Supporting information for

Cephalotaxine-type and homoerythrina-type alkaloids with antiproliferative effects from *Cephalotaxus fortunei*

Chun-Xue Zhao [a], Hui Liu [b], Xin Zhang [a], Meng-Yue Yang [a], Yue-Tong Wang [b], Yi-Jia Xing [a], Jun-Xin Hua [a], Qin Zhang [a], Da-Hong Li [a], Jiao Bai *, [a], Yong-Kui Jing *, [b], Hui-Ming Hua *, [a]

a Key Laboratory of Structure-Based Drug Design & Discovery, Ministry of Education, Shenyang Pharmaceutical University, Shenyang 110016, PR China

b Wuya College of Innovation, Shenyang Pharmaceutical University, Shenyang 110016, PR China

*Corresponding author.

E-mail address: huimhua@163.com (Hui-Ming Hua); jingyk@syphu.edu.cn (Yong-Kui Jing); baijiao@hotmail.com (Jiao Bai)

Content

General experimental procedures

The HRESIMS data were performed on the Bruker micro-TOFQ-Q mass spectrometer. The NMR spectra data were measured on a Bruker NMR spectrometer (600 MHz). ECD spectra were measured on a Bio-Logic Science MOS-450 spectropolarimeter. Optical rotations were measured with an Anton Paar MCP 200 polarimeter. UV spectra were recorded on a Shimadzu spectrophotometer with a model UV-1700. Silica gel (200–300 mesh, Qingdao Haiyang Chemical Co., Ltd., Qingdao, PR China), ODS (50 μm, YMC Co. Ltd., Kyoto, Japan), Sephadex LH-20 (GE Healthcare, Uppsala, Sweden). TLC analyses were carried out on silica gel plates (GF254, Qingdao Haiyang Chemical Co., Ltd., Qingdao, PR China). X-ray crystallographic analysis was performed on a Bruker PHOTON-II detector (Bruker Biospo Rheinstetten, Germany). Semi-preparative HPLC was performed on YMC ODS-A column (250 × 10 mm I. D., 5 μm) equipped with Shimadzu SPD-20A UV-Vis detector and LC-6AD pump.

Plant material

The twigs and leaves of *C. fortunei* were purchased from Zhenyuantang Pharmaceutical Co., Ltd., Bozhou City, Anhui Province, PR China, in August 2017. The seeds of *C. fortunei* were purchased from Futaba Seed Company, Wuxi City, Jiangsu Province, PR China, in August 2017. The plant species were identified by Assoc. Prof. Jiuzhi Yuan, School of Traditional Chinese Medicine, Shenyang Pharmaceutical University, PR China. The plant specimens (voucher no. SJS-201708-3 and SJS-201708-4) were deposited at Key Laboratory of Structure-Based Drug Design & Discovery, Ministry of Education, Shenyang Pharmaceutical University, PR China.

Extraction and isolation

The dried twigs and leaves of *C. fortunei* (45.8 kg) were extracted with 75% EtOH (400 L) three times for two hours each time. After removal of the solvent, the crude extract (6.45 kg) was dissolved in 3% HCl (12 L) solution to pH 2–3 and filtered to obtain a precipitate and an acidic filtrate, respectively. The acidic aqueous solution was partitioned with CH_2Cl_2 (30 L) to afford part C (20 g). Then the acid

aqueous solution was basified with solid Na_2CO_3 to pH 9–10 and extracted again with CH_2Cl_2 to afford part A (30 g). The above-mentioned precipitate was suspended in water and adjusted to the neutral pH with anhydrous sodium carbonate, which was extracted with CH_2Cl_2 to obtain part B (105 g).

Part A was subjected to an ODS open column chromatography with MeOH-H_2O (10:100–100:0, v/v) to give six fractions (AI-AV). Fraction AI (5.0 g) was separated by column chromatography (CC) over silica gel, and eluted with CH_2Cl_2-MeOH (100:0–0:100, v/v) to give subfractions AI-1–AI-6. Fraction AI-1 (3.0 g) was isolated by silica gel CC eluted with CH_2Cl_2-MeOH (100:0–0:100, v/v) to give subfractions AI-1-1–AI-1-8. **30** (500.0 mg) was precipitated as crystals from fraction AI-1-1 (1 g) and the remaining mother liquid was isolated by semi-preparative HPLC with MeOH-H_2O (39:61, containing 0.005% diethylamine (DEA)) to yield **8** (9.0 mg, t_R 55.0 min). Fraction AI-1-2 (1.0 g) was isolated by silica gel CC eluted with CH_2Cl_2-MeOH (100:0–0:100, v/v) to give subfractions AI-1-2-1–AI-1-2-6. **9** (18.0 mg) was precipitated as crystals from fraction AI-1-2-1 (100 mg). Fraction AI-1-4 (300 mg) was isolated by semi-preparative HPLC with MeOH-H_2O (35:65, containing 0.005% DEA) to obtain **14** (100.0 mg, t_R 16.0 min), and **1** (20.0 mg, t_R 26.0 min). **14a** (3.0 mg) was precipitated as crystals from fraction AI-1-6 (100 mg) and **13** (5.5 mg) was obtained as crystals from fraction AI-1-7 (100 mg). Fraction AII (1.0 g) was isolated by silica gel CC eluted with petroleum ether-ethyl acetate (100:10–0:100, v/v) to give subfractions AII-1–AII-6. Fraction AII-1 (200 mg) was isolated by semi-preparative HPLC with MeOH-H_2O (35:65, containing 0.005% DEA) to obtain **10** (5.0 mg, t_R 38.0 min), and **22** (3.0 mg, t_R 45.0 min). Fraction AII-2 (100 mg) was purified on a Sephadex LH-20 column (eluted with MeOH) to obtain **21** (5 mg). Fraction AII-3 (1.0 g) was separated by silica gel CC eluted with CH_2Cl_2-acetone (100:0–0:100, v/v) to give subfractions AII-3-1–AII-3-5. Fraction AII-3-1 (100 mg) was purified on a Sephadex LH-20 column (eluted with MeOH) to obtain **20** (10 mg). **5** (100.0 mg) was crystallized from fraction AIII (1.2 g). Fraction AIV (1.5 g) precipitated crystals (MeOH) to obtain **24** (150 mg).

Part B was separated by CC over silica gel eluted with CH_2Cl_2-MeOH (100:0–0:100, v/v) to give subfractions BI-BV. Fraction BV (4.5 g) was separated by silica gel CC and eluted with CH_2Cl_2-MeOH (100:0–0:100, v/v) to give subfractions BV-1–BV-6. **7** (20.0 mg) was crystallized from fraction BV-1 (800 mg) and the remaining part was isolated by semi-preparative HPLC with MeOH-H_2O (33:67, containing 0.005% DEA) to obtain **6** (56.0 mg, t_R 70.5 min). Fraction BV-2 (600 mg) was subjected to an ODS CC (MeOH-H_2O, 10% to 100%, v/v) to give five fractions (BV-2-1–BV-2-5). Fraction BV-2-1 (200 mg) was isolated by semi-preparative HPLC with MeOH-H_2O (60:40, containing 0.005% DEA) to obtain **23** (3.0 mg, t_R 25.0 min) and **4** (2.0 mg, t_R 29.0 min). Fraction BV-2-2 (50 mg) was isolated by semi-preparative HPLC with MeOH-H_2O (40:60, containing 0.005% DEA) to obtain **3** (2.0 mg, t_R 16.5 min). Fraction BV-3 (100 mg) was isolated by semi-preparative HPLC with MeOH-H_2O (45:55, containing 0.005% DEA) to obtain **2** (5.0 mg, t_R 45.2 min). Fraction BV-3 (300 mg) was separated by CC over silica gel eluted with CH_2Cl_2-MeOH (100:0–0:100, v/v) to give subfractions BV-3-1–BV-3-5. Fraction BV-3-1 (85 mg) yielded **31** (3.0 mg) by recrystallization (MeOH).

The seed kernels of *C. fortunei* (15.0 kg) were immersed and degreased with petroleum ether (90 L) at room temperature to obtain 6.3 kg of defatted seed kernels. Defatted seed kernels were extracted with 85% EtOH and concentrated by refluxing to obtain 1146 g of EtOH extract. The extract was suspended in water and extracted with petroleum ether to obtain part D (247 g). The aqueous layer was adjusted to pH 2–3 by adding 2–3% HCl (3 L) and filtered to obtain acid aqueous solution and precipitate. The aqueous acid solution was extracted with CH_2Cl_2 (40 L) to obtain part E (43 g), and then was adjusted to pH 9–10 with solid Na_2CO_3 and extracted with CH_2Cl_2 (80 L) again to obtain part F (152 g).

Part F was subjected to a silica gel CC eluted with CH_2Cl_2-MeOH (100:0–0:100, v/v) to give six fractions (FI-FVI). Fraction FII (5.0 g) was separated by CC over silica gel, and eluted with petroleum ether-ethyl acetate (100:0–0:100, v/v) to give subfractions FII-1–FII-7. Fraction FII-3 was separated on an ODS column with MeOH-H_2O (10:100–100:0, v/v) to give six fractions (FII-3-1–FII-3-6). Fraction FII-

3-1 was isolated by semi-preparative HPLC with MeOH-H_2O (18:82, containing 0.005% DEA) to obtain **18** (0.8 mg, t_R 71.0 min). **26** (3.8 mg) was precipitated as crystals from fraction FIII and the remaining mother liquid was separated on an ODS column (MeOH-H_2O, 10% to 100%, v/v) to obtain five fractions FIII-3-1–FIII-3-5. Fractions FIII-3-1 was separated by silica gel CC and eluted with CH_2Cl_2-MeOH (100:0–0:100, v/v) to give subfractions FIII-3-1-1–FIII-3-1-2. **19** was precipitated as crystals from fractions FIII-3-1-1. **29** was precipitated as crystals from fraction FIII-3-2. Fraction FIII-3-2 was purified on a Sephadex LH-20 column (eluted with MeOH) to obtain six fractions (FII-3-2-1–FII-3-2-6). Fraction FII-3-2-6 was isolated by semi-preparative HPLC with MeOH-H_2O (48:52, containing 0.005% DEA) to obtain **25** (8.3 mg, t_R 20.0 min) and **12** (1.8 mg, t_R 26.0 min). Fraction FIV was separated on an ODS column (MeOH-H_2O, 10% to 100%, v/v) to obtain five fractions FIV-1–FIV-6. Fraction FIV-2 was isolated by semi-preparative HPLC with MeOH-H_2O (40:60, containing 0.005% DEA) to obtain **27** (5.4 mg, t_R 34.0 min). FIV-4 was isolated by semi-preparative HPLC with MeOH-H_2O (40:60, containing 0.005% DEA) to obtain **17** (2.6 mg, t_R 39.0 min), **15** (2.5 mg, t_R 42.0 min) and **28** (5.1 mg, t_R 63.0 min). FIV-5 was isolated by semi-preparative HPLC with MeOH-H_2O (41:59, containing 0.005% DEA) to obtain **11** (12.0 mg, t_R 27.0 min) and **16** (11.0 mg, t_R 50.0 min). FIV-6 was isolated by semi-preparative HPLC with MeOH-H_2O (50:50, containing 0.005% DEA) to obtain **32** (4.5 mg, t_R 50.0 min).

Spectroscopic data of compounds

Cephalofortunine A *β*-*N*-oxide (**1**): colorless needle crystal; $[\alpha]_D^{20}$ + 45.0 (*c* 0.3, CH_3OH); UV (CH_3OH) λ_{max} (logε) 209 (5.08), 238 (3.12), 280 (1.63) nm; ECD (CH_3OH) λ_{max} ($\Delta\varepsilon$) 209 (+10.08), 228 (-15.02), 249 (+20.06), 282 (-13.9) nm; ^1H and ^{13}C NMR (DMSO-d_6) see Table 1; HRESIMS *m*/*z* 378.1927 ($[M+H]^+$, calcd. 378.1911, $C_{20}H_{27}NO_6$).

Cephalofortunine A (**2**): colorless solid; $[\alpha]_D^{20}$ + 51.6 (*c* 0.3, CH_3OH); UV (CH_3OH) λ_{max} (logε) 208 (5.66) nm, 233 (3.60), 280 (1.88) nm; ECD (CH_3OH) λ_{max} ($\Delta\varepsilon$) 218 (-9.82), 242 (-29.80), 279 (-10.80) nm; ^1H and ^{13}C NMR (DMSO-d_6) see Table 1; HRESIMS *m*/*z* 362.1970 ($[M+H]^+$, calcd. 362.1962, $C_{20}H_{27}NO_5$).

Cephalofortunine B (**3**): colorless solid; $[\alpha]_D^{20}$ + 15.0 (*c* 0.05, CH_3OH); UV (CH_3OH) λ_{max} (logε) 206 (5.08), 233 (3.07), 283 (1.62) nm; ECD (CH_3OH) λ_{max} ($\Delta\varepsilon$) 212 (+22.08), 227 (-7.20), 243 (+7.92) nm; ^1H and ^{13}C NMR (DMSO-d_6) see Table 1; HRESIMS *m*/*z* 348.1794 ($[M+H]^+$, calcd. 348.1805, $C_{19}H_{25}NO_5$).

Fortuneicyclidin C (**11**): colorless solid; $[\alpha]_D^{20}$ – 31.0 (*c* 0.23, CH_3OH); UV (CH_3OH) λ_{max} (logε) 294 (0.20), 241 (0.18), 205 (1.63) nm; ECD (CH_3OH) λ_{max} ($\Delta\varepsilon$) 219 (-11.5), 241 (+2.02), 282 (-2.50) nm; ^1H and ^{13}C NMR (DMSO-d_6) see Table 2; HRESIMS *m*/*z* 318.1340 ($[M+H]^+$, calcd. 318.1336, $C_{17}H_{20}NO_5$).

Cephalocyclidin B (**13**): colorless needle crystal; $[\alpha]_D^{20}$ – 62.6 (*c* 0.3, CH_3OH); UV (CH_3OH) λ_{max} (logε) 210 (4.62), 248 (1.98), 294 (1.02) nm; ECD (CH_3OH) λ_{max} ($\Delta\varepsilon$) 230 (-6.36), 252 (+29.80), 292 (-19.02) nm; ^1H and ^{13}C NMR (DMSO-d_6) see Table 2; HRESIMS *m*/*z* 366.1115 ($[M]^+$, calcd. 366.1104, $C_{18}H_{21}ClNO_5$).

11-Deoxycephalofortine B (**15**): colorless needle crystal; $[\alpha]_D^{20}$ + 26.0 (*c* 0.2, CH_3OH); UV (CH_3OH) λ_{max} (logε) 205 (4.83), 239 (1.52), 291 (1.86) nm; ECD (CH_3OH) λ_{max} ($\Delta\varepsilon$) 215 (+7.50), 235 (+5.05), 270 (-5.05), 298 (+2.50) nm; ^1H and ^{13}C NMR (DMSO-d_6) see Table 3; HRESIMS *m*/*z* 304.1569 ($[M+H]^+$, calcd. 304.1543, $C_{17}H_{22}NO_4$).

Cephalotine A 3-*O*-*β*-glucopyranoside (**17**): colorless needle crystal; $[\alpha]_D^{20}$ – 27.6 (*c* 0.25, CH_3OH); UV (CH_3OH) λ_{max} (logε) 291 (0.51) nm; ECD (CH_3OH) λ_{max} ($\Delta\varepsilon$) 215 (+4.95), 292 (-6.80) nm; ^1H and ^{13}C NMR (DMSO-d_6) see Table 3; HRESIMS *m*/*z* 480.1872 ($[M+H]^+$, calcd. 480.1864, $C_{23}H_{30}NO_{10}$).

Single-crystal X-ray crystallographic analysis

The X-ray crystallographic data of compounds **1**, **6** and **13** were acquired on a Bruker APEX-II CCD diffractometer and deposited at the Cambridge Crystallographic Data Center (CCDC, 2179041, 2179042 and 2179045). Detailed parameters are also available in Supporting Information.

Computational methods

The Spartan 14.0 (Wavefunction Inc., Irvine, CA, USA) search using molecular mechanics MMFF was performed for (3*R*, 5*R*, 6*S*, 7*S*)-**2**. The low-energy conformers of them were further optimized in the gas phase by semi-empirical method in

Gaussian 09 program package,[1, 2] which were reoptimized and analysed by using the density functional theory (DFT) at the B3LYP/6-31 G (d, p) level, resulted in no imaginary frequencies. The ECD was calculated using TD-DFT-B3LYP/6-31 G (d, p) level with the CPCM model in methanol solution. The overall calculated ECD curves of all compounds were generated by Boltzmann weighting of their selected low-energy conformers using SpecDis 1.51.[3] The ECD spectra of **2**, **3**, **11**, **15** and **17** were calculated in the same method.

Antitumor activity assay

Two human leukemia cell lines (THP-1 and K562) were obtained from the American Type Culture Collection, ATCC (Lockville, MD, USA). The test cells were cultured in RPMI 1640 media (Gibco, New York, USA) supplemented with 10% fetal bovine serum (ExCell Bio), 100 U/mL penicillin, and 100 μg/mL streptomycin. All cells were cultured at 37 ◦C in a 5% CO_2 incubator. Antitumor activity was evaluated by the method as described previously.[4]

References

1 H. Goto and E. Osawa. An efficient algorithm for searching low-energy conformers of cyclic and acyclic molecules. *J. Chem. Soc. Perkin Trans*. 2008, 2, 187–198.

2 H. Goto and E. Osawa. Corner flapping: a simple and fast algorithm for exhaustive generation of ring conformations. *J. Am. Chem. Soc*. 1989, 111, 8950–8951.

3 T. Bruhn, A. Schaumlöffel, Y. Hemberger and G. Bringmann. SpecDis: quantifying the comparison of calculated and experimental electronic circular dichroism spectra. *Chirality* 2013, 25, 243–249.

4 Y. Z. Li, Z. L. Li, S. L. Yin, G. Shi, M. S. Liu, Y. K. Jing and H. M. Hua, Triterpenoids from *Calophyllum inophyllum* and their growth inhibitory effects on human leukemia HL-60 cells. *Fitoterapia* 2010, 81, 586–589.

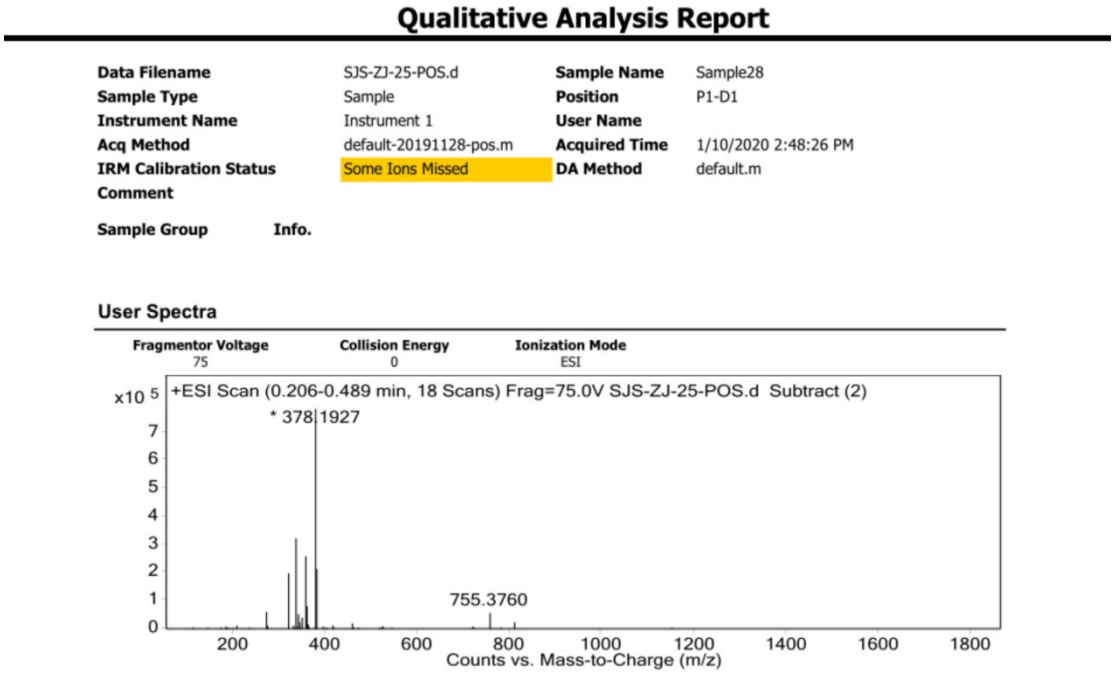

Figure S1. HRESIMS spectrum of **1**

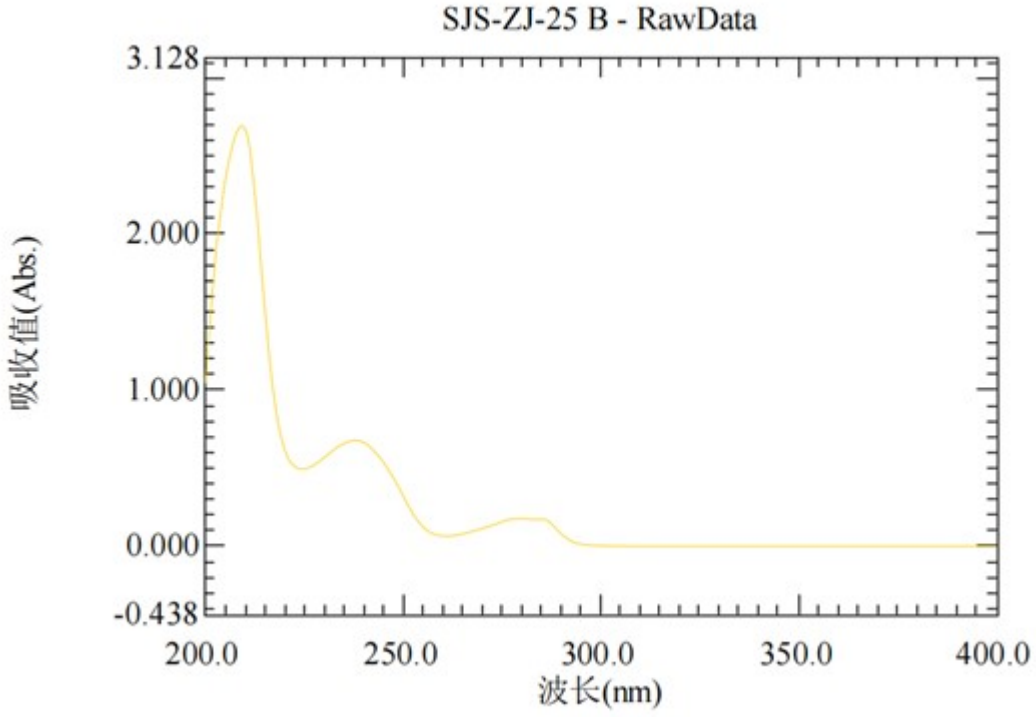

Figure S2. UV spectrum of **1**

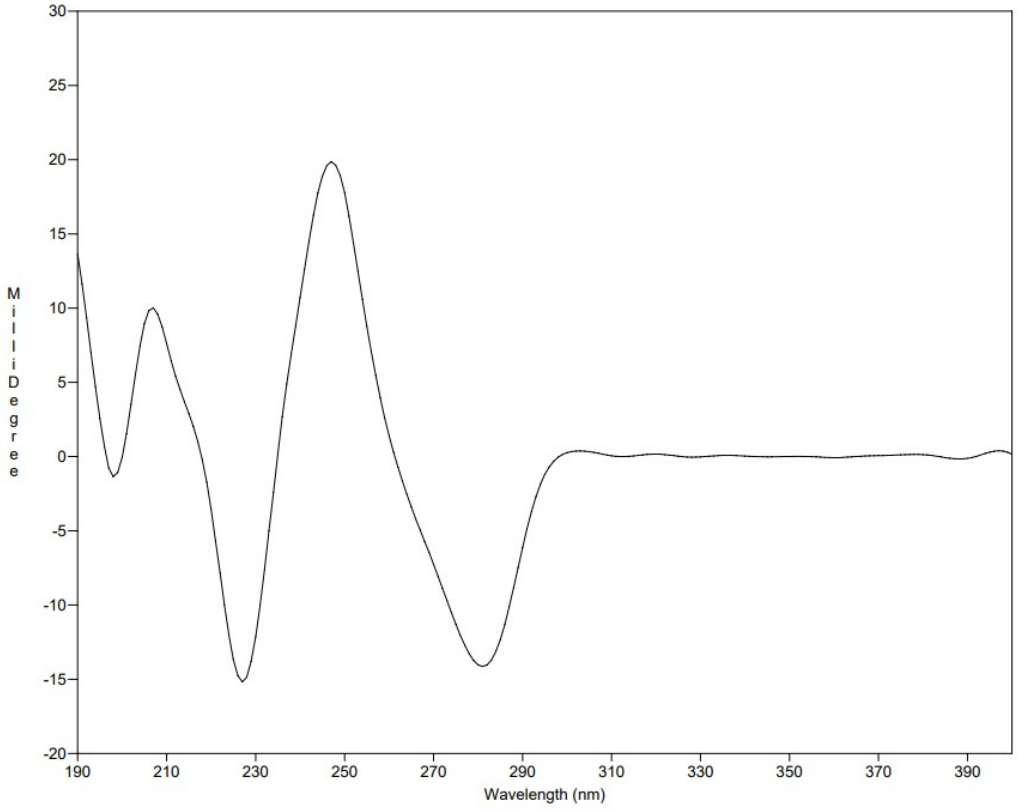

Figure S3. Experimental ECD spectrum of **1**

Z

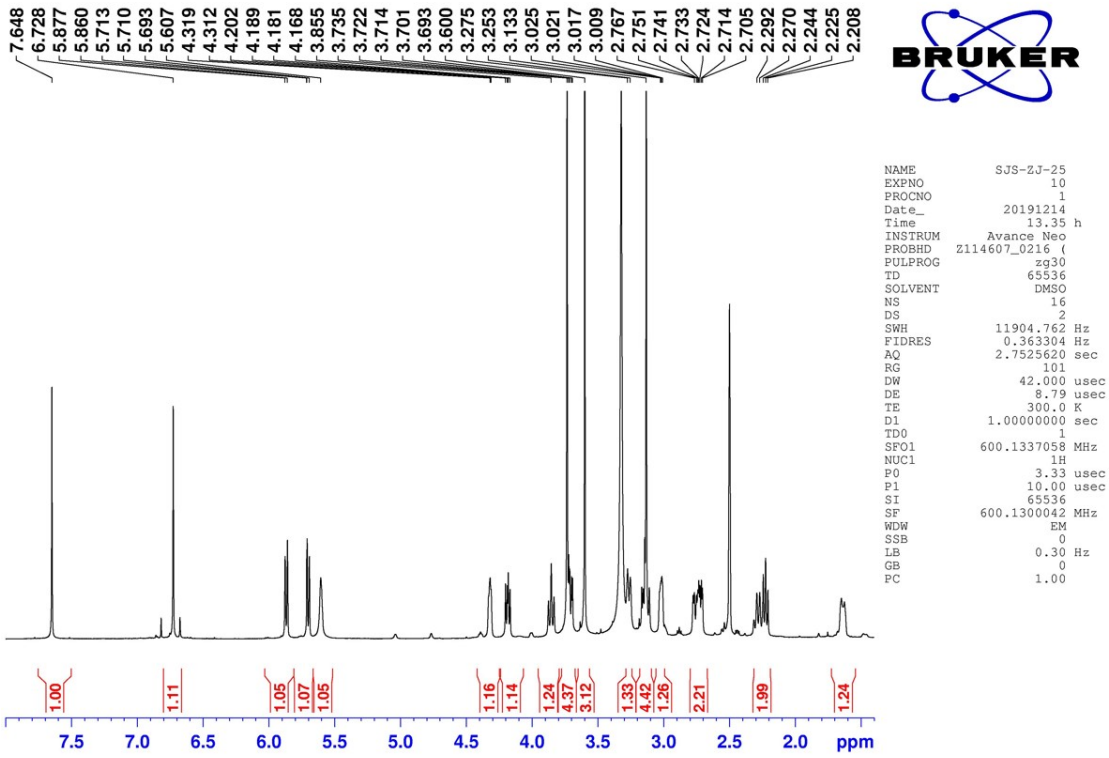

Figure S4. ^{1}H NMR spectrum of compound **1** (600 MHz, DMSO-d_6)

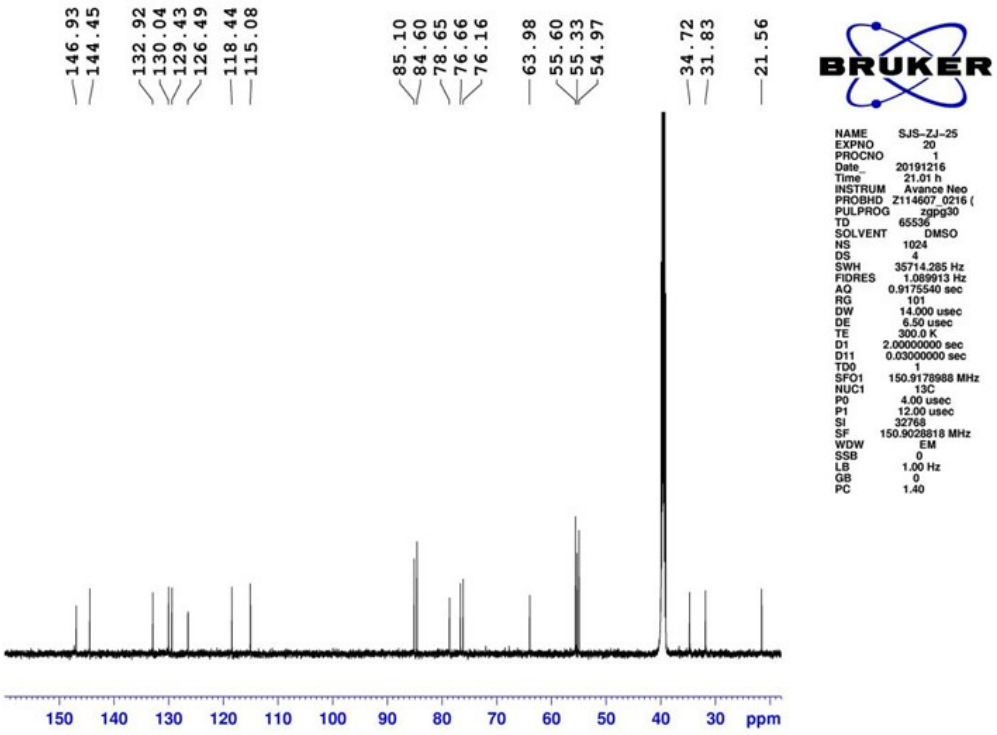

Figure S5. ^{13}C NMR spectrum of compound **1** (150 MHz, DMSO-d_6)

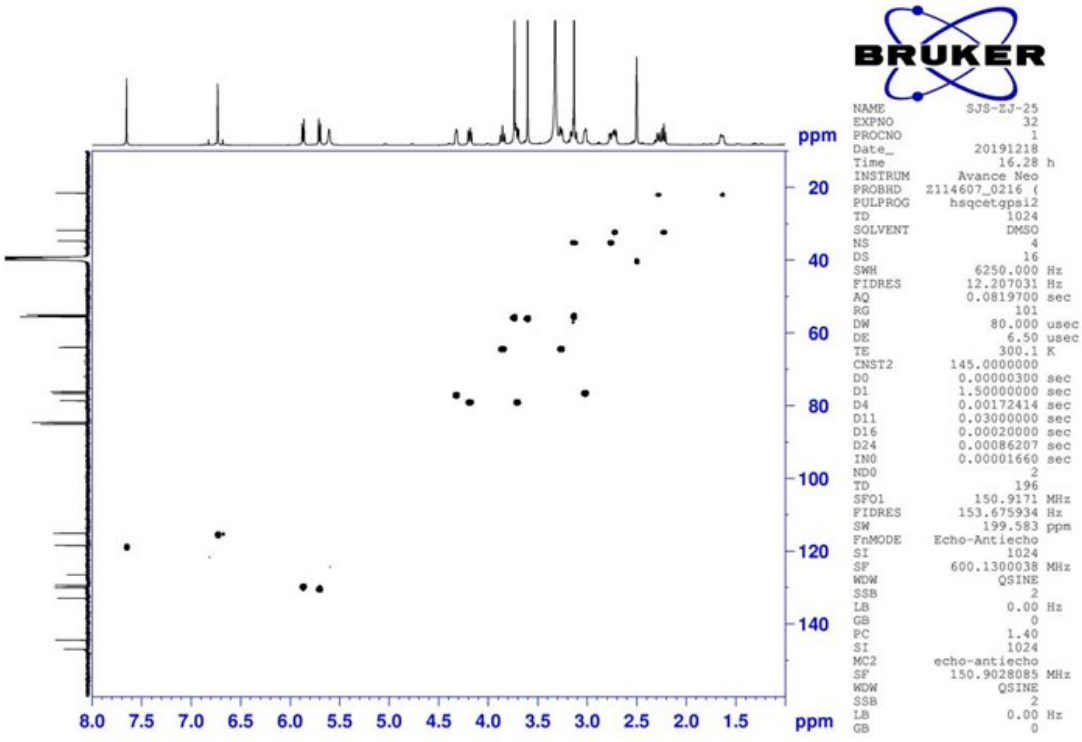

Figure S6. HSQC spectrum of compound **1** (600 MHz, DMSO-d_6)

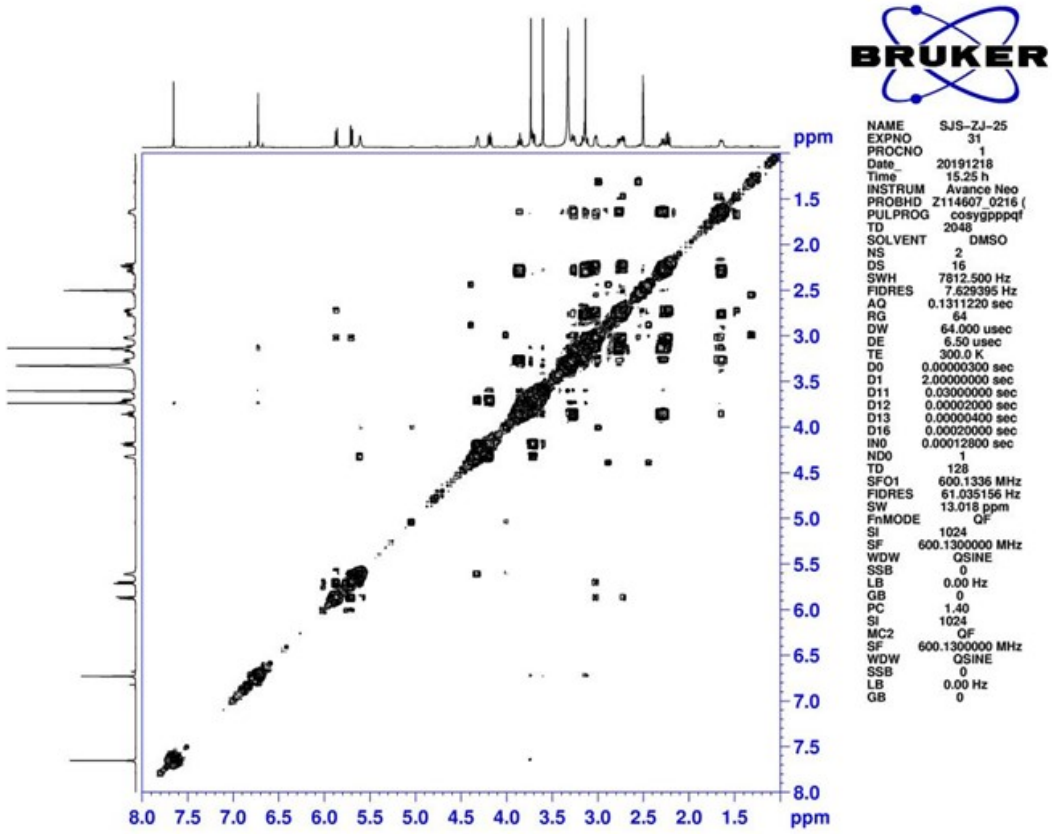

Figure S7. ^{1}H-^{1}H COSY spectrum of compound **1** (600 MHz, DMSO-d_6)

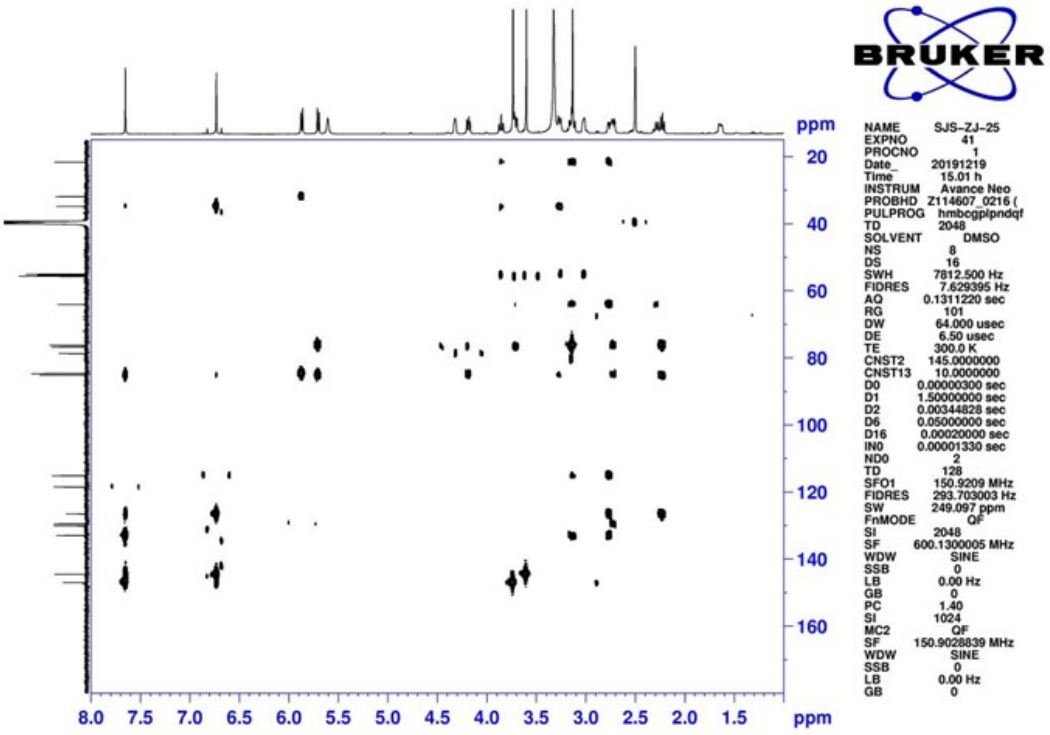

Figure S8. HMBC spectrum of compound **1** (600 MHz, DMSO-d_6)

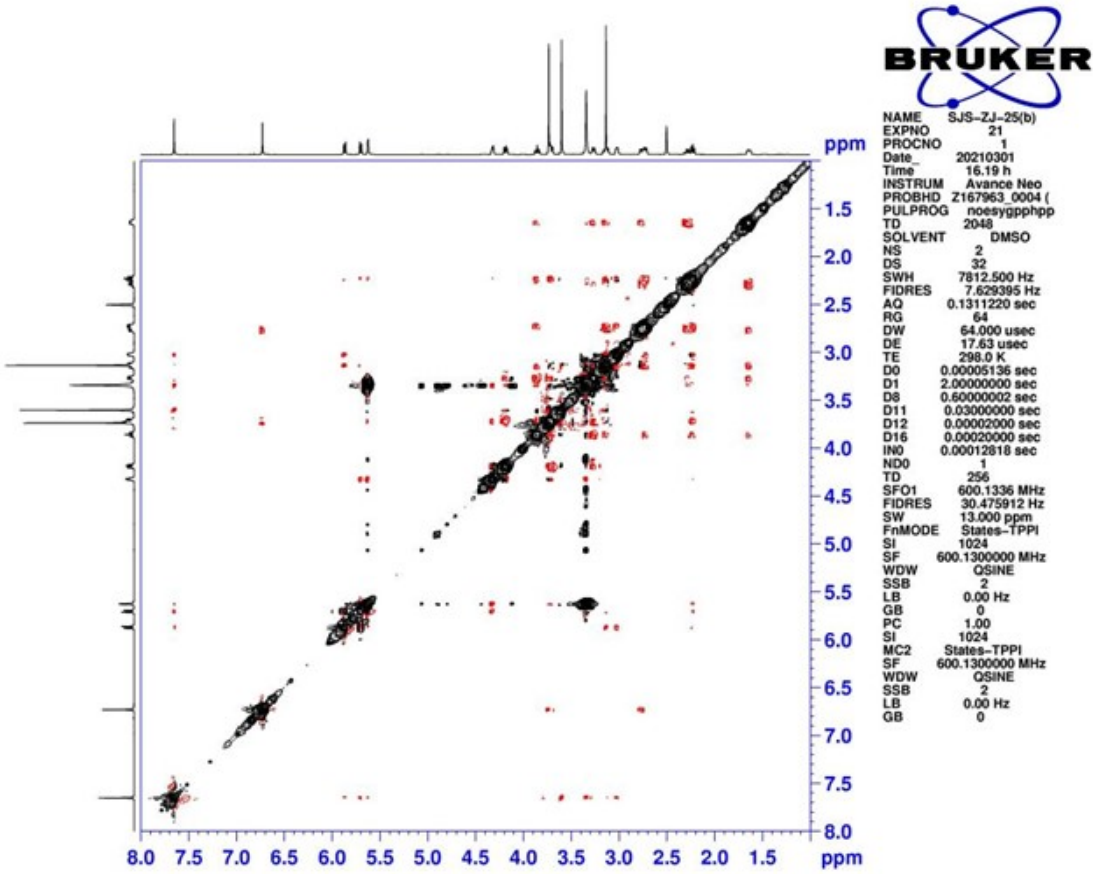

Figure S9. NOESY spectrum of compound **1** (600 MHz, DMSO-d_6)

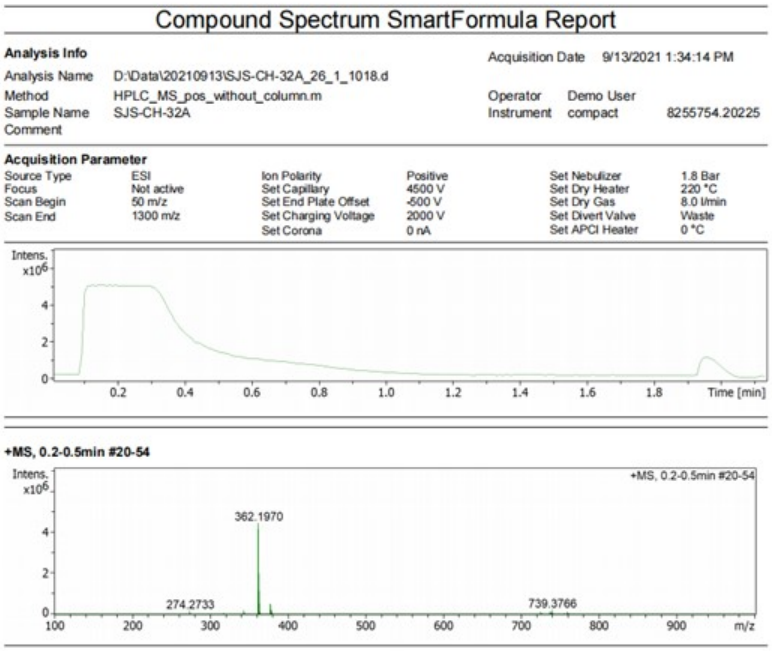

Figure S10. HRESIMS spectrum of **2**

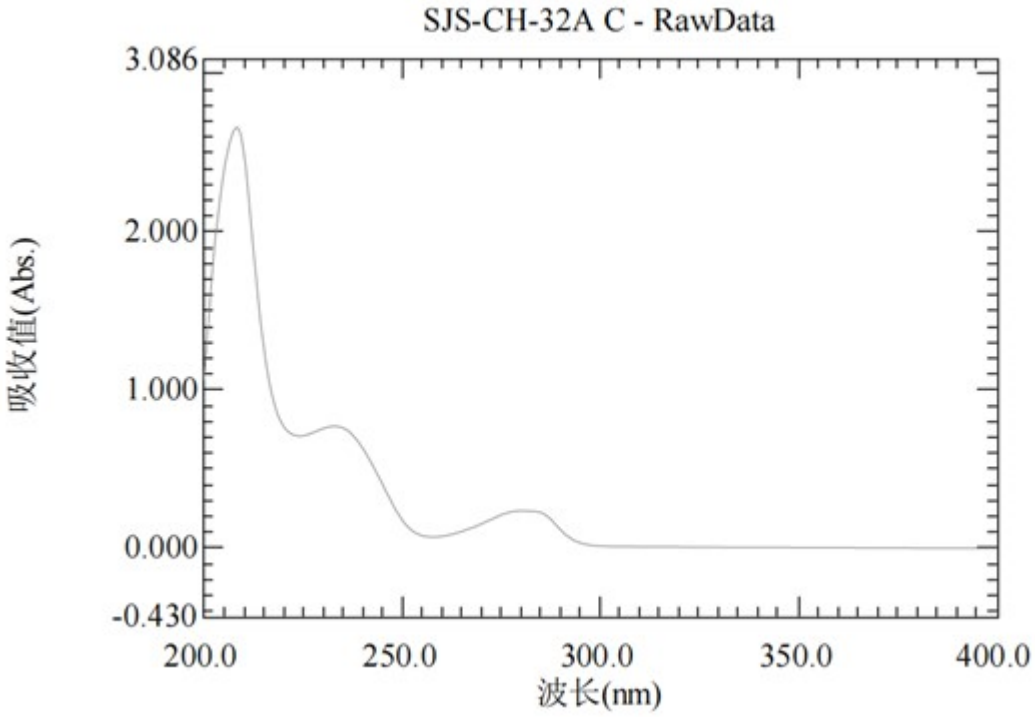

Figure S11. UV spectrum of **2**

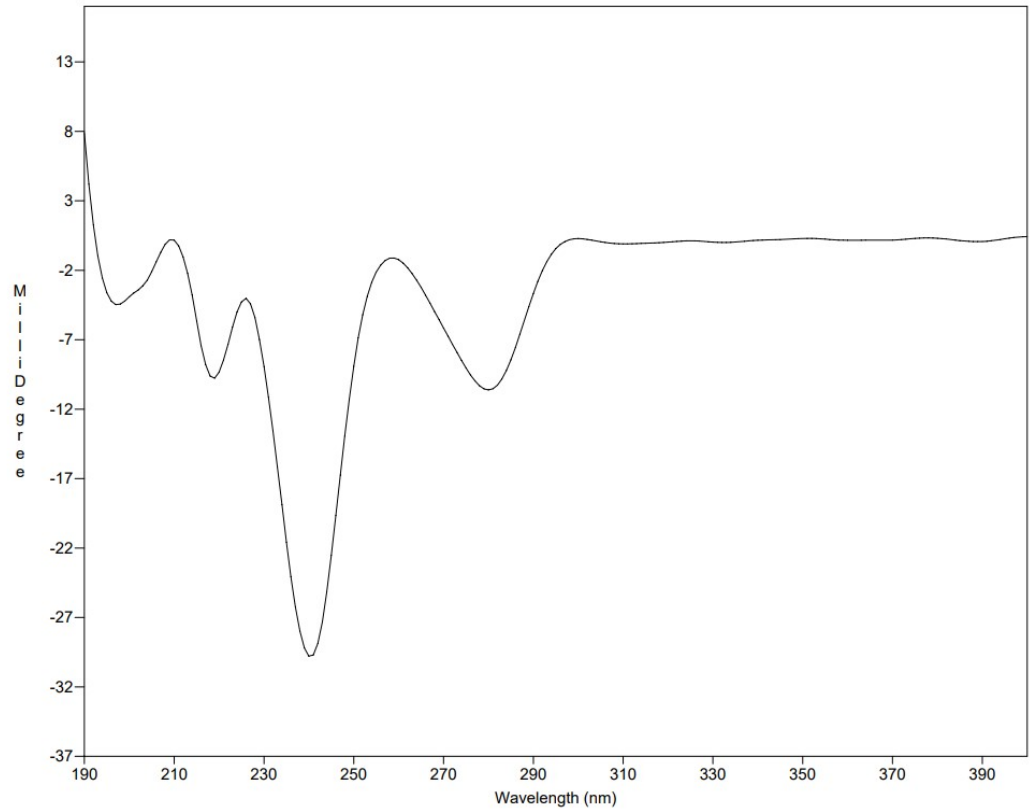

Figure S12. Experimental ECD spectrum of **2**

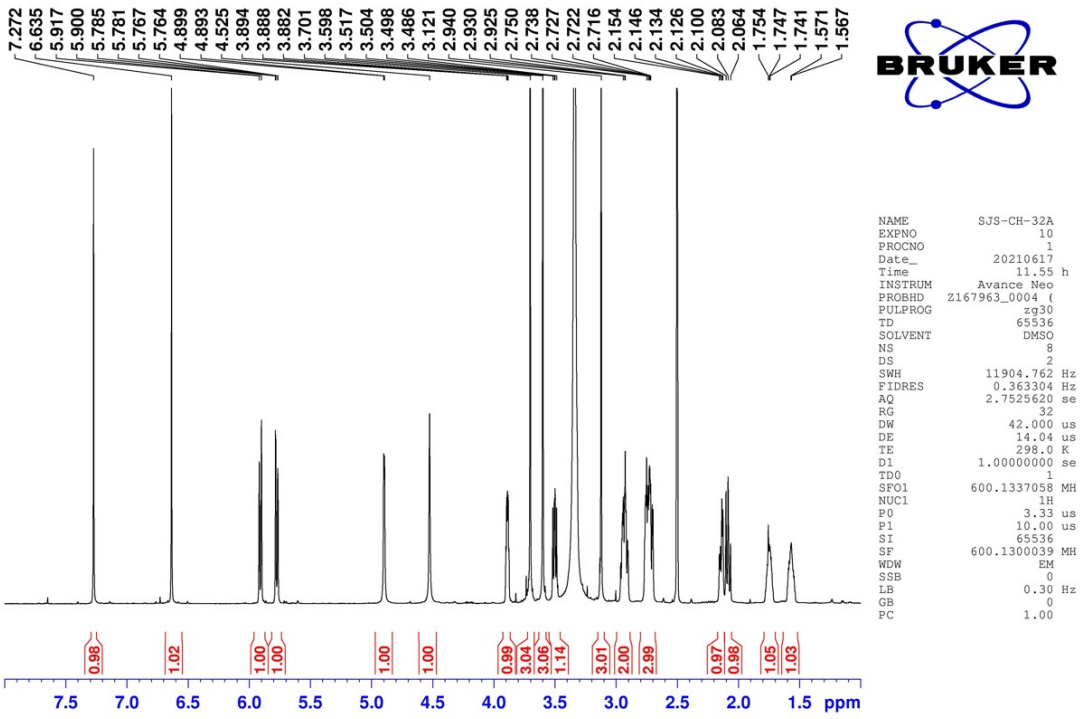

Figure S13. ^{1}H NMR spectrum of compound **2** (600 MHz, DMSO-d_6)

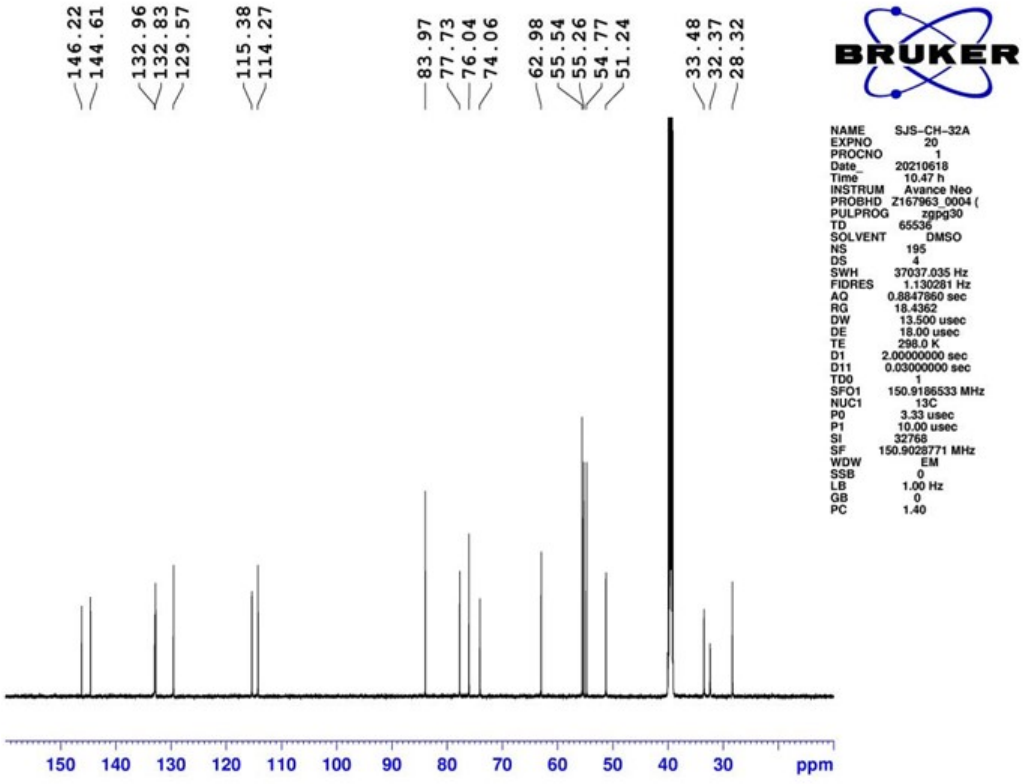

Figure S14. ^{13}C NMR spectrum of compound **2** (150 MHz, DMSO-d_6)

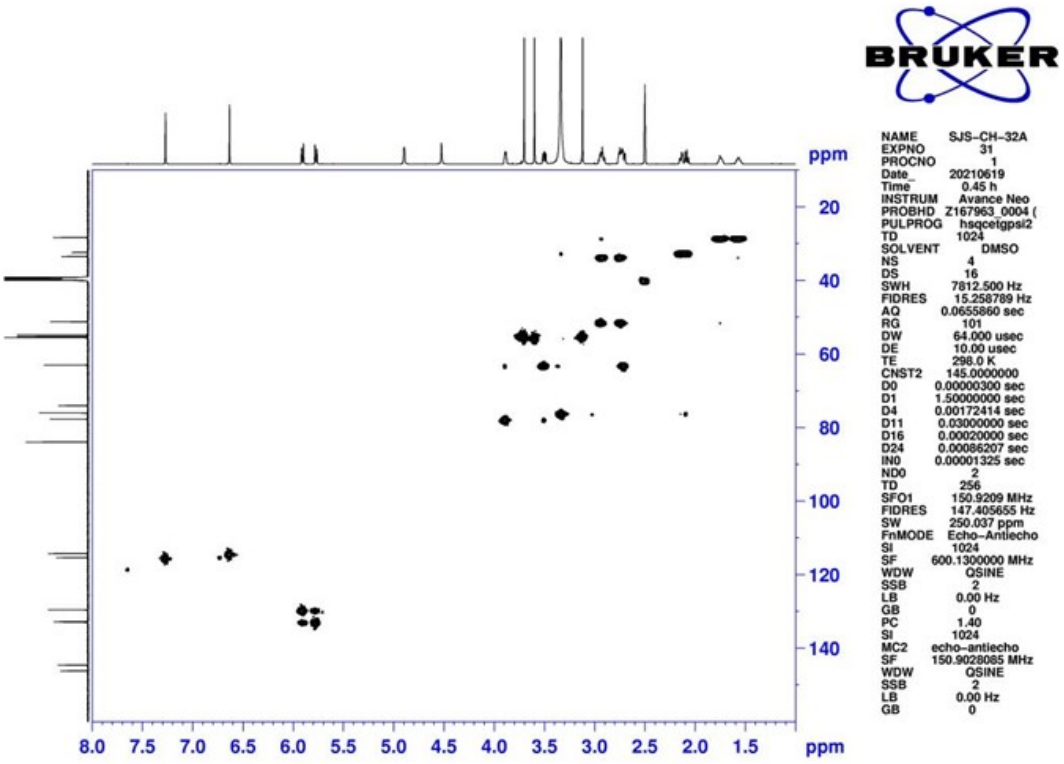

Figure S15. HSQC spectrum of compound **2** (600 MHz, DMSO-d_6)

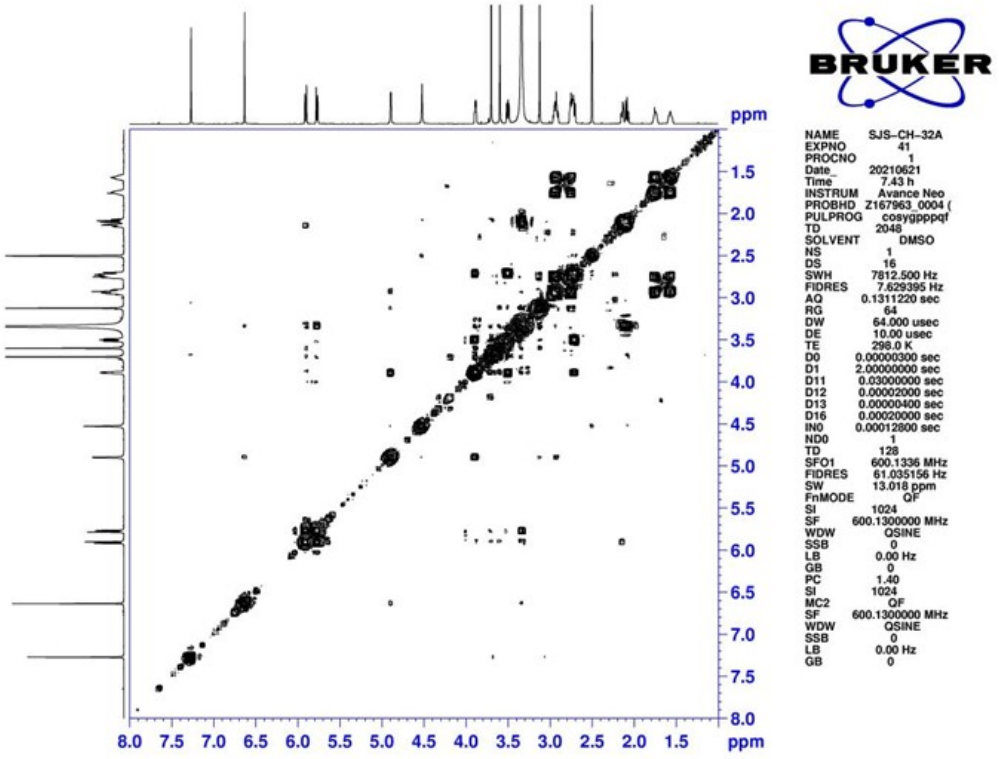

Figure S16. ^{1}H-^{1}H COSY spectrum of compound **2** (600 MHz, DMSO-d_6)

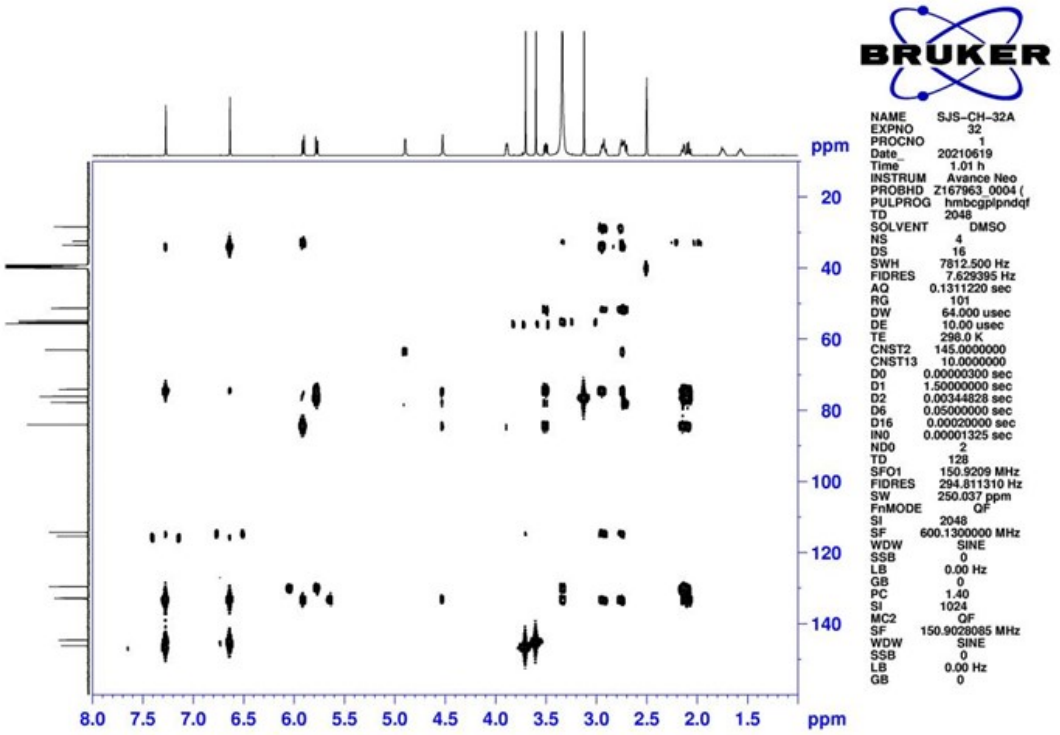

Figure S17. HMBC spectrum of compound **2** (600 MHz, DMSO-d_6)

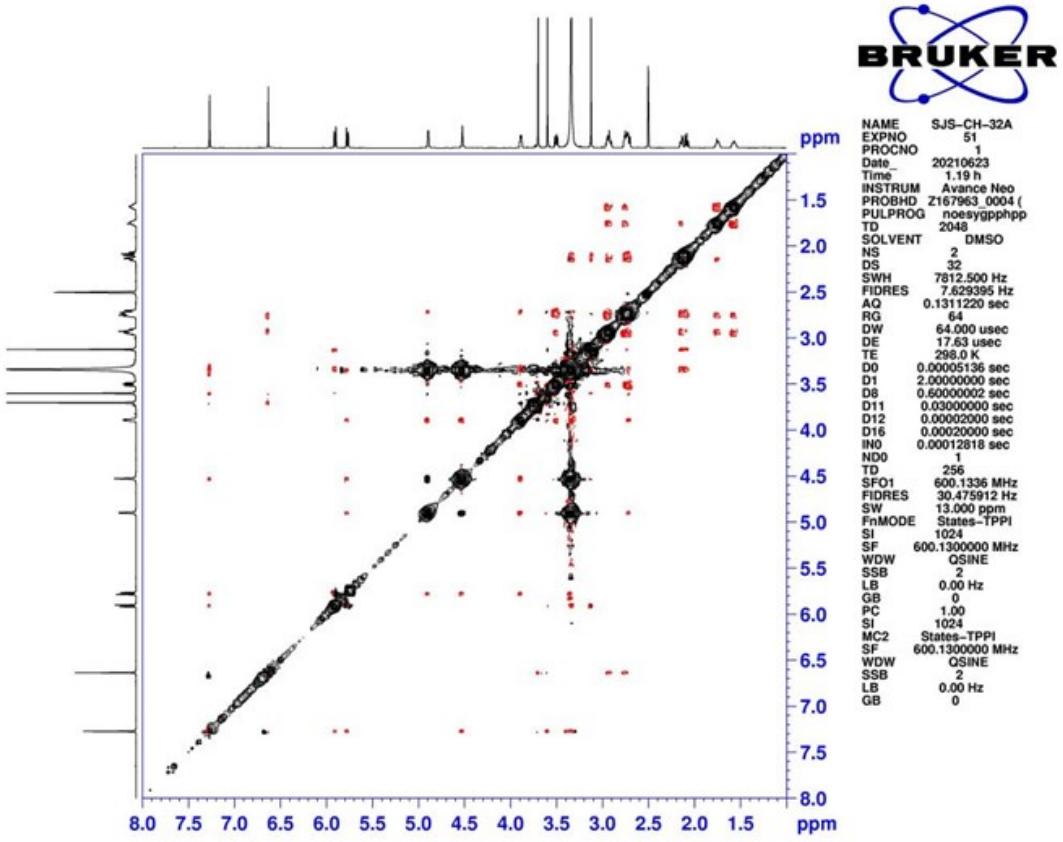

Figure S18. NOESY spectrum of compound **2** (600 MHz, DMSO-d_6)

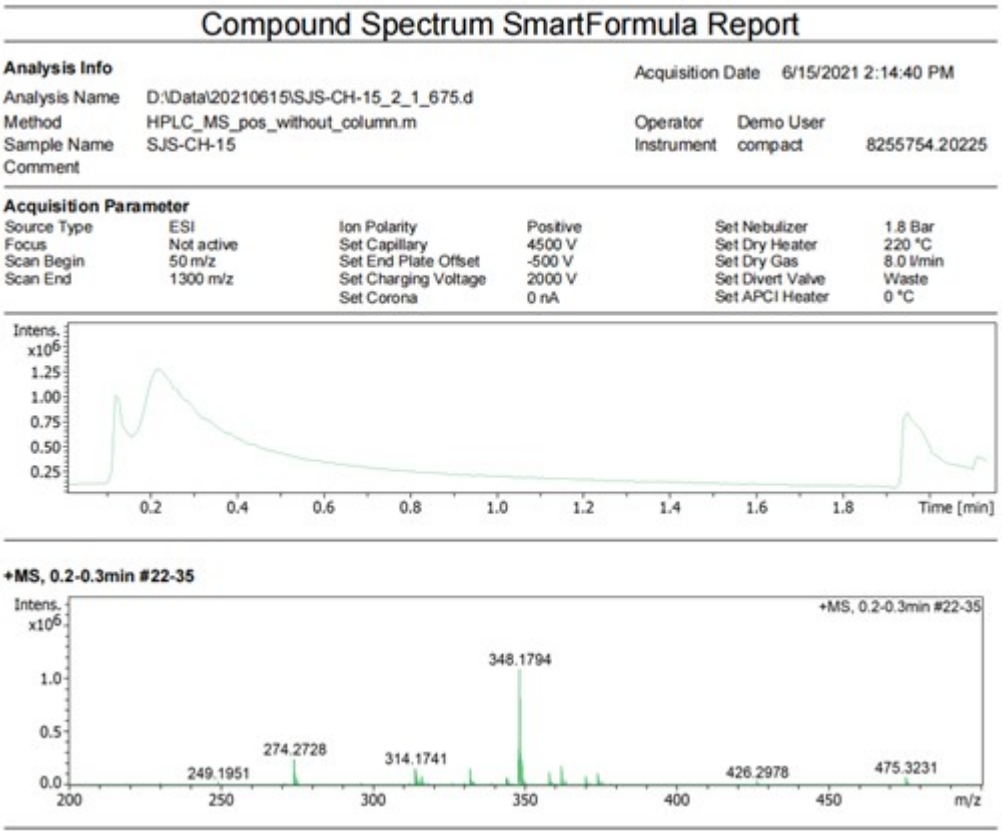

Figure S19. HRESIMS spectrum of **3**

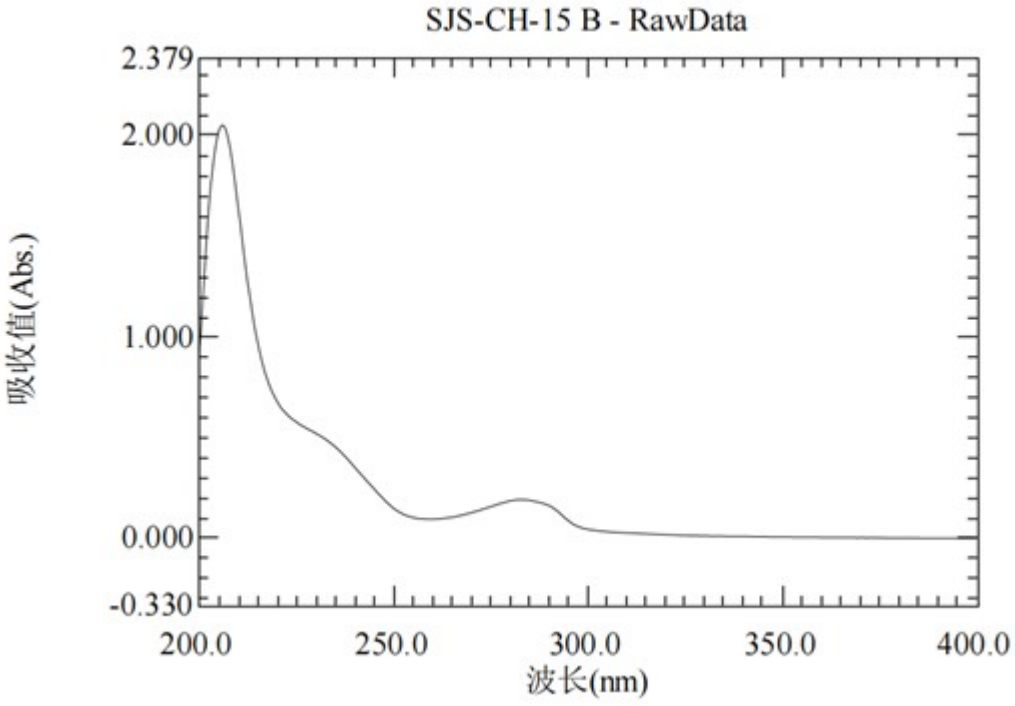

Figure S20. UV spectrum of **3**

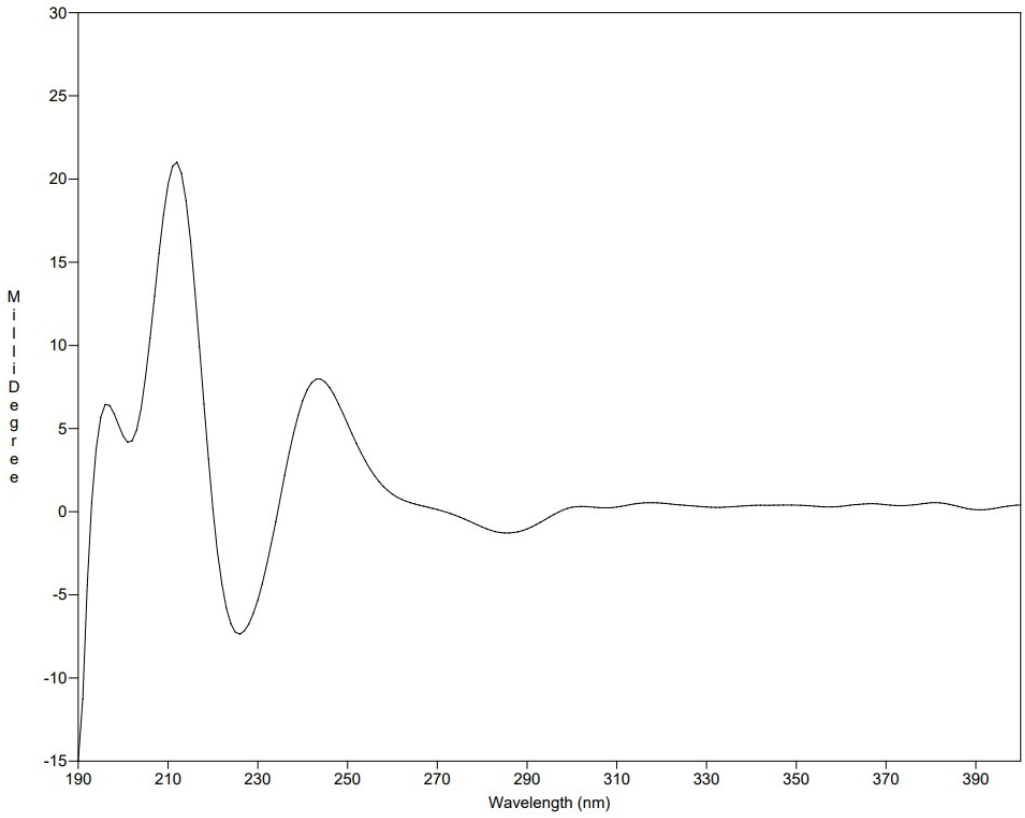

Figure S21. Experimental ECD spectrum of **3**

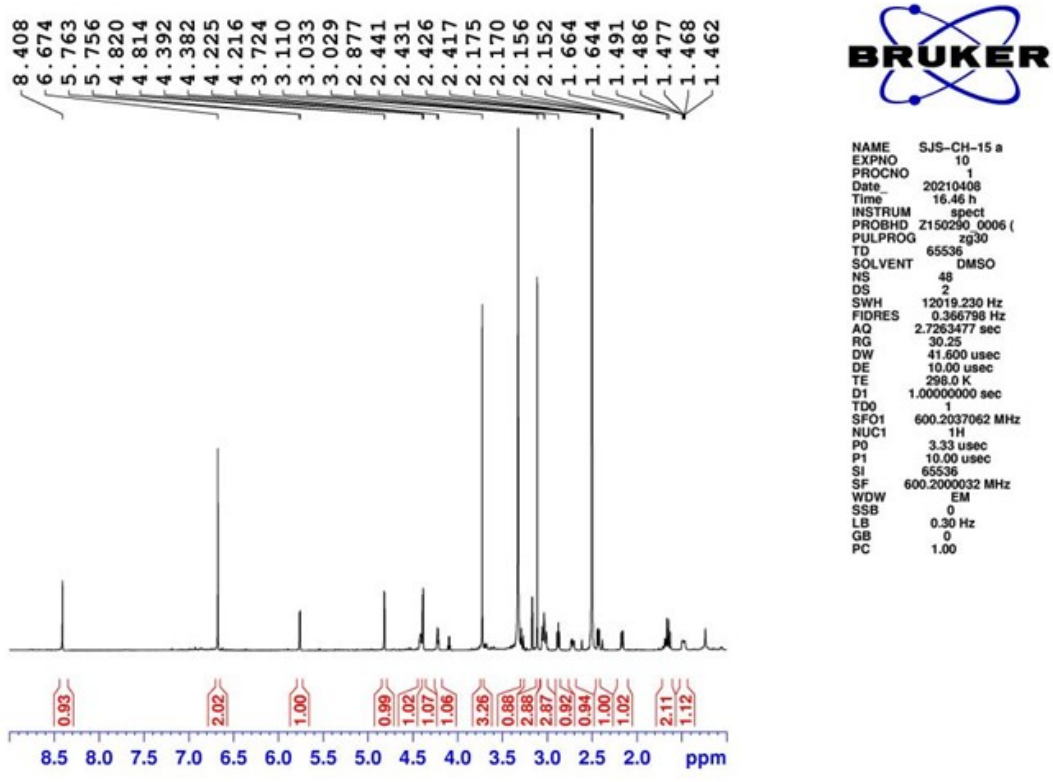

Figure S22. ^{1}H NMR spectrum of compound **3** (600 MHz, DMSO-d_6)

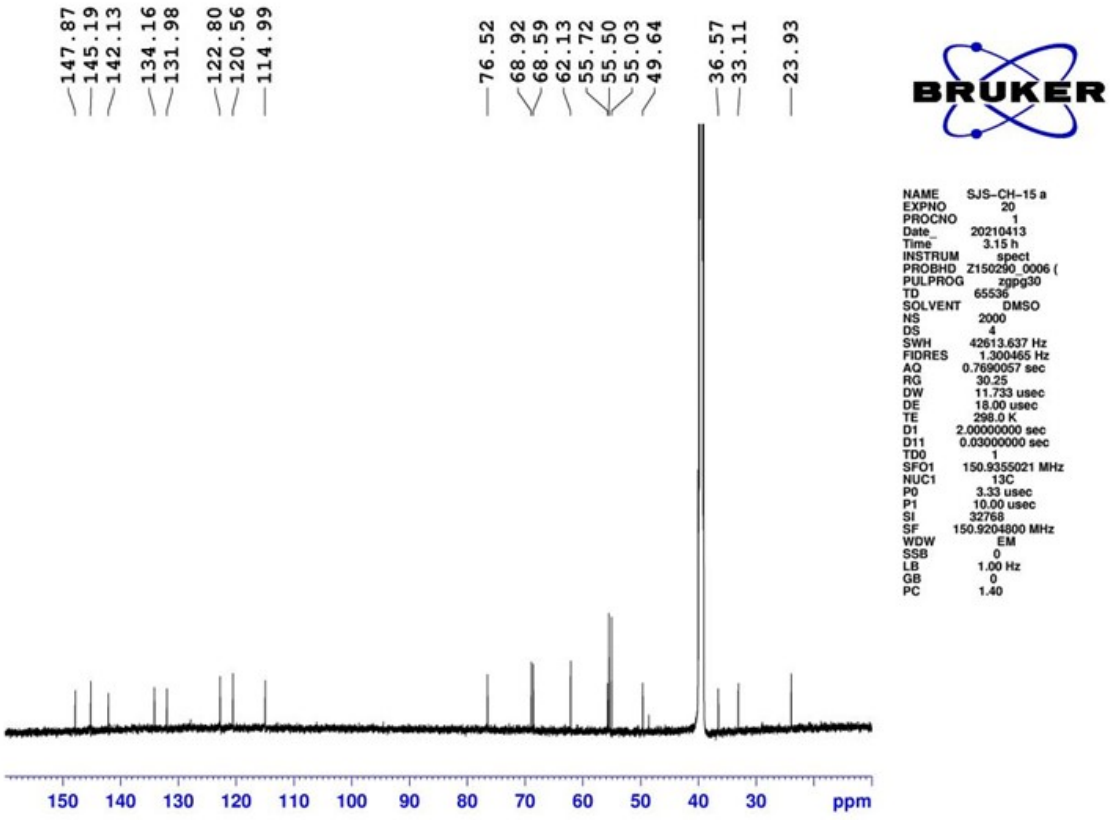

Figure S23. ^{13}C NMR spectrum of compound **3** (150 MHz, DMSO-d_6)

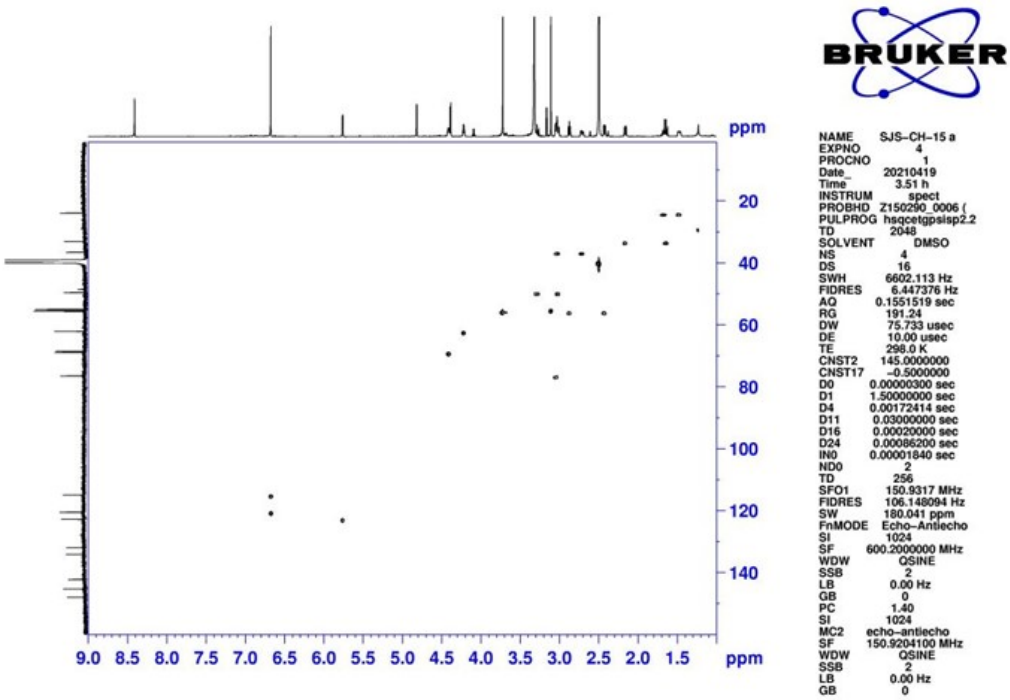

Figure S24. HSQC spectrum of compound **3** (600 MHz, DMSO-d_6)

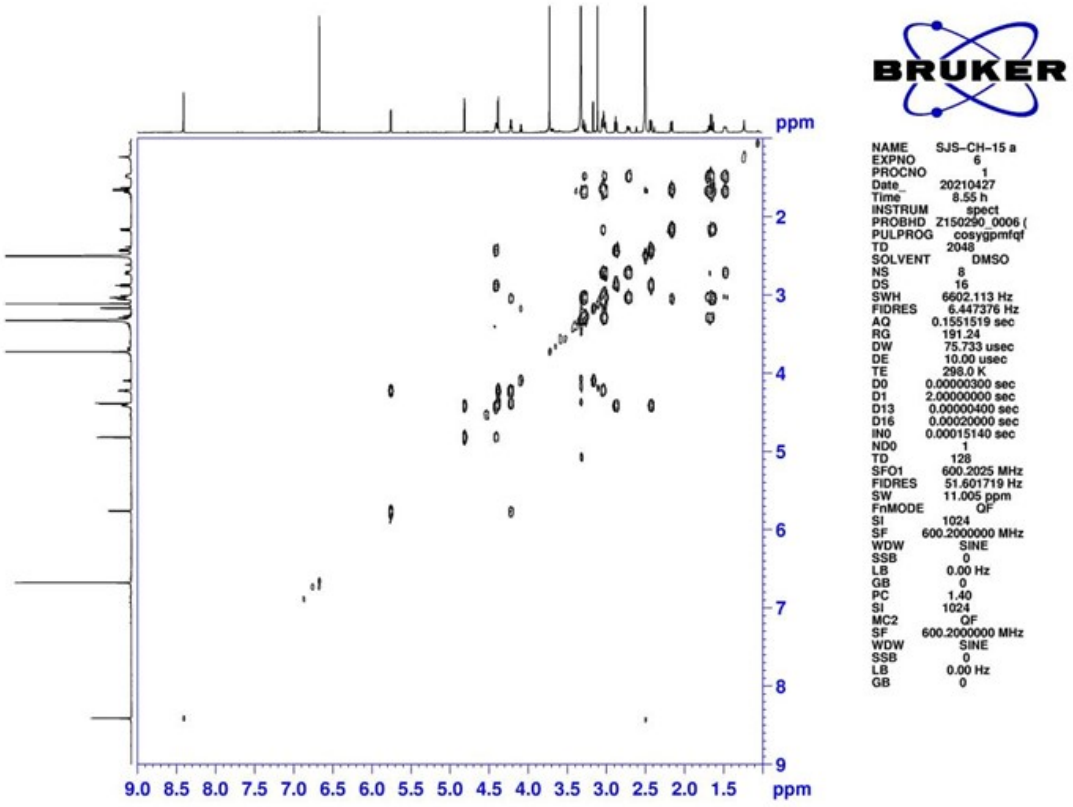

Figure S25. ^{1}H-^{1}H COSY spectrum of compound **3** (600 MHz, DMSO-d_6)

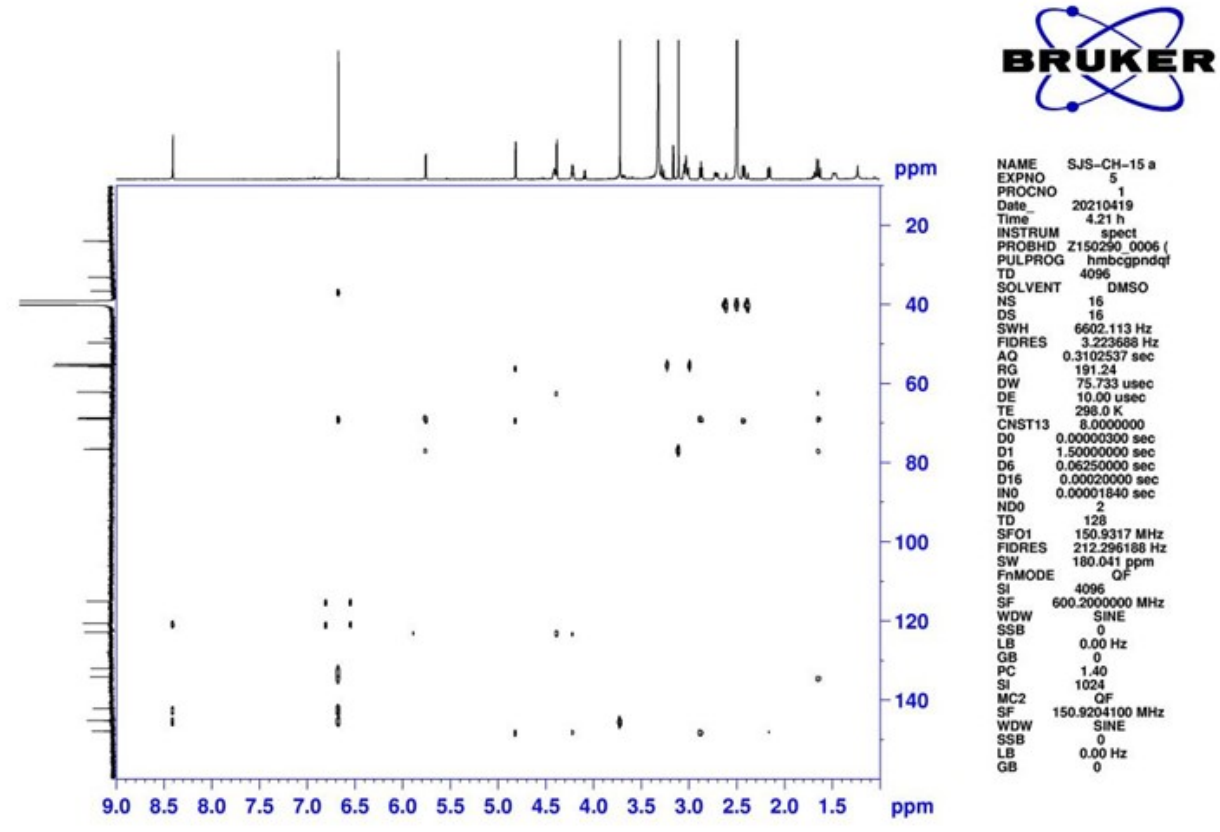

Figure S26. HMBC spectrum of compound **3** (600 MHz, DMSO-d_6)

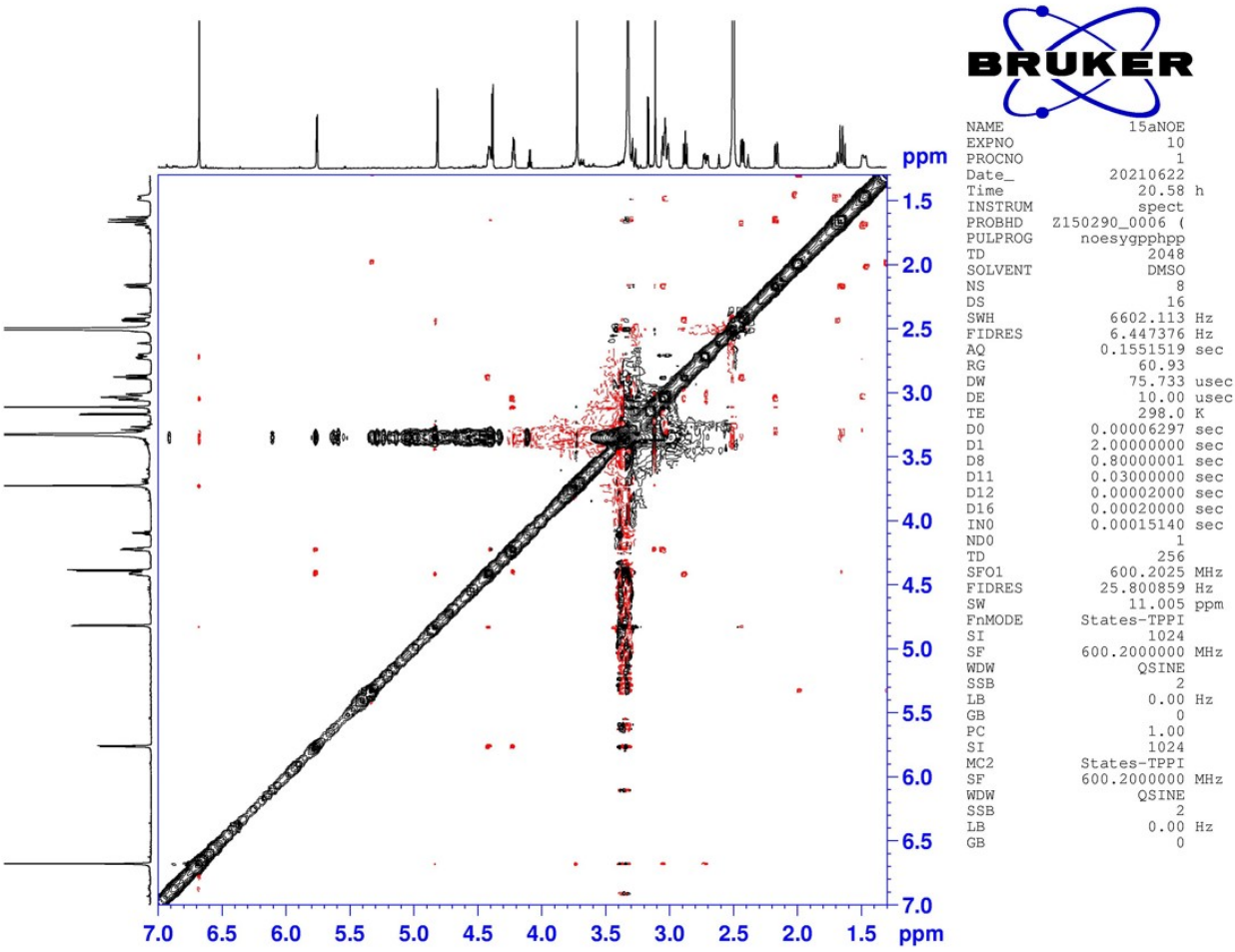

Figure S27. NOESY spectrum of compound **3** (600 MHz, DMSO-d_6)

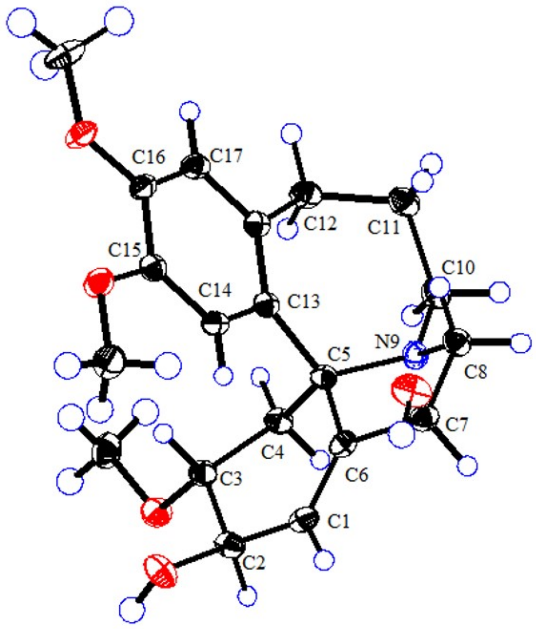

Figure S28. ORTEP drawing of compound **6**

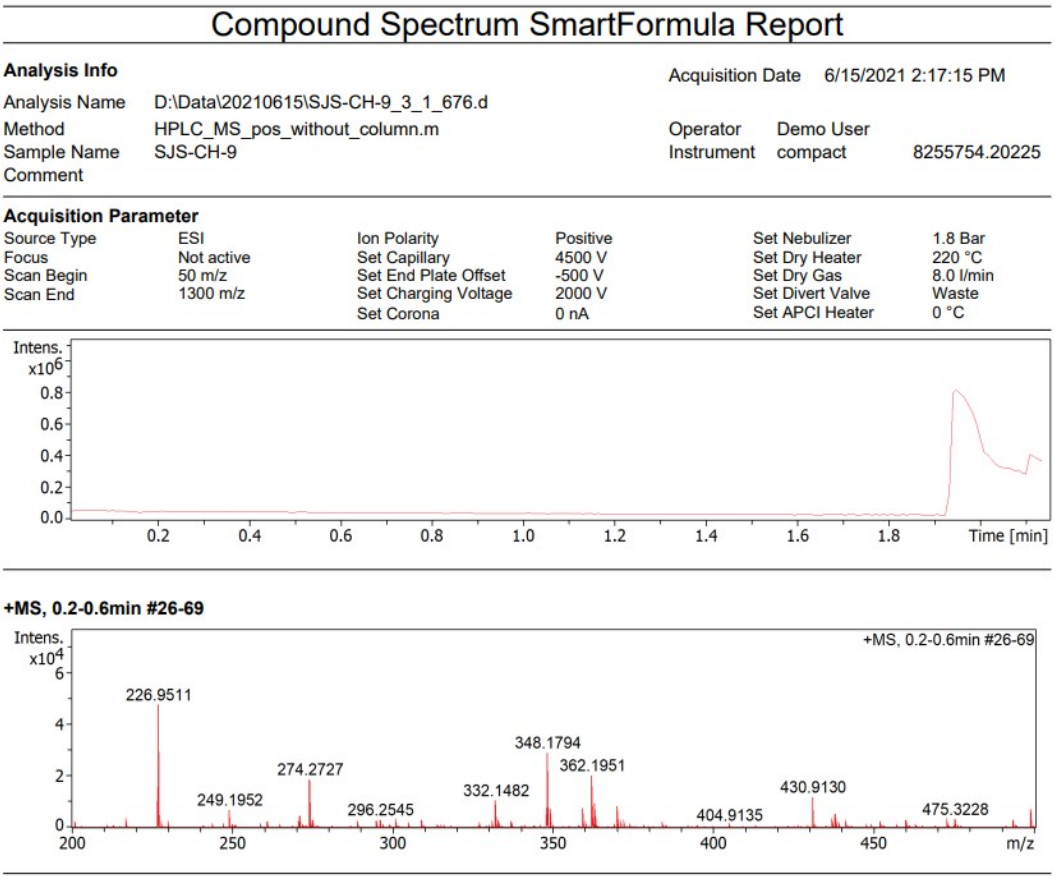

Figure S29. HRESIMS spectrum of **6**

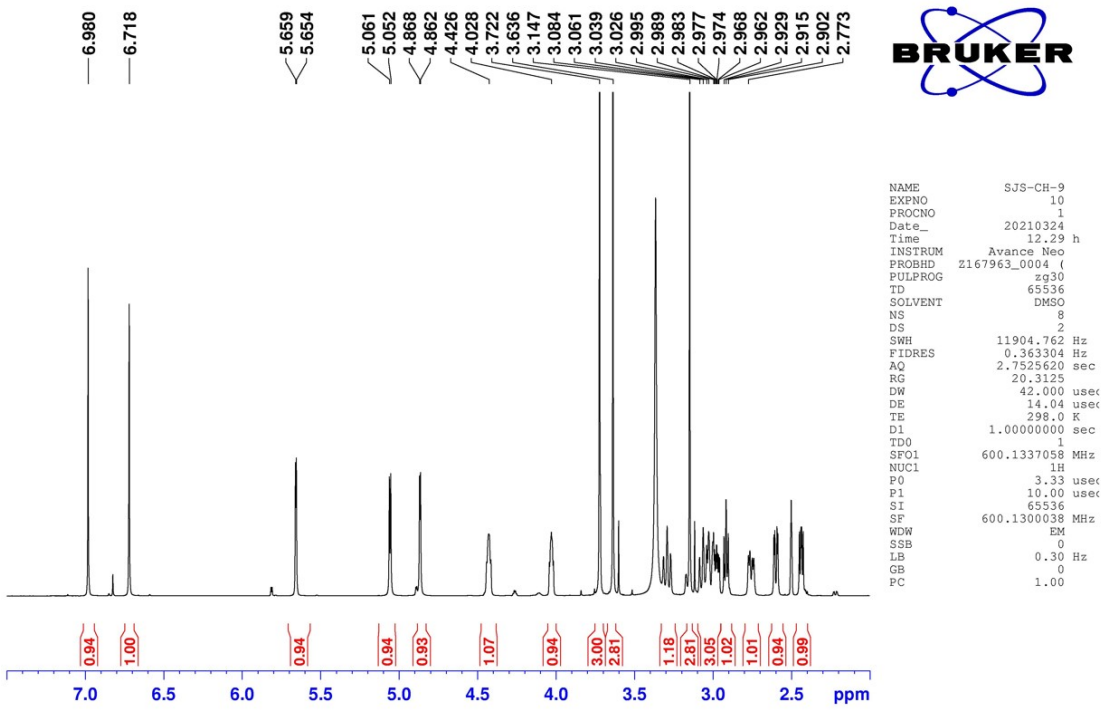

Figure S30. ^{1}H NMR spectrum of compound **6** (600 MHz, DMSO-d_6)

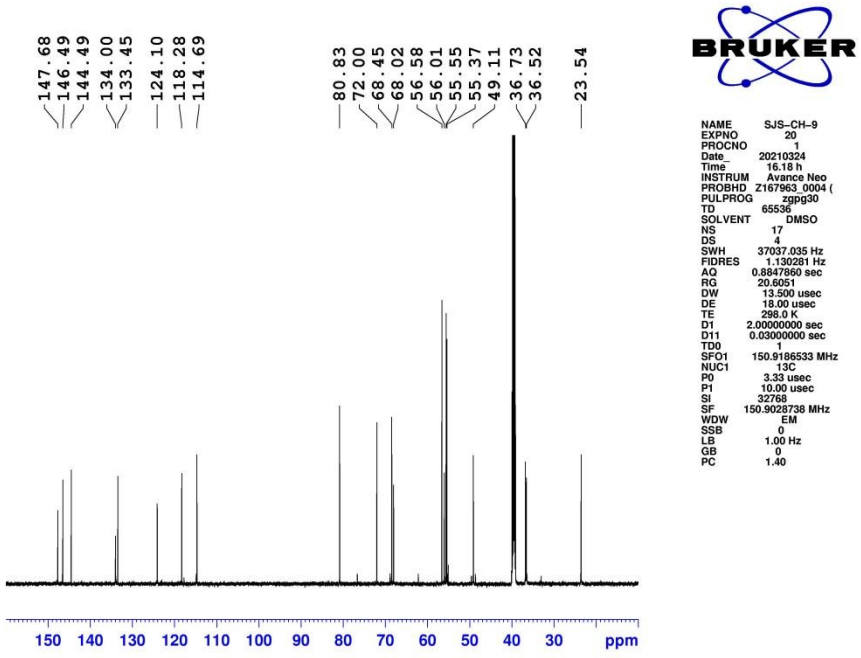

Figure S31. ^{13}C NMR spectrum of compound **6** (600 MHz, DMSO-d_6)

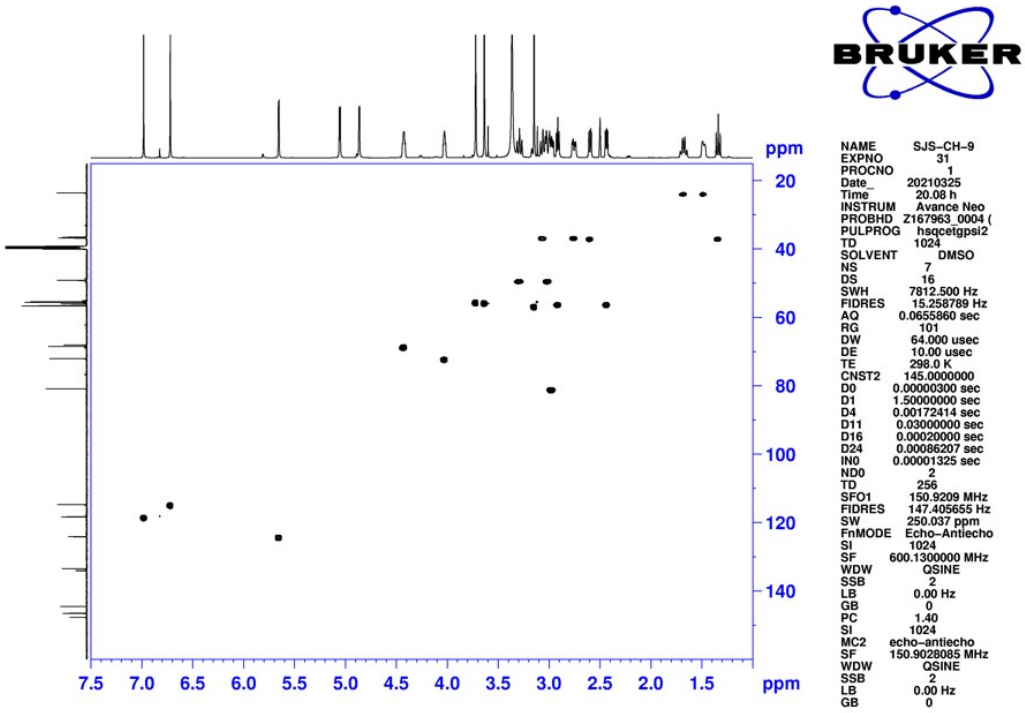

Figure S32. HSQC spectrum of compound **6**

Elemental Composition Report **Page 1**

Single Mass Analysis
Tolerance = 5.0 mDa / DBE: min = -1.5, max = 50.0
Element prediction: Off
Number of isotope peaks used for i-FIT = 3

Monoisotopic Mass, Even Electron Ions
136 formula(e) evaluated with 1 results within limits (up to 50 best isotopic matches for each mass)
Elements Used:
C: 17-17 H: 0-880 N: 0-7 O: 0-200
SZJ-D-12 86 (0.492)
1: TOF MS ES+

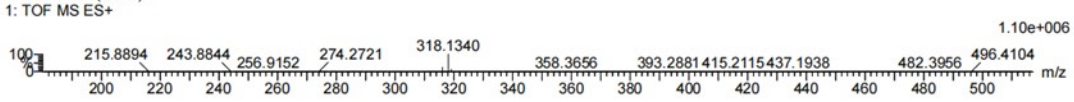

Minimum:				-1.5				
Maximum:		5.0	10.0	50.0				
Mass	Calc. Mass	mDa	PPM	DBE	i-FIT	Norm	Conf(%)	Formula
318.1340	318.1341	-0.1	-0.3	8.5	658.2	n/a	n/a	C17 H20 N O5

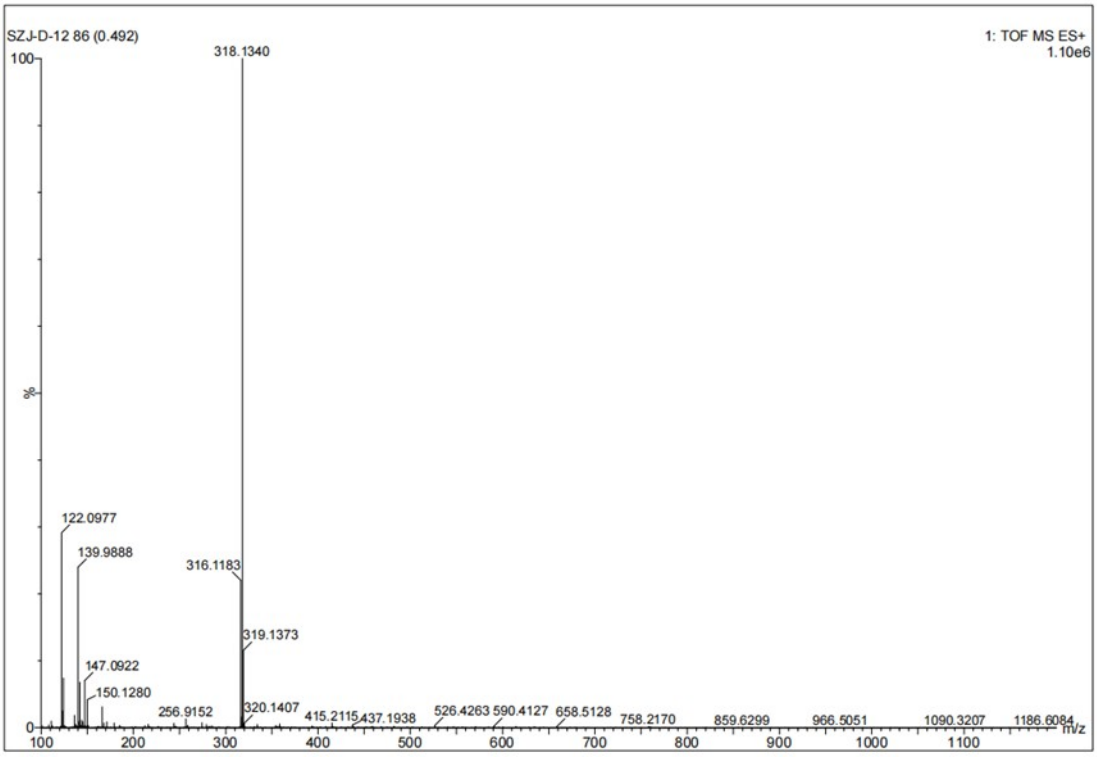

Figure S33. HRESIMS spectrum of **11**

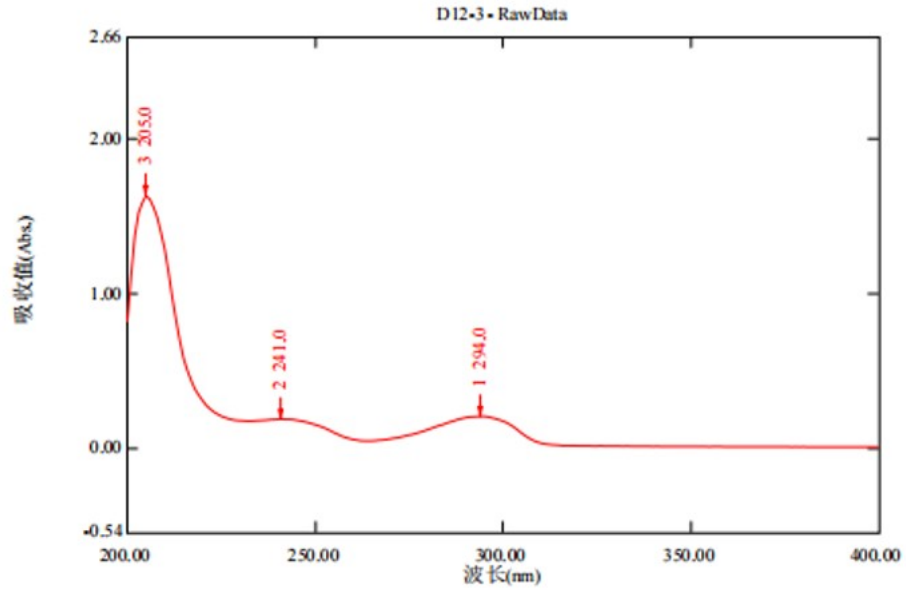

Figure S34. UV spectrum of **11**

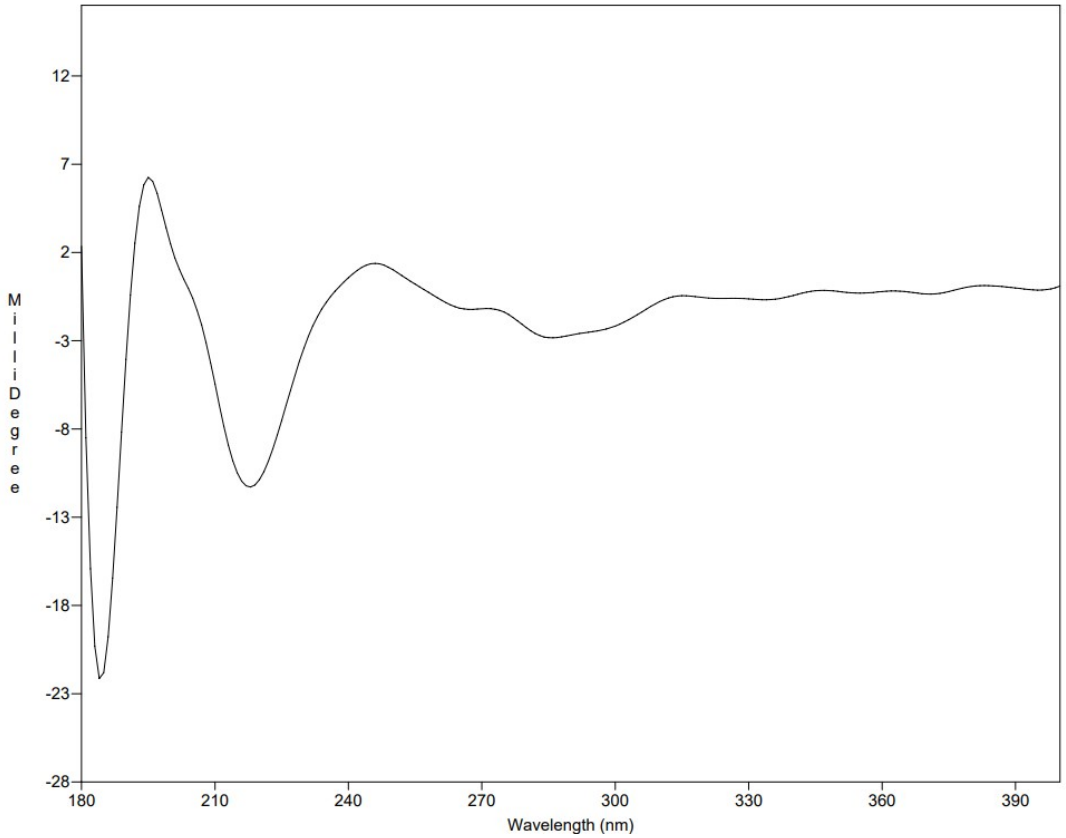

Figure S35. Experimental ECD spectrum of **11**

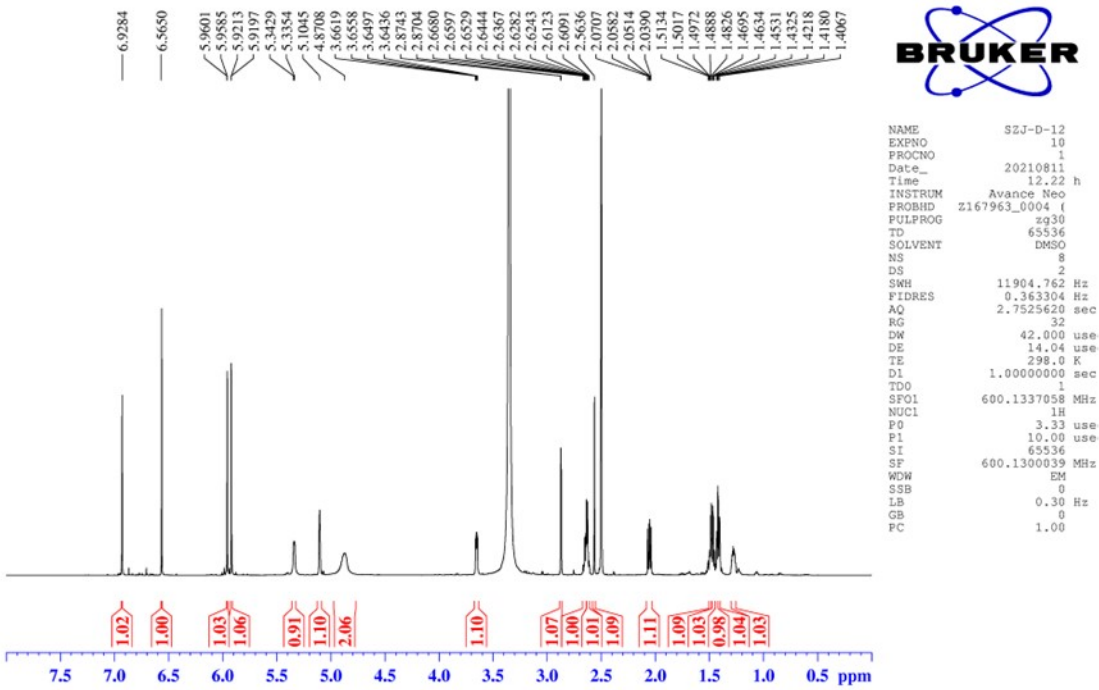

Figure S36. ^{1}H NMR spectrum of compound **11** (600 MHz, DMSO-d_6)

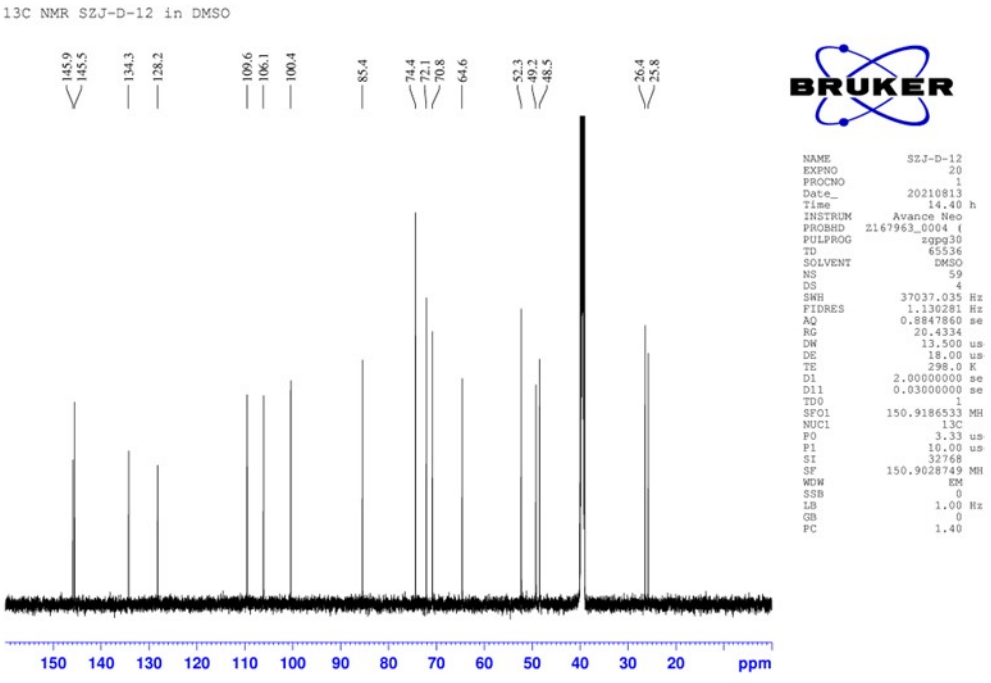

Figure S37. ^{13}C NMR spectrum of compound **11** (150 MHz, DMSO-d_6)

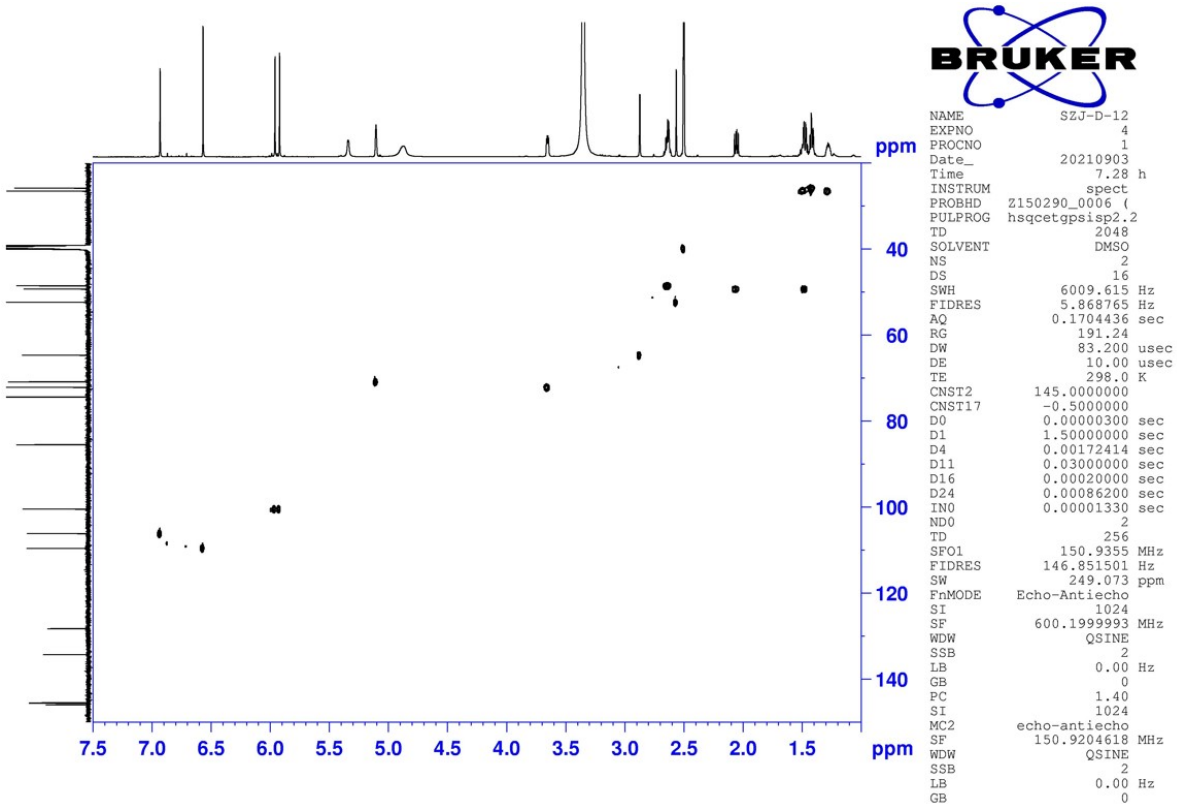

Figure S38. HSQC spectrum of compound **11** (600 MHz, DMSO-d_6)

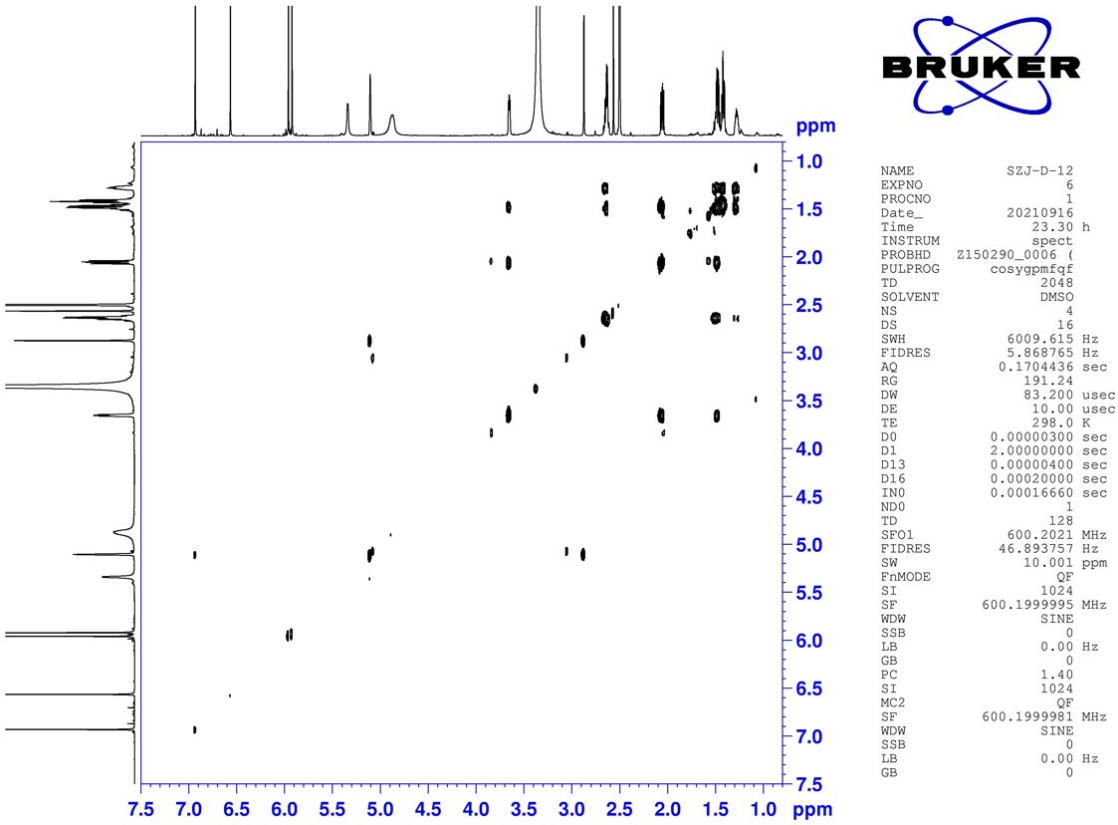

Figure S39. ^{1}H-^{1}H COSY spectrum of compound **11** (600 MHz, DMSO-d_6)

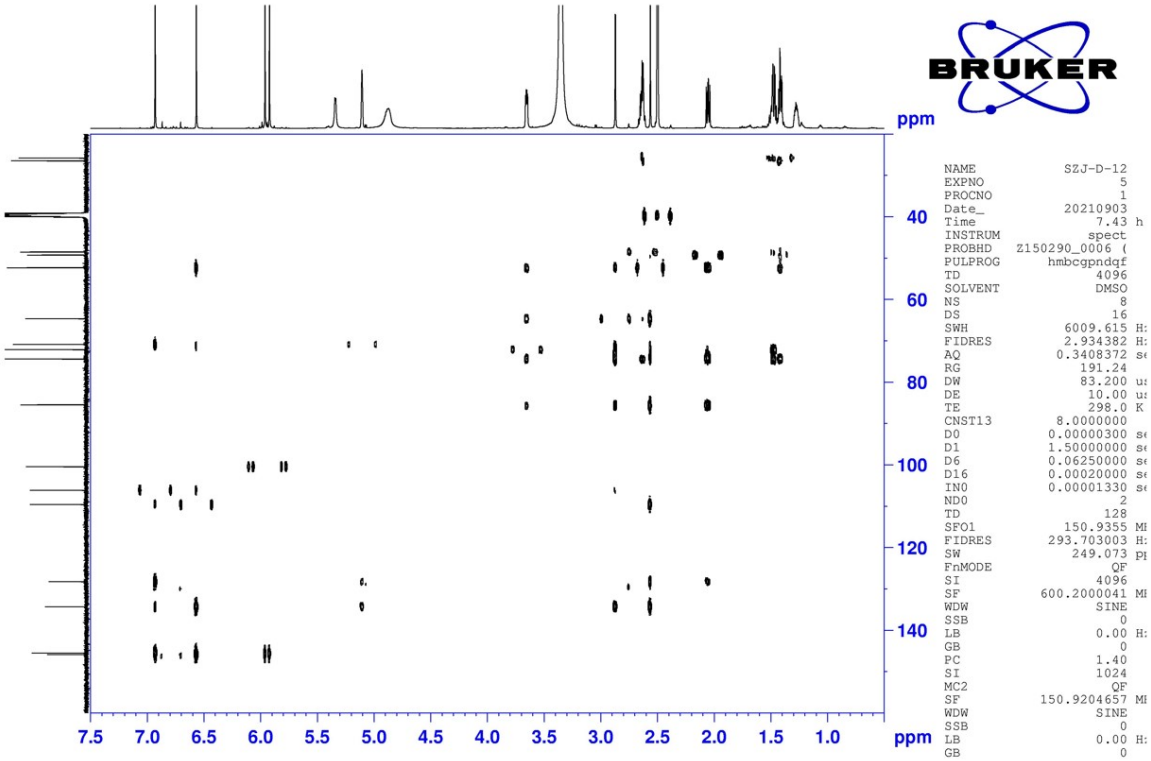

Figure S40. HMBC spectrum of compound **11** (600 MHz, DMSO-d_6)

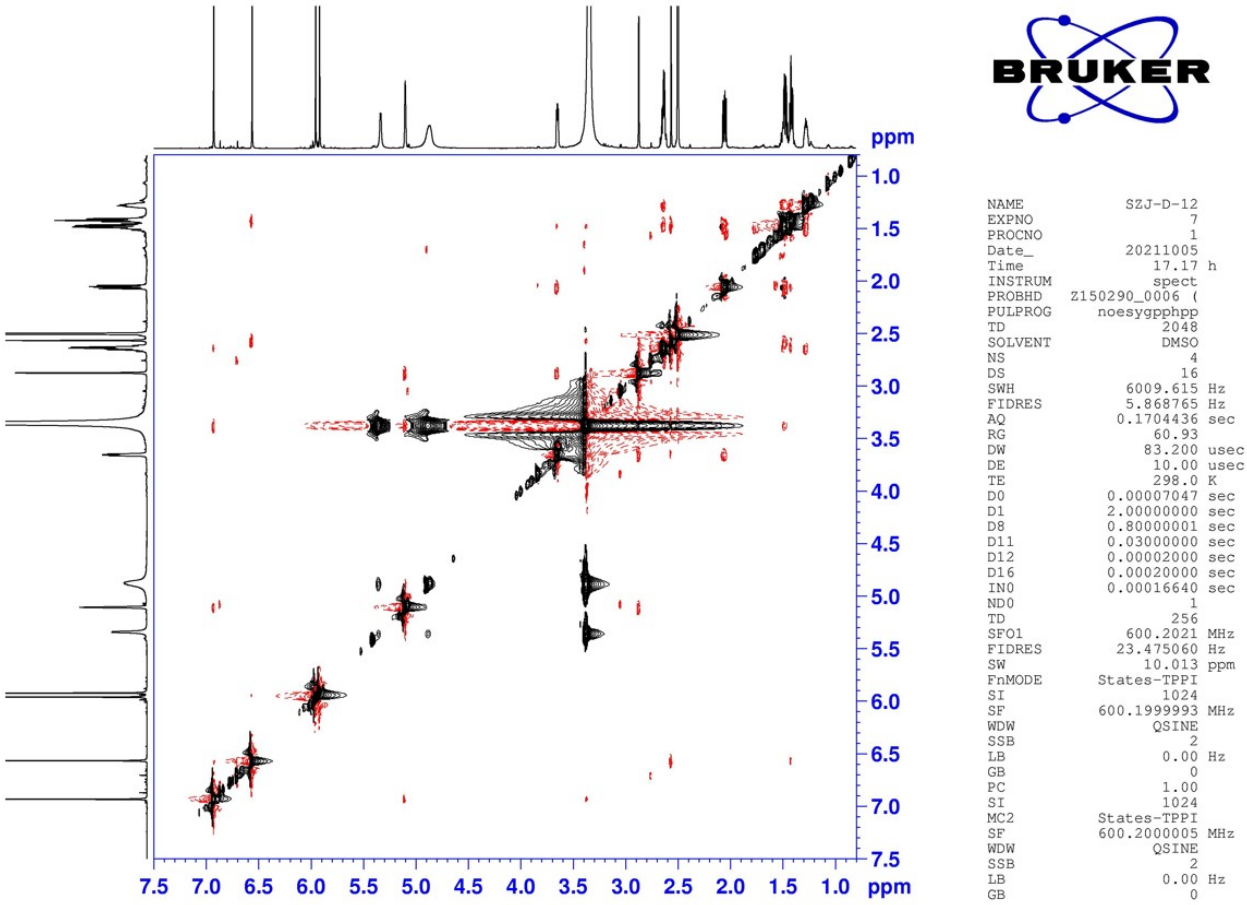

Figure S41. NOESY spectrum of compound **11** (600 MHz, DMSO-d_6)

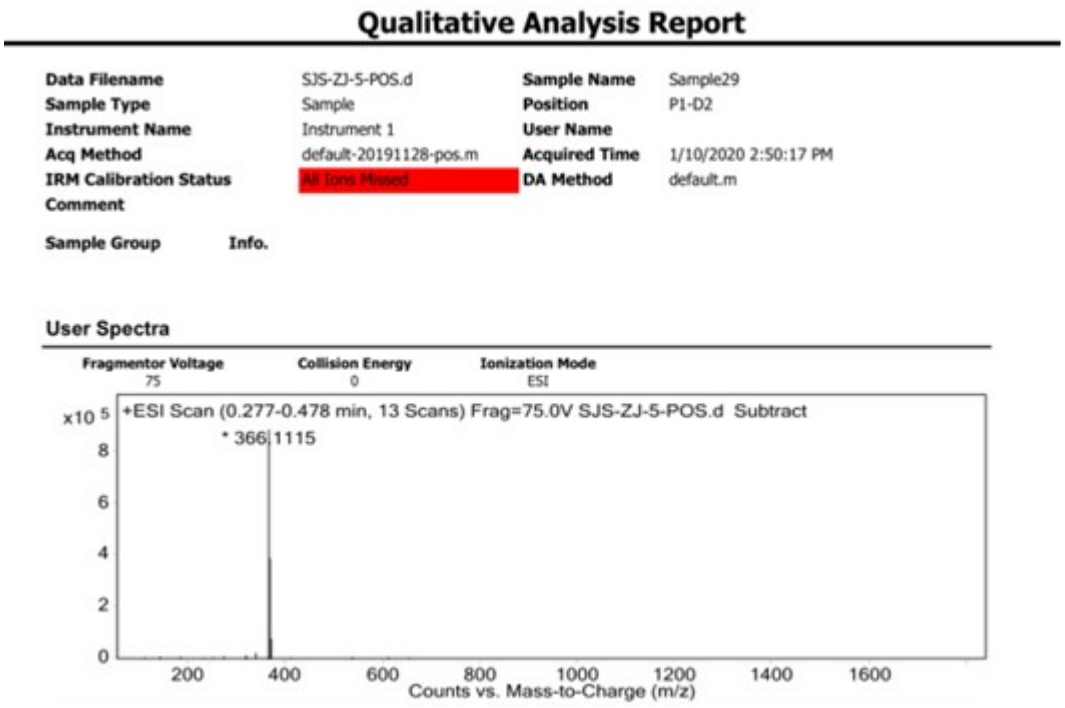

Figure S42. HRESIMS spectrum of **13**

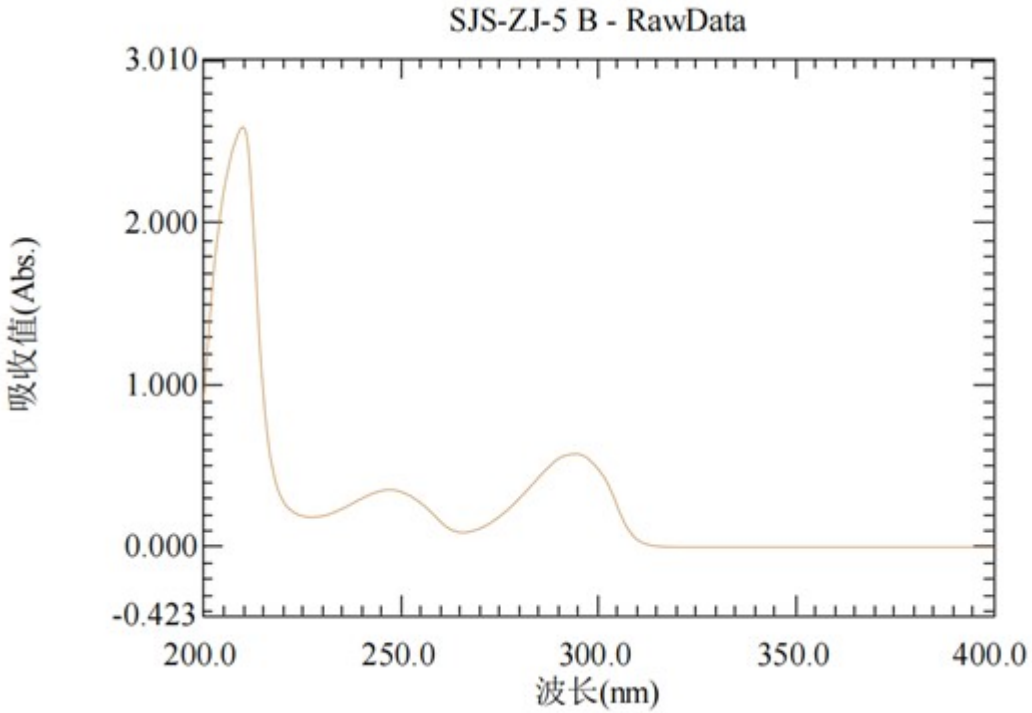

Figure S43. UV spectrum of compound **13**

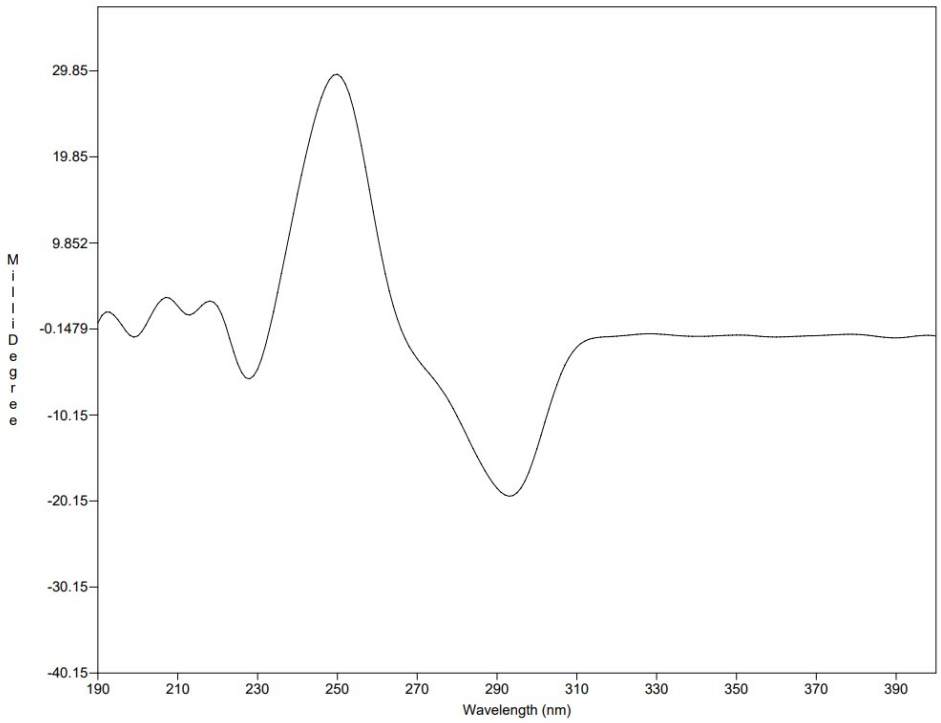

Figure S44. Experimental ECD spectrum of **13**

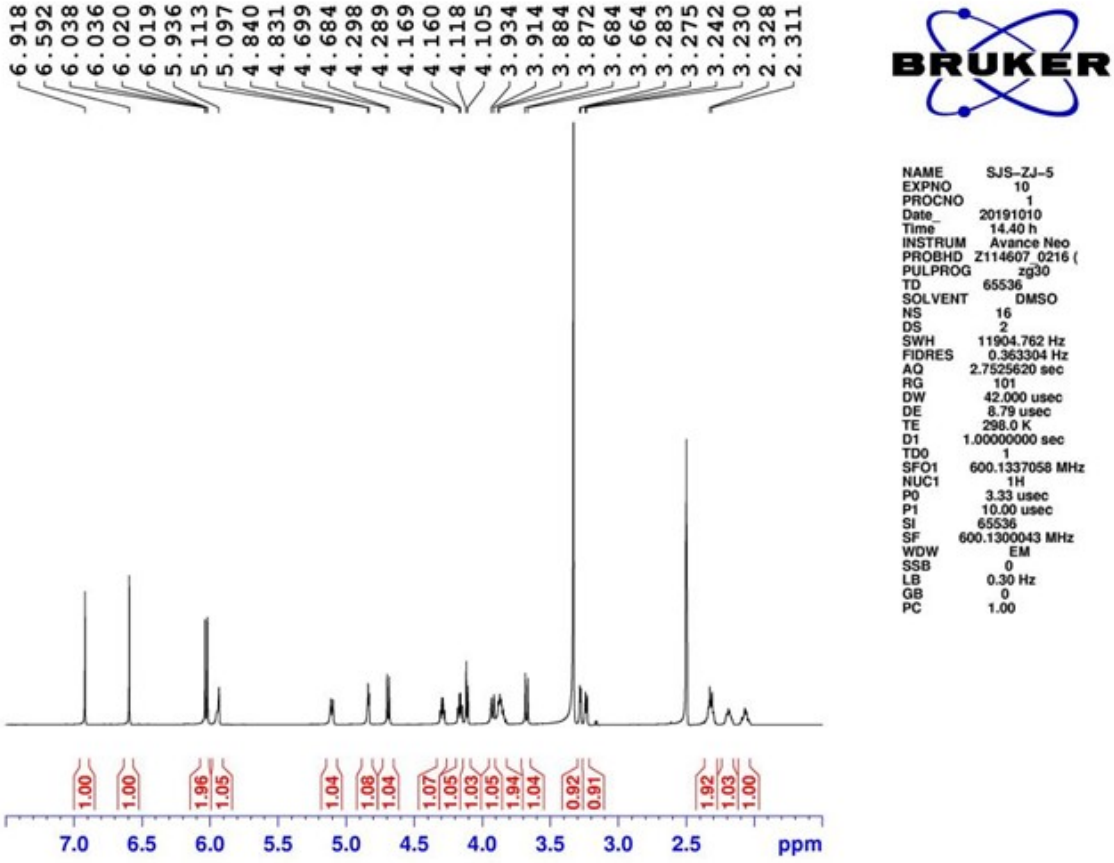

Figure S45. ^{1}H NMR spectrum of compound **13** (600 MHz, DMSO-d_6)

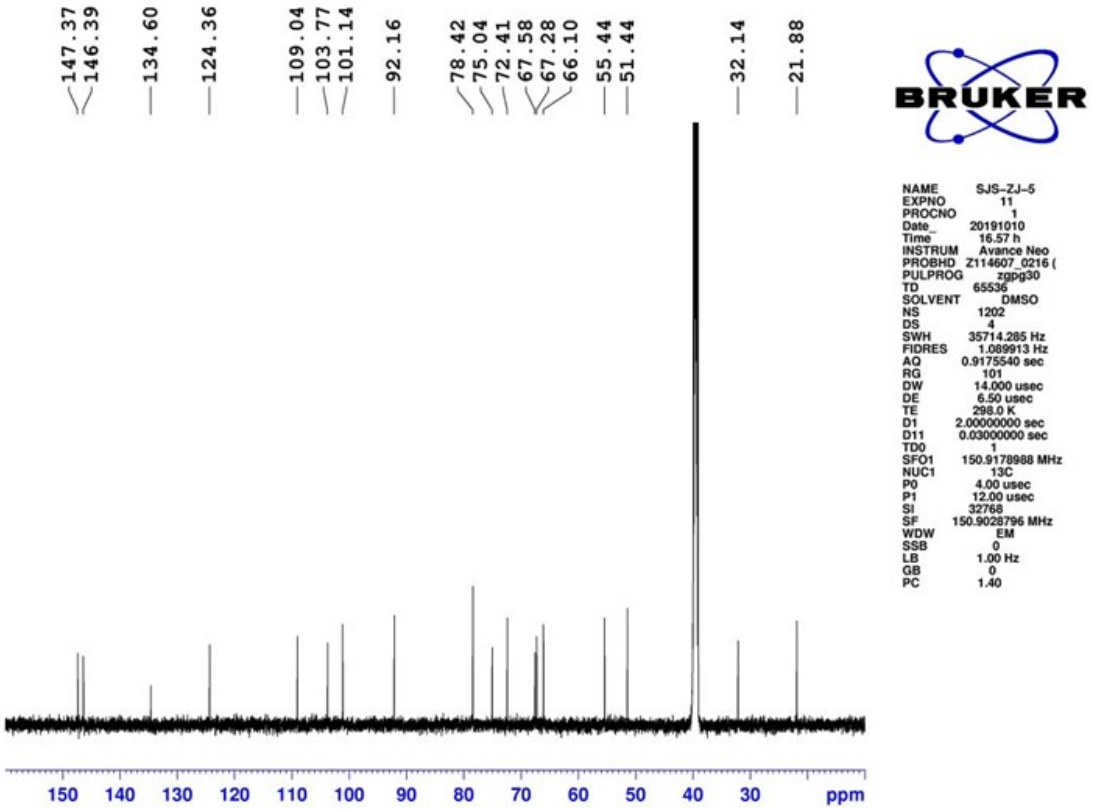

Figure S46. ^{13}C NMR spectrum of compound **13** (150 MHz, DMSO-d_6)

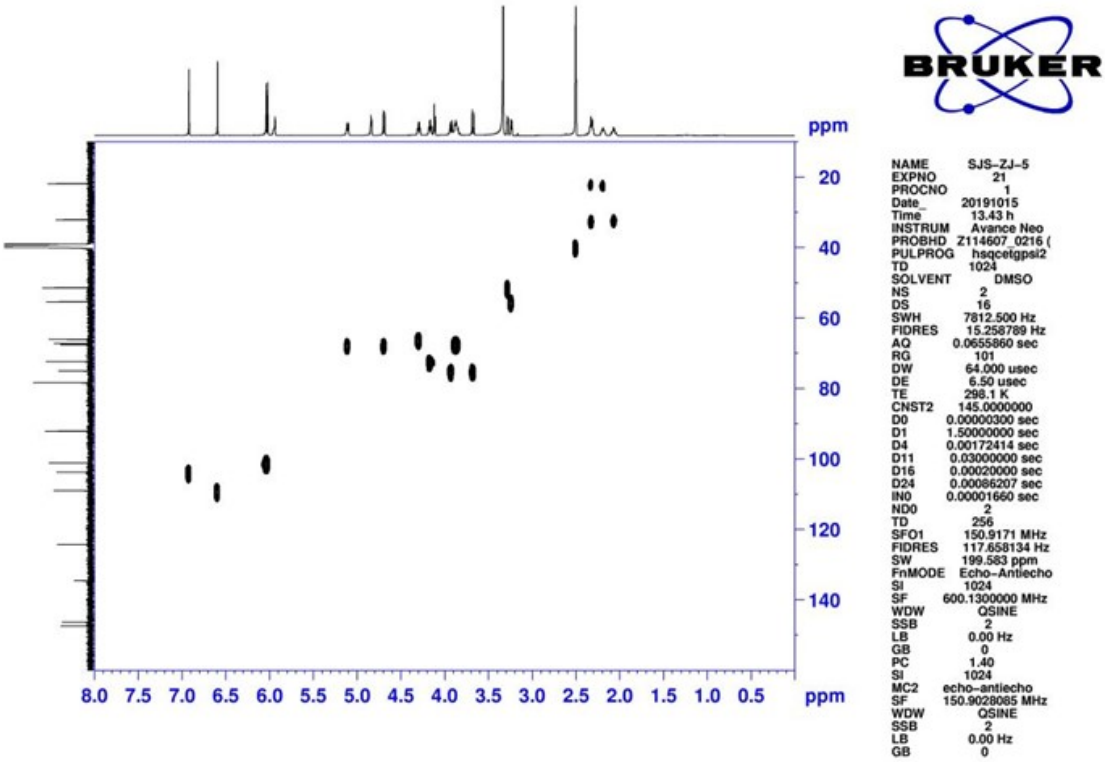

Figure S47. HSQC spectrum of compound **13** (600 MHz, DMSO-d_6)

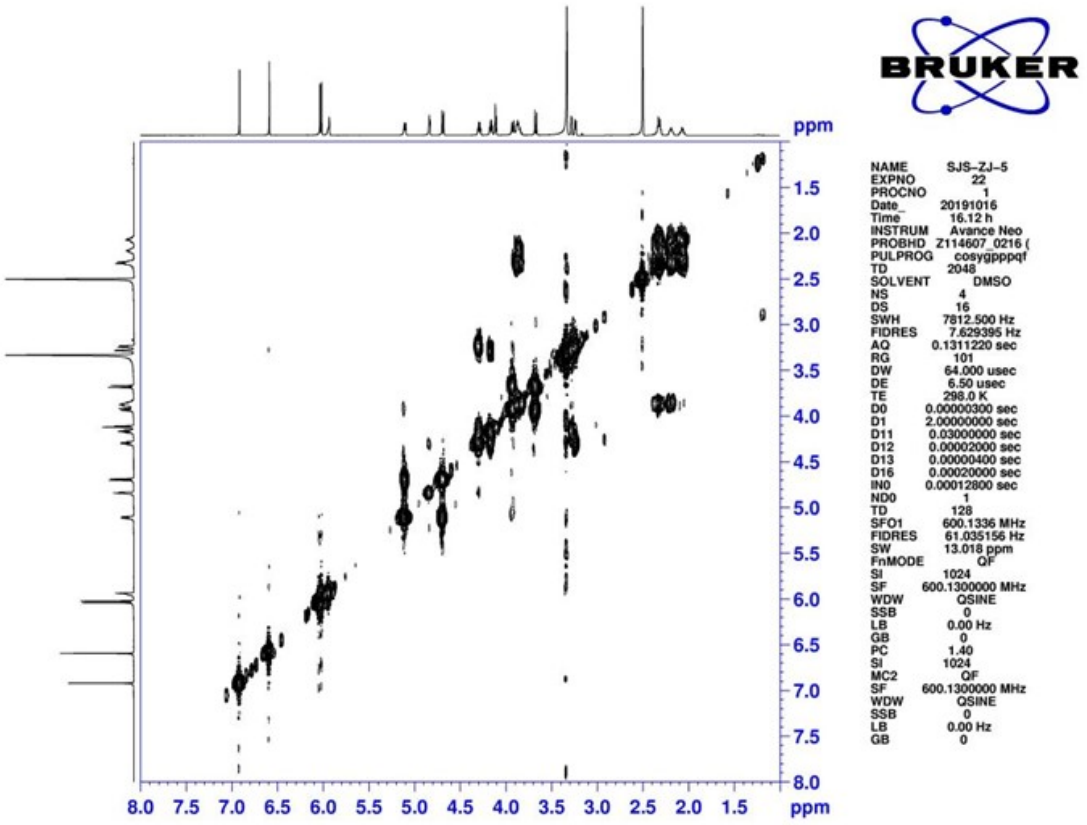

Figure S48. ^{1}H-^{1}H COSY spectrum of compound **13** (600 MHz, DMSO-d_6)

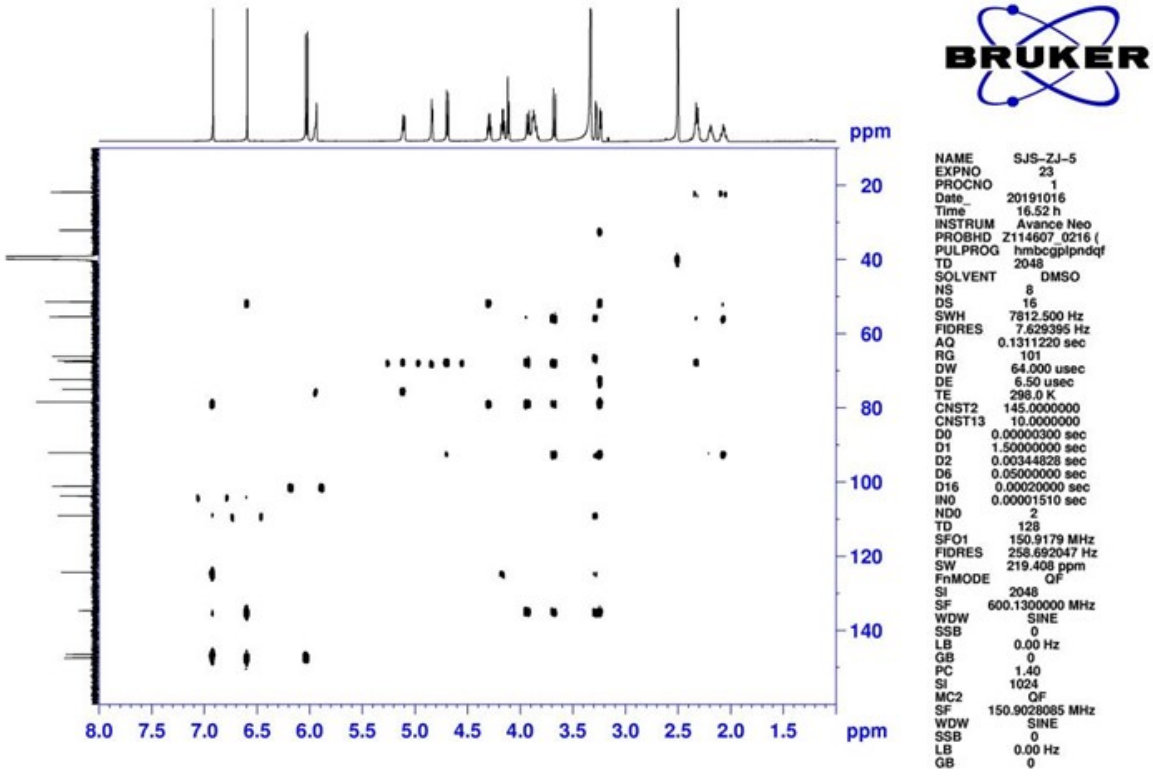

Figure S49. HMBC spectrum of compound **13** (600 MHz, DMSO-d_6)

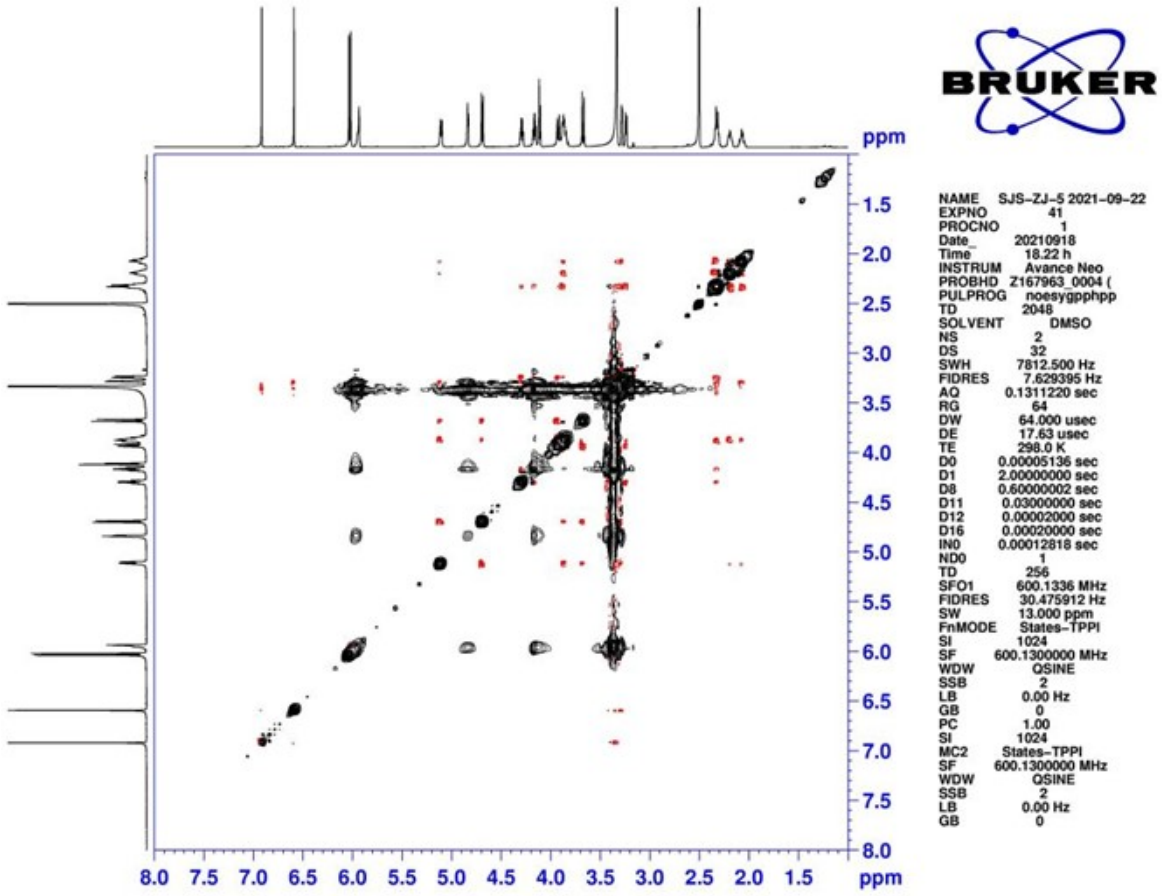

Figure S50. NOESY spectrum of compound **13** (600 MHz, DMSO-d_6)

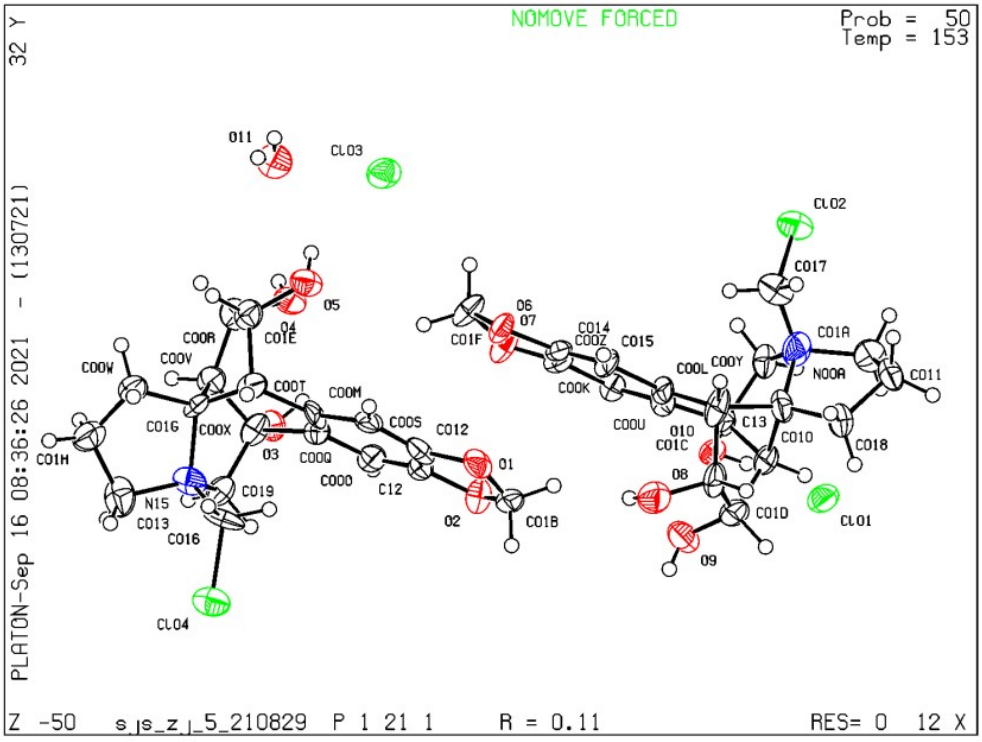

Figure S51. ORTEP drawing of compound **13**

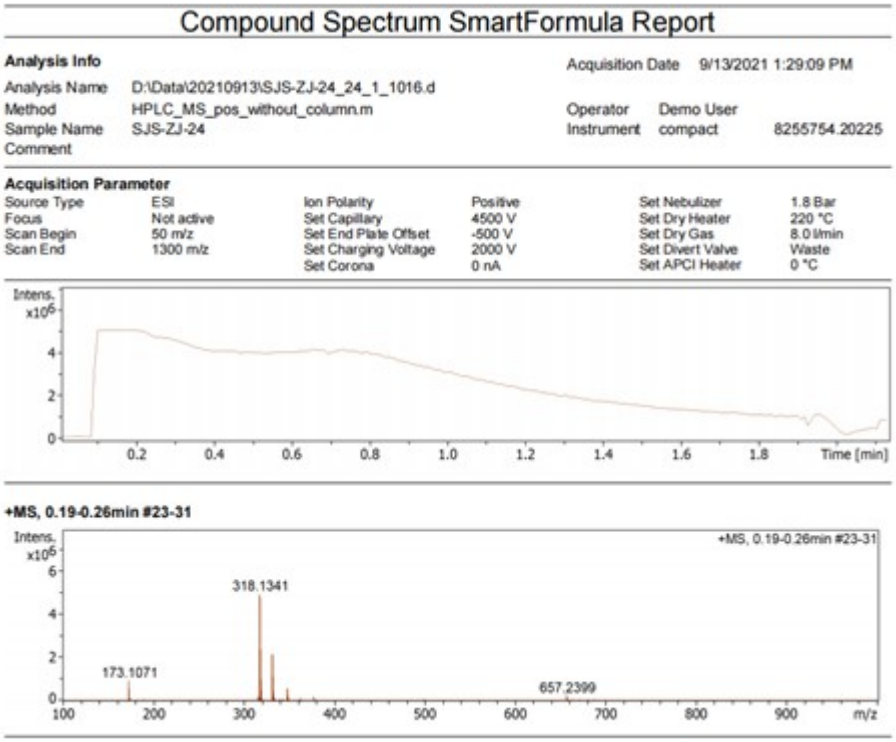

Figure S52. HRESIMS date of **14**

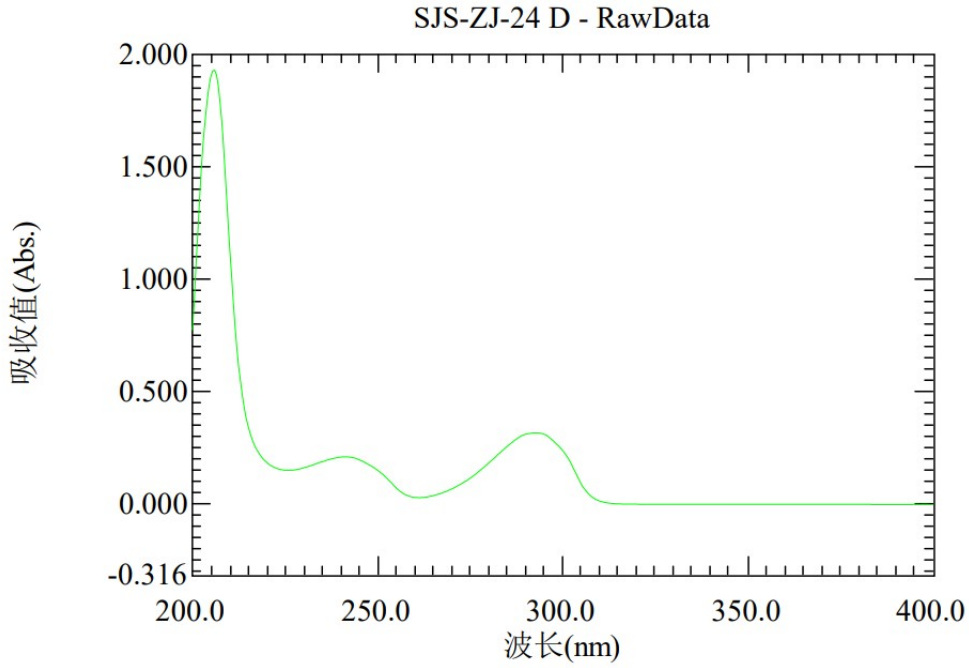

Figure S53. UV spectrum of **14**

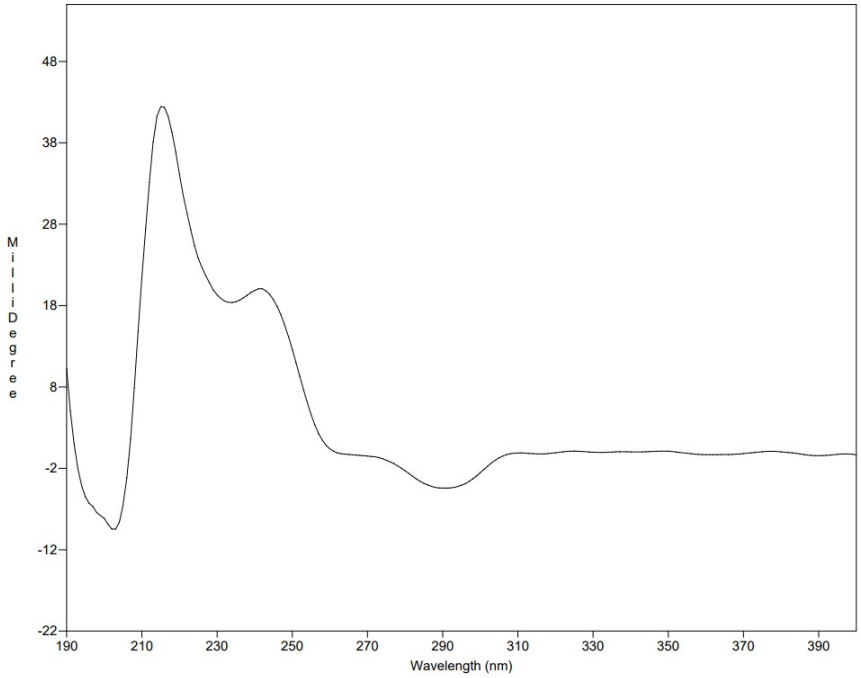

Figure S54. Experimental ECD spectrum of **14**

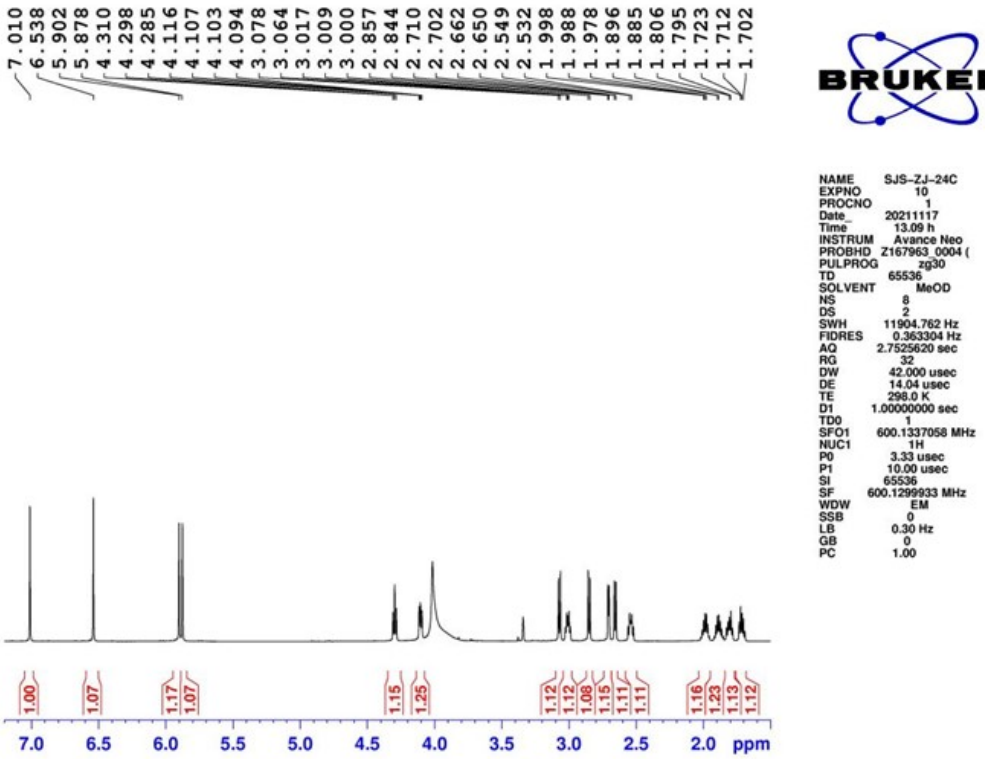

Figure S55. ^{1}H NMR spectrum of compound **14** ($CDCl_3$/CD_3OD (4:1) at 310 K)

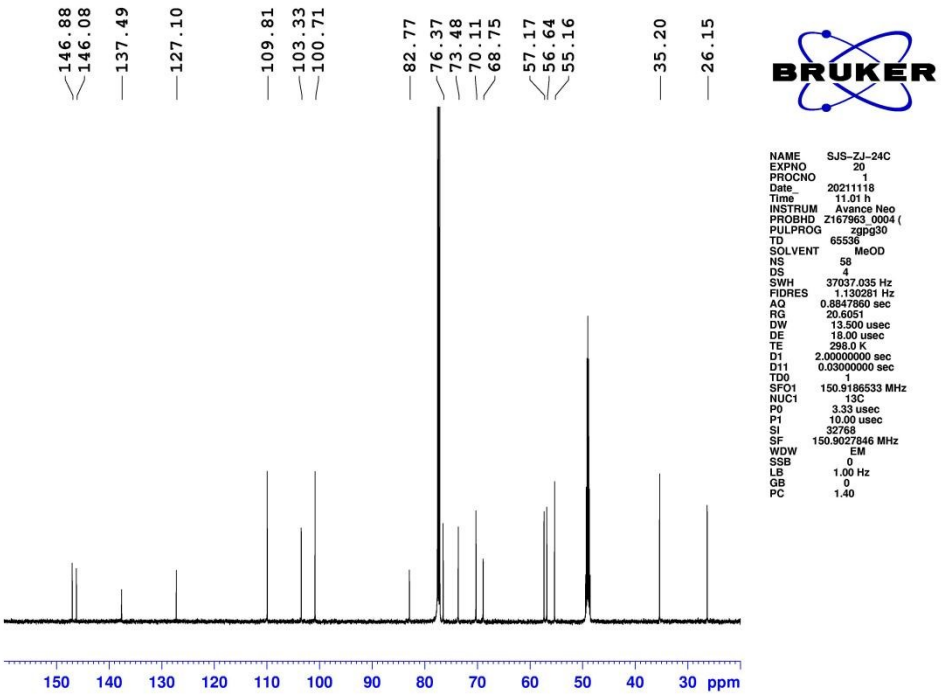

Figure S56. ^{13}C NMR spectrum of compound **14** ($CDCl_3/CD_3OD$ (4:1) at 310 K)

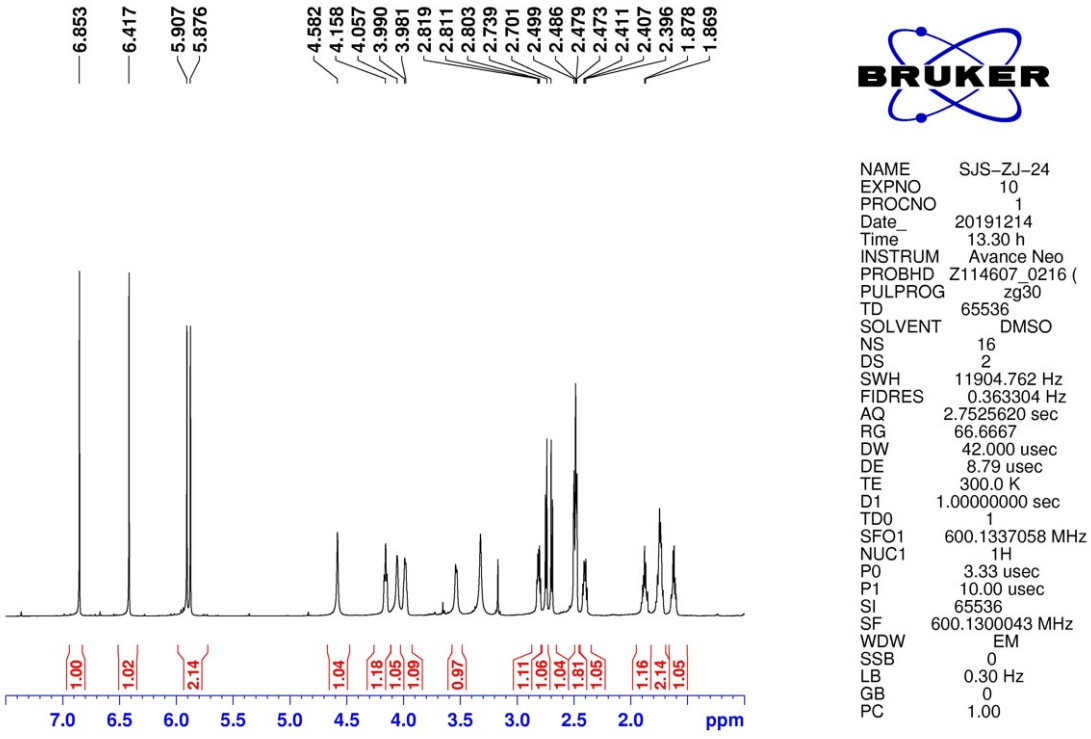

Figure S57. ^{1}H NMR spectrum of compound **14** (600 MHz, DMSO-d_6)

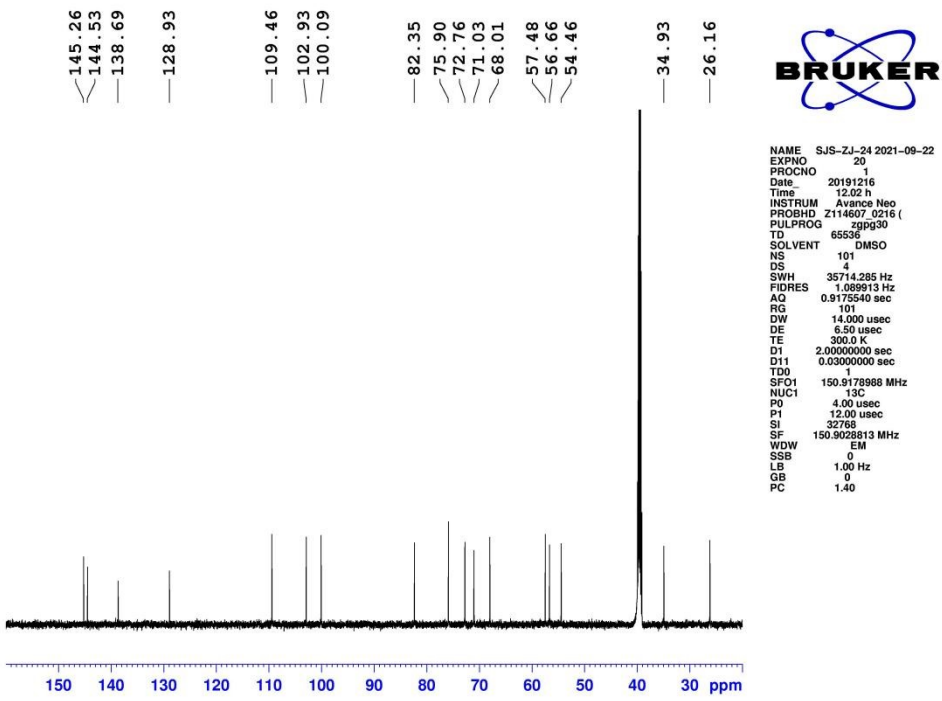

Figure S58. ^{13}C NMR spectrum of compound **14** (150 MHz, DMSO-d_6)

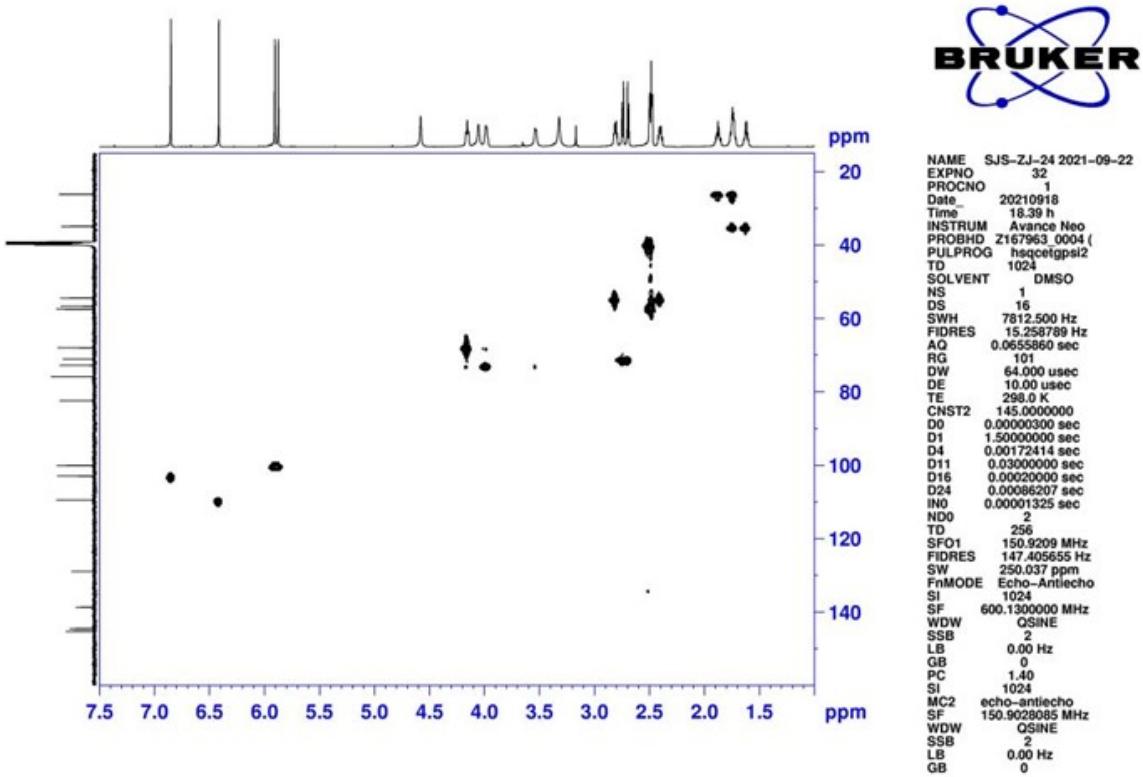

Figure S59. HSQC spectrum of compound **14** (600 MHz, DMSO-d_6)

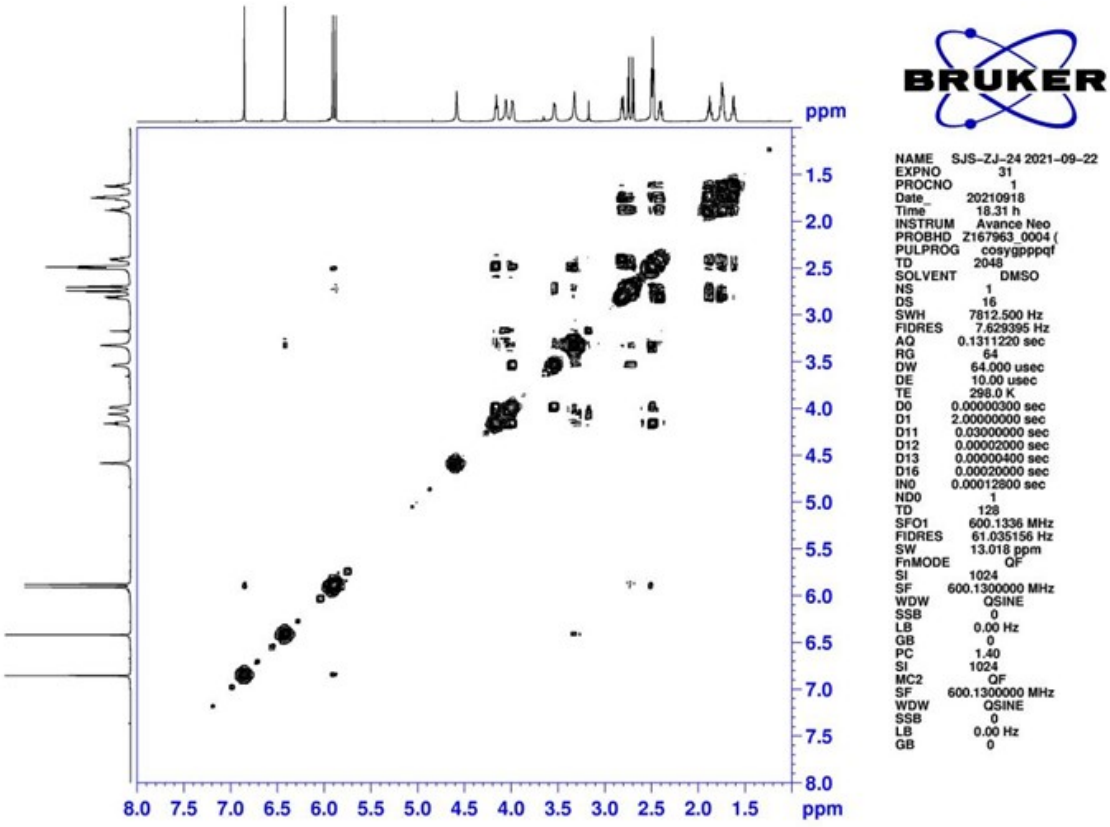

Figure S60. ^{1}H-^{1}H COSY spectrum of compound **14** (600 MHz, DMSO-d_6)

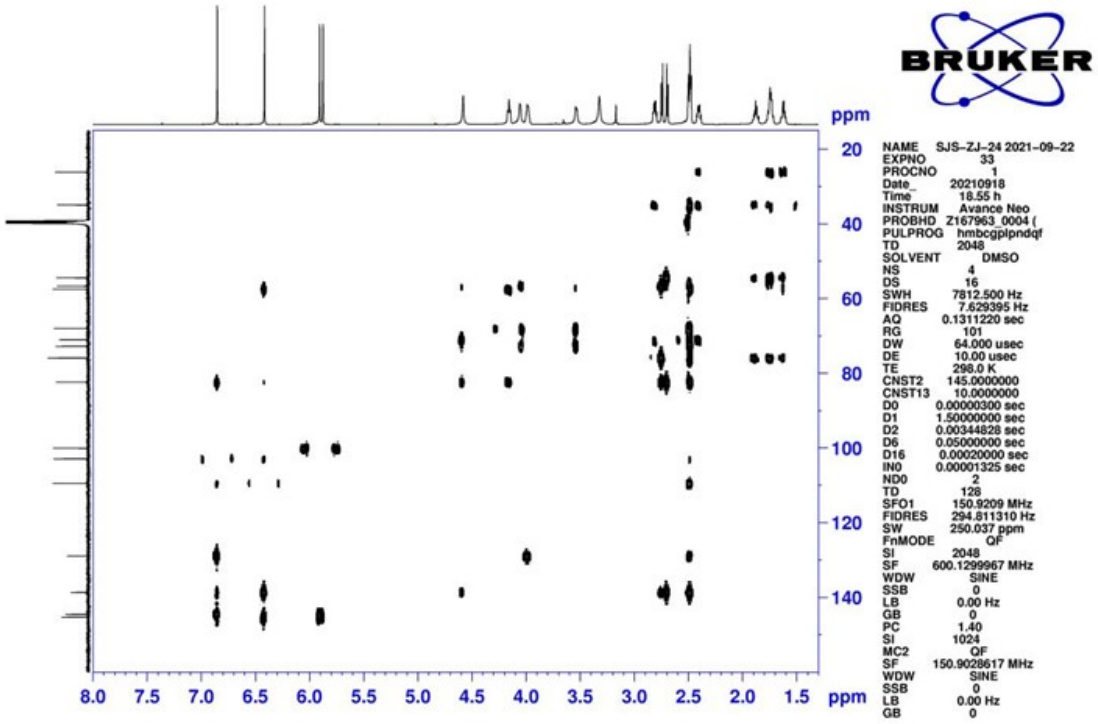

Figure S61. HMBC spectrum of compound **14** (600 MHz, DMSO-d_6)

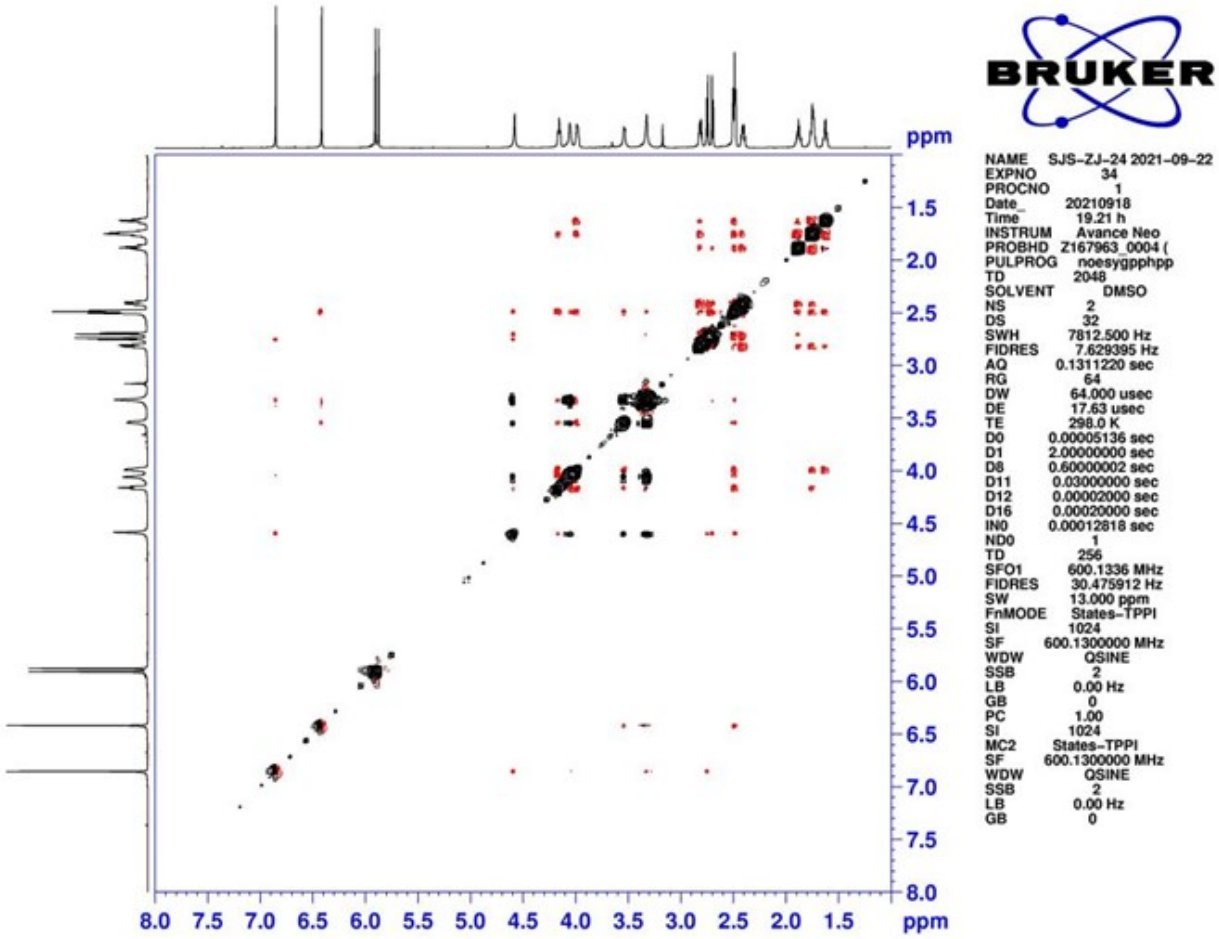

Figure S62. NOESY spectrum of compound **14** (600 MHz, DMSO-d_6)

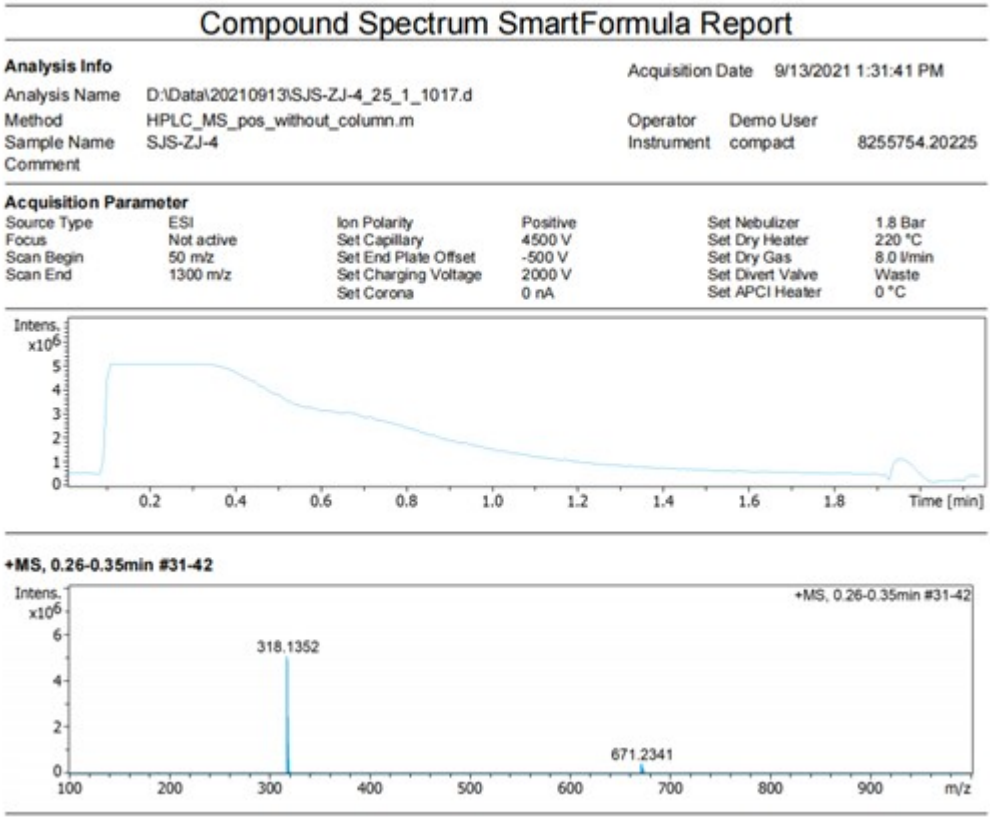

Figure S63. HRESIMS spectrum of **14a**

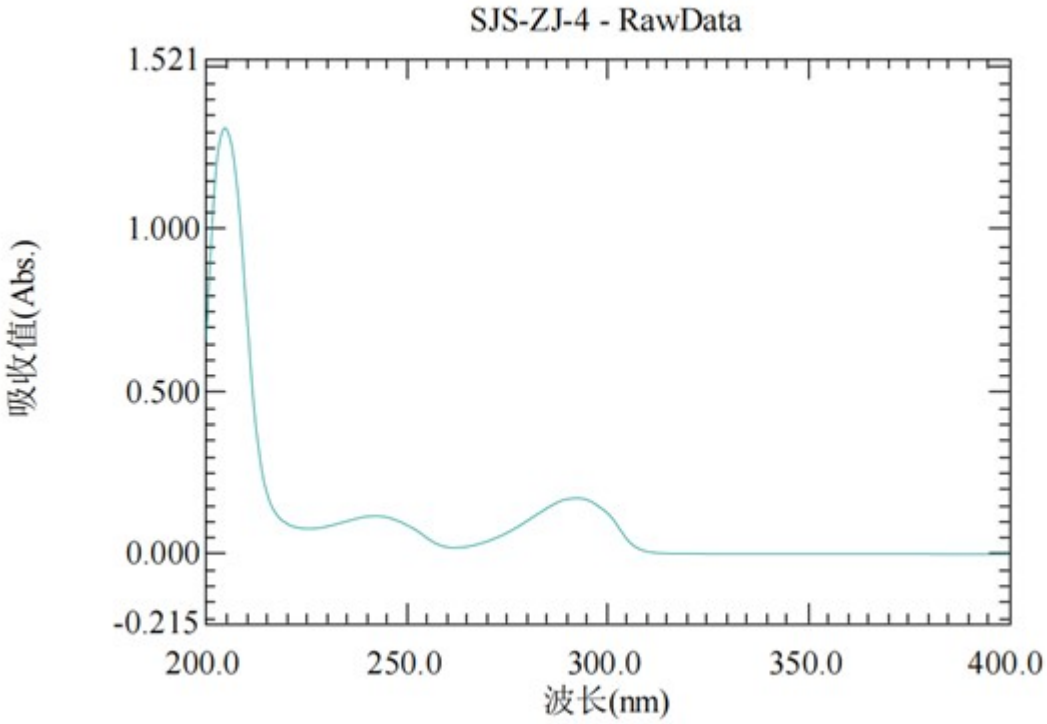

Figure S64. UV spectrum of **14a**

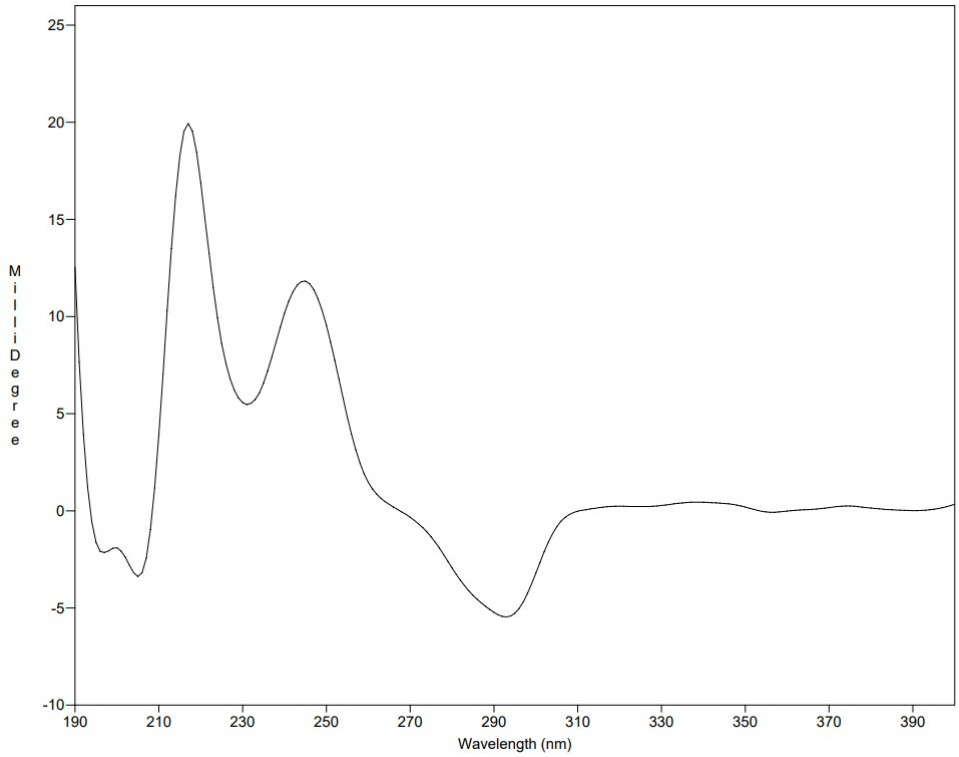

Figure S65. Experimental ECD spectrum of **14a**

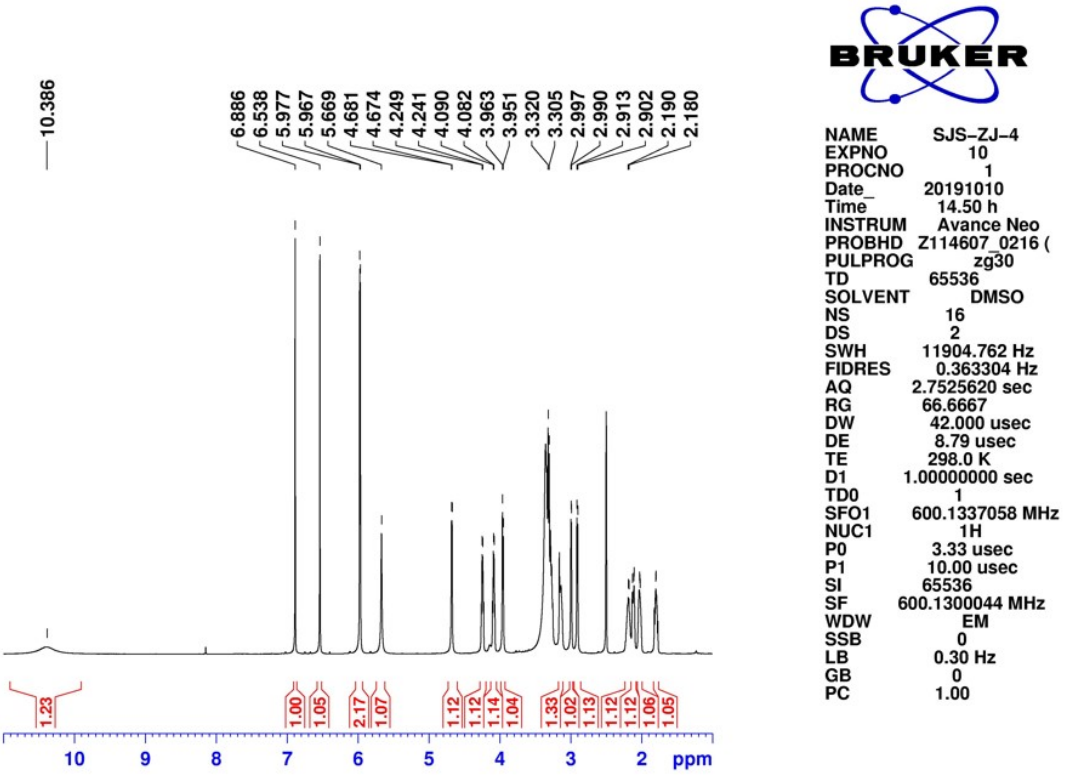

Figure S66. ^{1}H NMR spectrum of compound **14a** (600 MHz, DMSO-d_6)

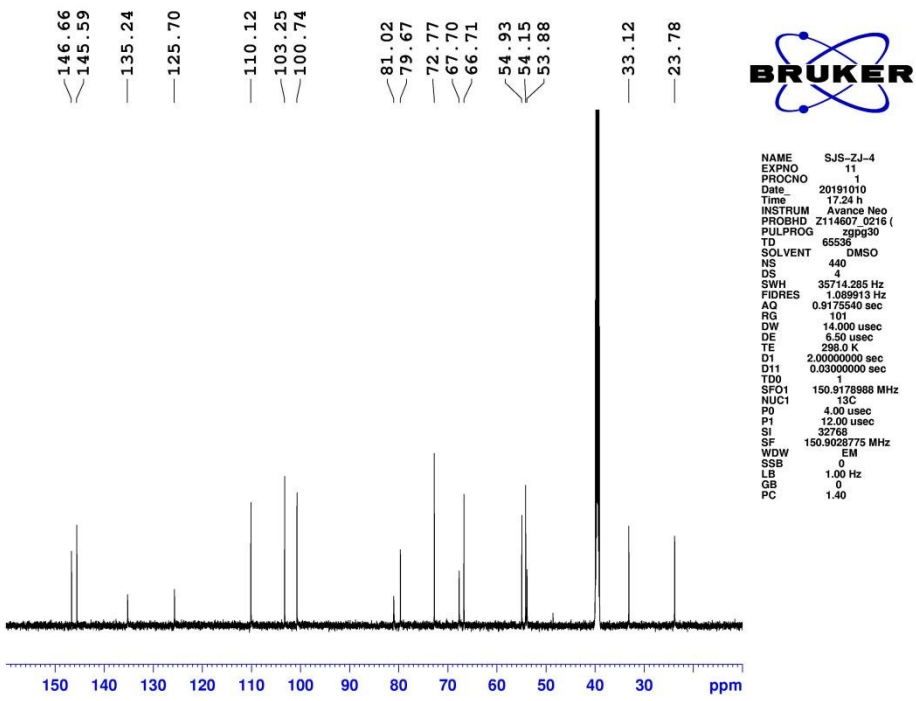

Figure S67. ^{13}C NMR spectrum of compound **14a** (150 MHz, DMSO-d_6)

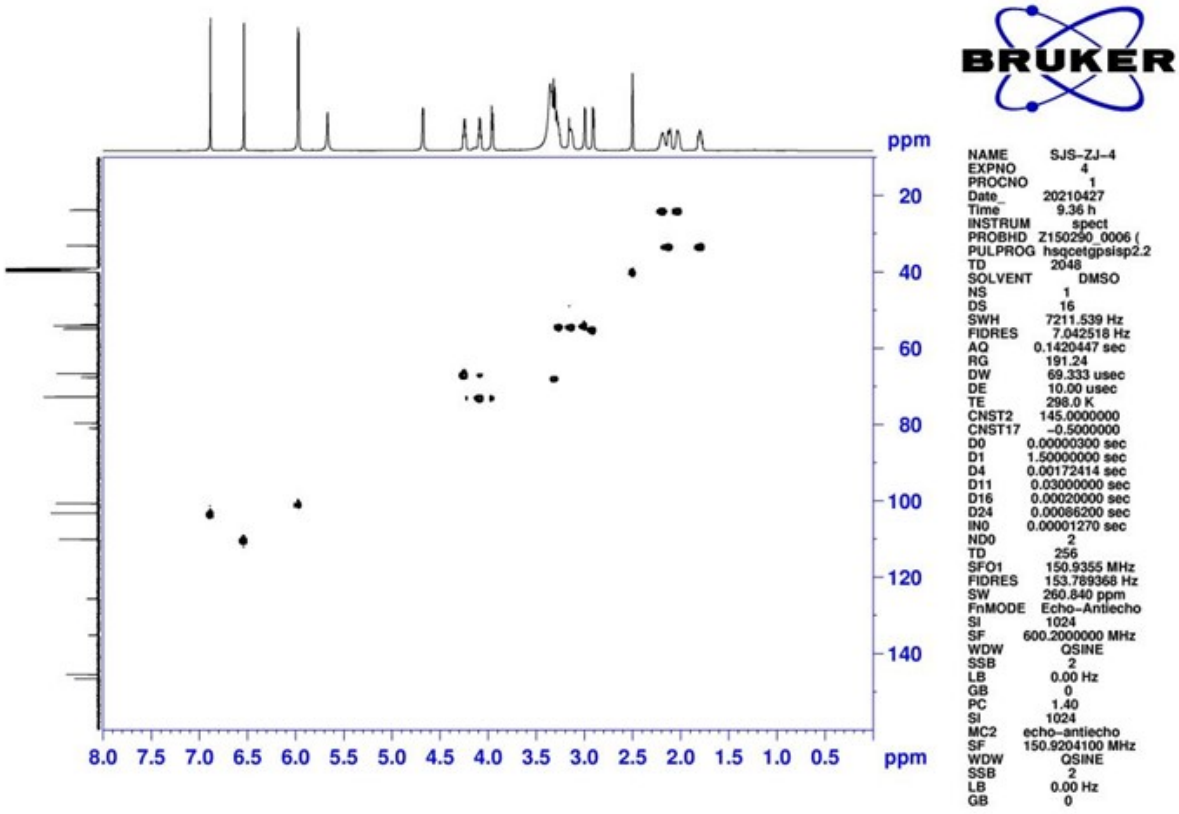

Figure S68. HSQC spectrum of compound **14a** (600 MHz, DMSO-d_6)

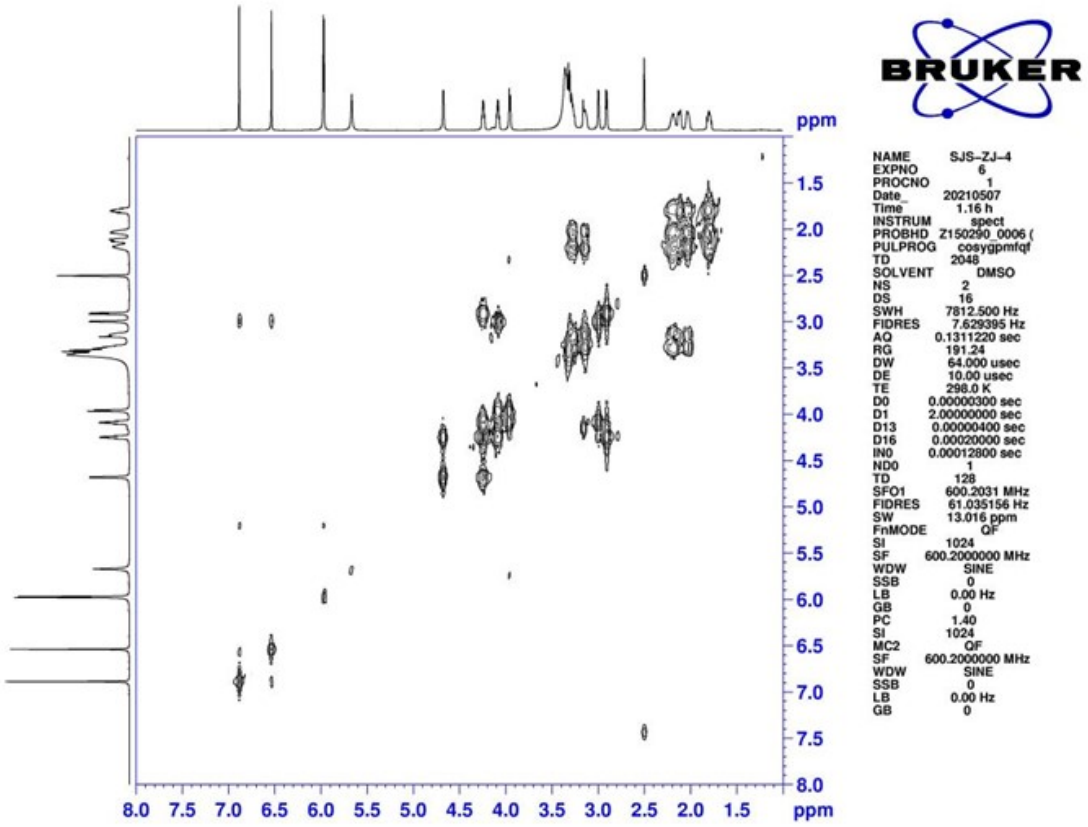

Figure S69. ^{1}H-^{1}H COSY spectrum of compound **14a** (600 MHz, DMSO-d_6)

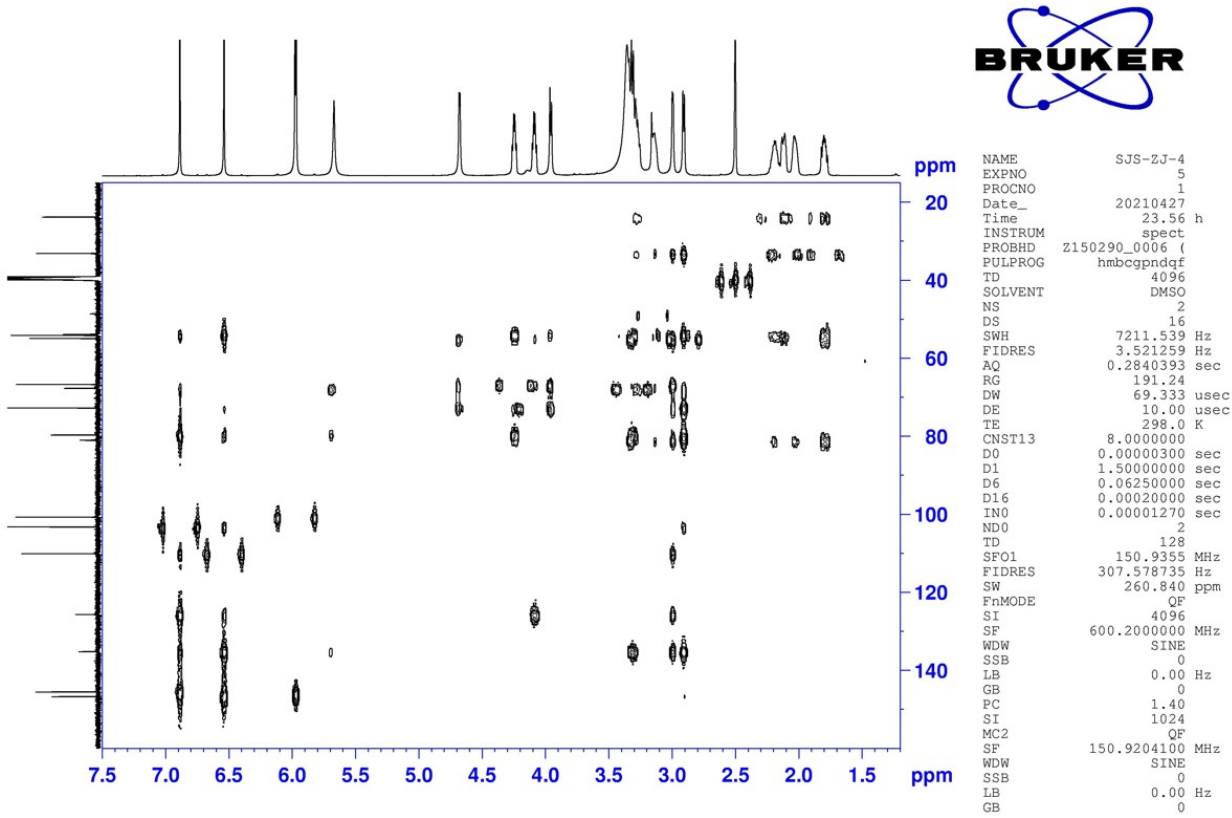

Figure S70. HMBC spectrum of compound **14a** (600 MHz, DMSO-d_6)

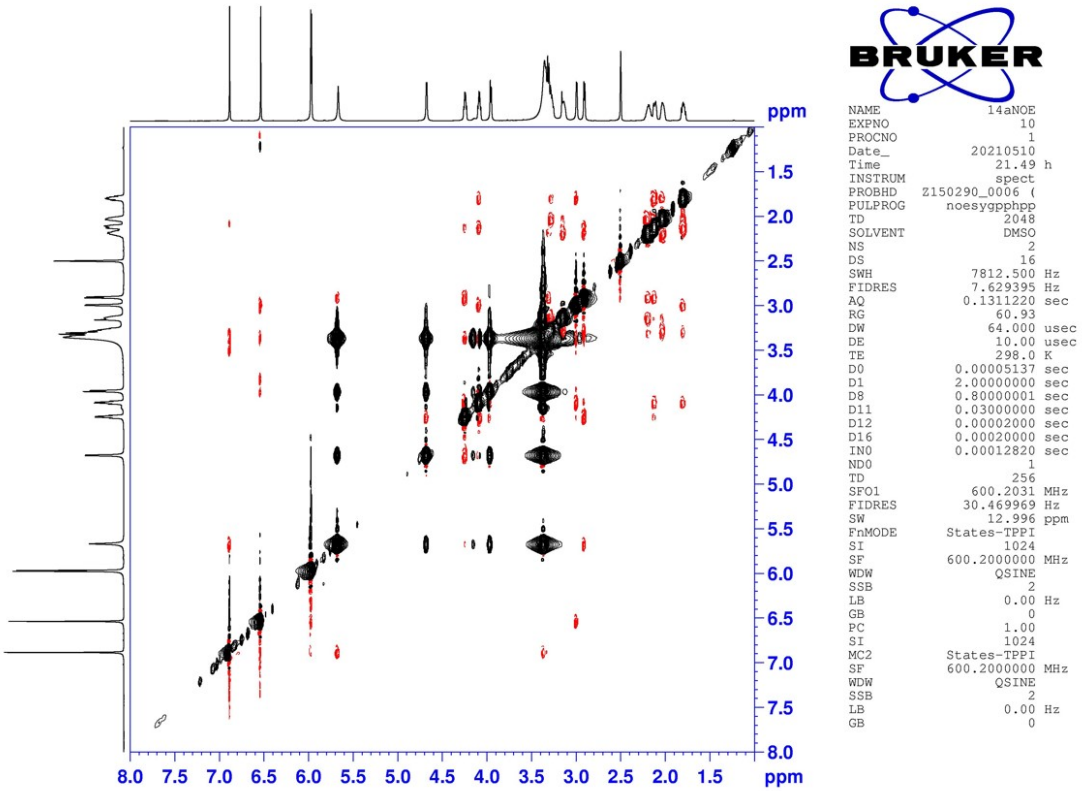

Figure S71. NOESY spectrum of compound **14a** (600 MHz, DMSO-d_6)

14a

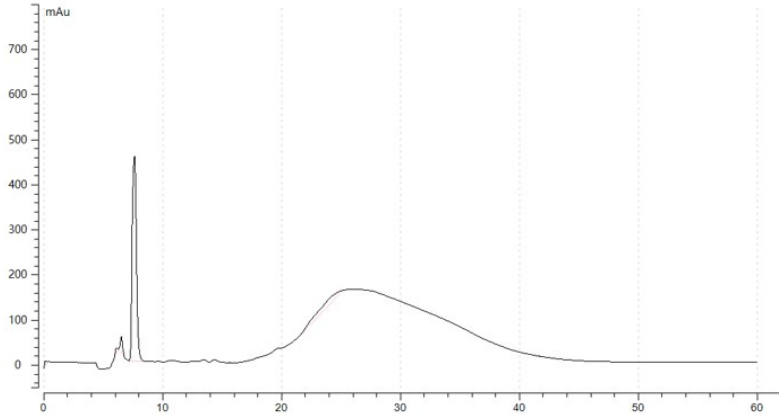

HPLC conditions:
MeOH-H_2O (32:68), t_R = 33.8 min,
low rate: 2.0 ml/min

14

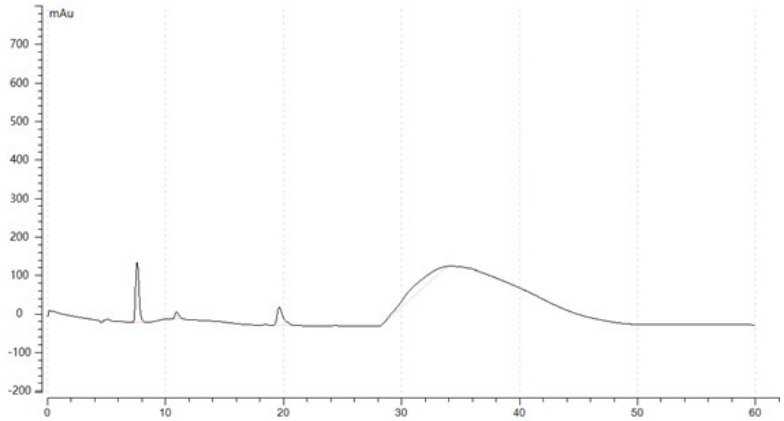

HPLC conditions:
MeOH-H_2O (32:68), t_R = 33.8 min,
low rate: 2.0 ml/min

14a

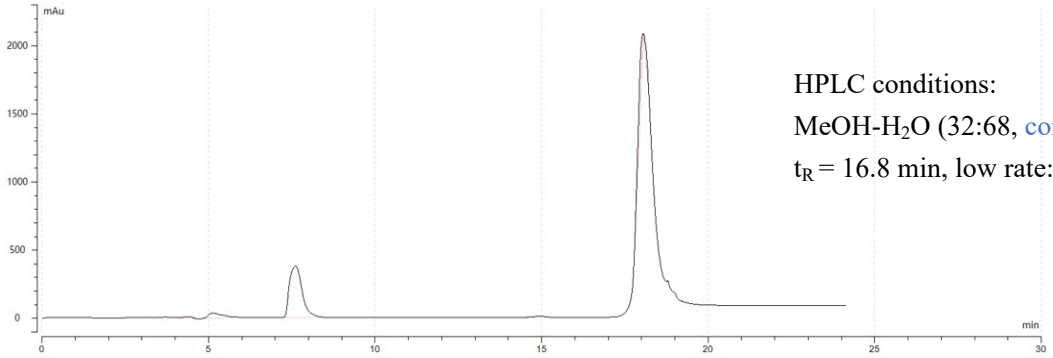

HPLC conditions:
MeOH-H_2O (32:68, containing 0.005% DEA),
t_R = 16.8 min, low rate: 2.0 ml/min

14

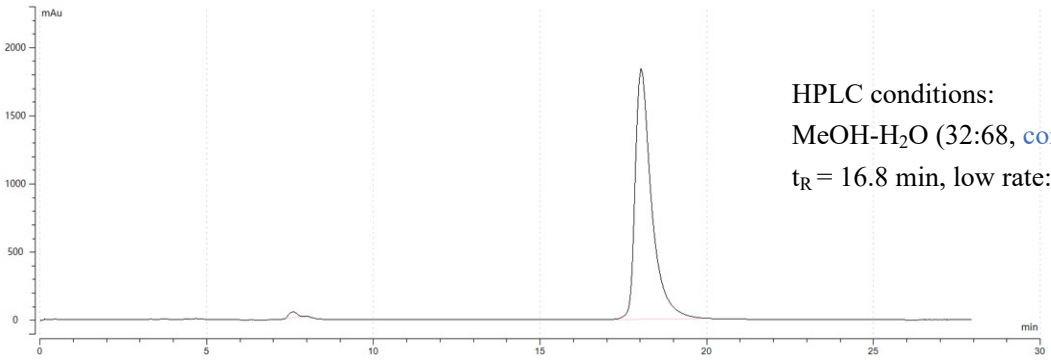

HPLC conditions:
MeOH-H_2O (32:68, containing 0.005% DEA),
t_R = 16.8 min, low rate: 2.0 ml/min

Mixture of **14** and **14a**

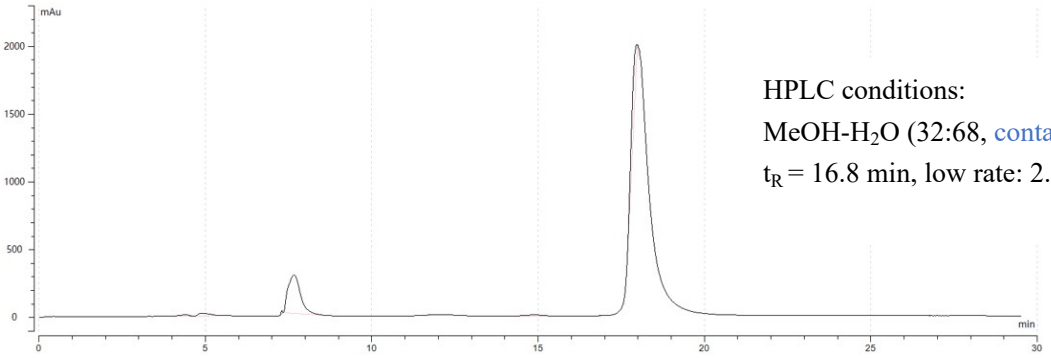

HPLC conditions:
MeOH-H_2O (32:68, containing 0.005% DEA),
t_R = 16.8 min, low rate: 2.0 ml/min

Figure S72. The HPLC chromatogram of **14a** and **14**

Elemental Composition Report **Page 1**

Single Mass Analysis
Tolerance = 10.0 PPM / DBE: min = -1.5, max = 50.0
Element prediction: Off
Number of isotope peaks used for i-FIT = 3

Monoisotopic Mass, Even Electron Ions
2918 formula(e) evaluated with 7 results within limits (up to 50 closest results for each mass)
Elements Used:
C: 0-100 H: 0-100 B: 0-1 N: 1-1 O: 0-100 S: 0-6 Cu: 0-5 Zn: 0-1 Se: 0-1 Br: 0-8 Ru: 0-1

1202-1-SZJ-D-14 43 (0.258) Cm (34:64)
1: TOF MS ES+

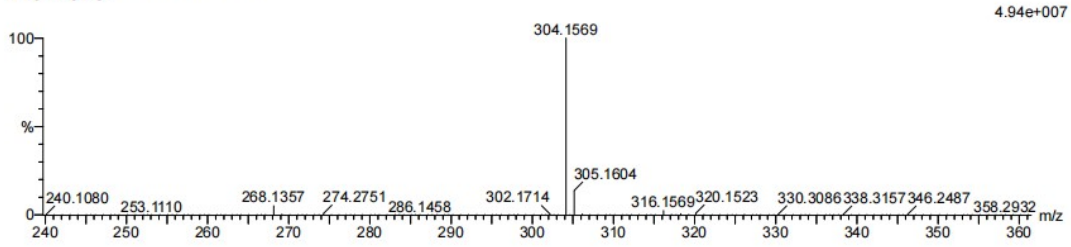

Minimum:				-1.5				
Maximum:		5.0	10.0	50.0				
Mass	Calc. Mass	mDa	PPM	DBE	i-FIT	Norm	Conf(%)	Formula
304.1569	304.1568	0.1	0.3	2.5	53.8	0.181	83.47	C12 H23 B N O7
	304.1576	-0.7	-2.3	1.5	63.8	10.154	0.00	C13 H27 B N O2 S2
	304.1578	-0.9	-3.0	-1.5	111.7	58.087	0.00	C13 H32 N Ru
	304.1583	-1.4	-4.6	2.5	58.5	4.843	0.79	C14 H26 N O4 S
	304.1549	2.0	6.6	7.5	55.5	1.849	15.73	C17 H22 N O4
	304.1543	2.6	8.5	2.5	113.1	59.441	0.00	C15 H30 N Se
	304.1543	2.6	8.5	6.5	64.6	11.018	0.00	C16 H23 B N O2 S

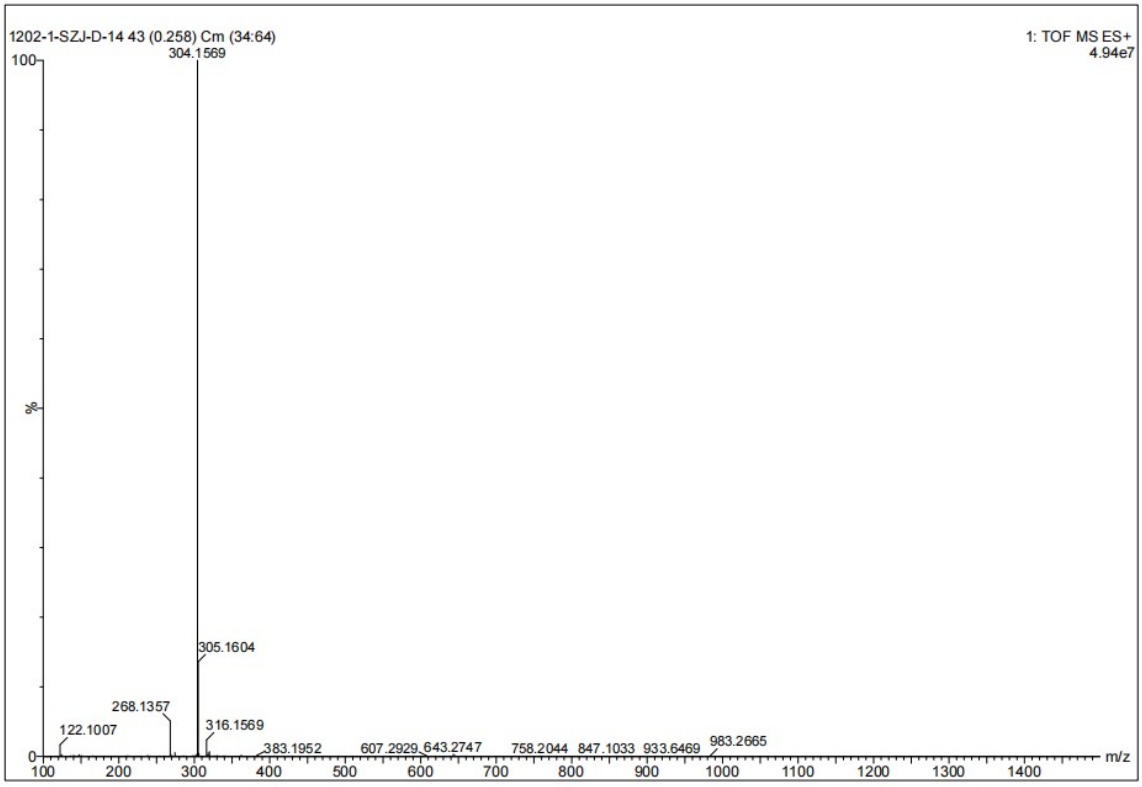

Figure S73. HRESIMS spectrum of **15**

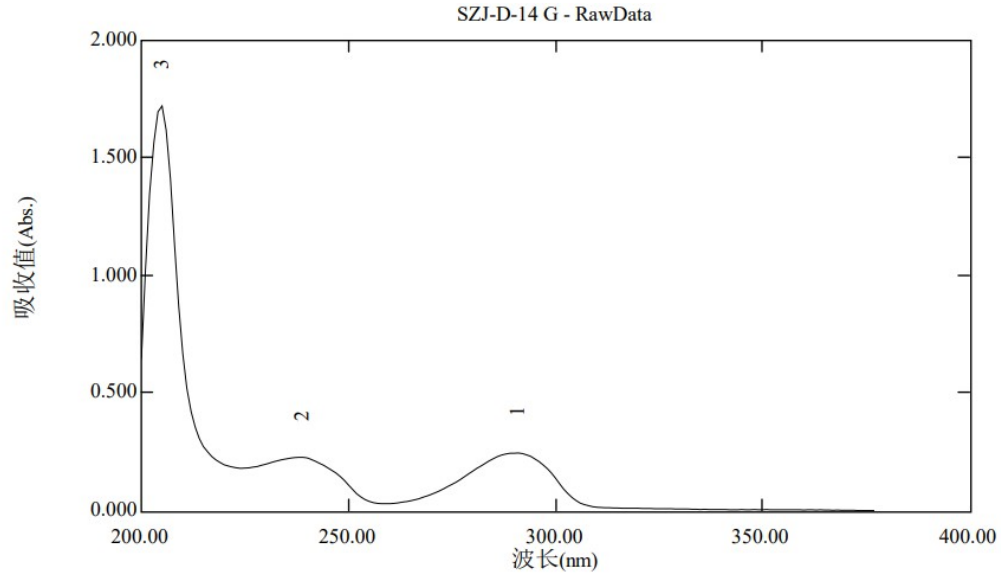

Figure S74. UV spectrum of **15**

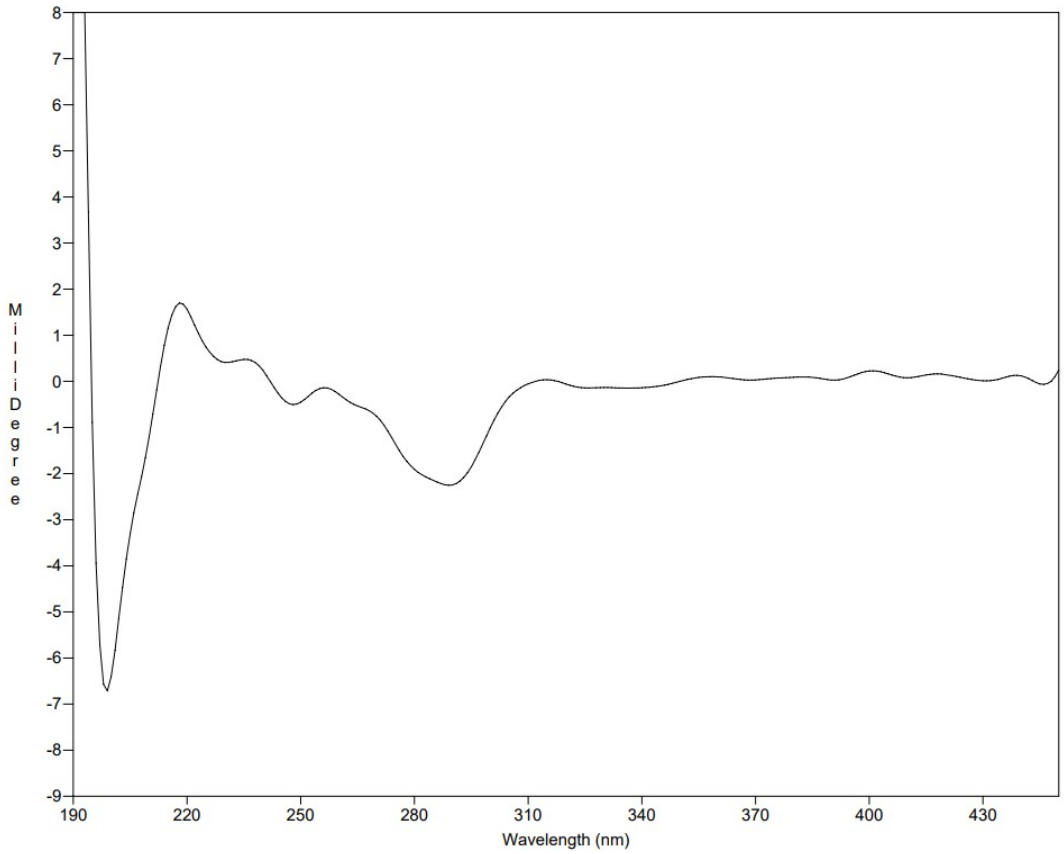

Figure S75. Experimental ECD spectrum of **15**

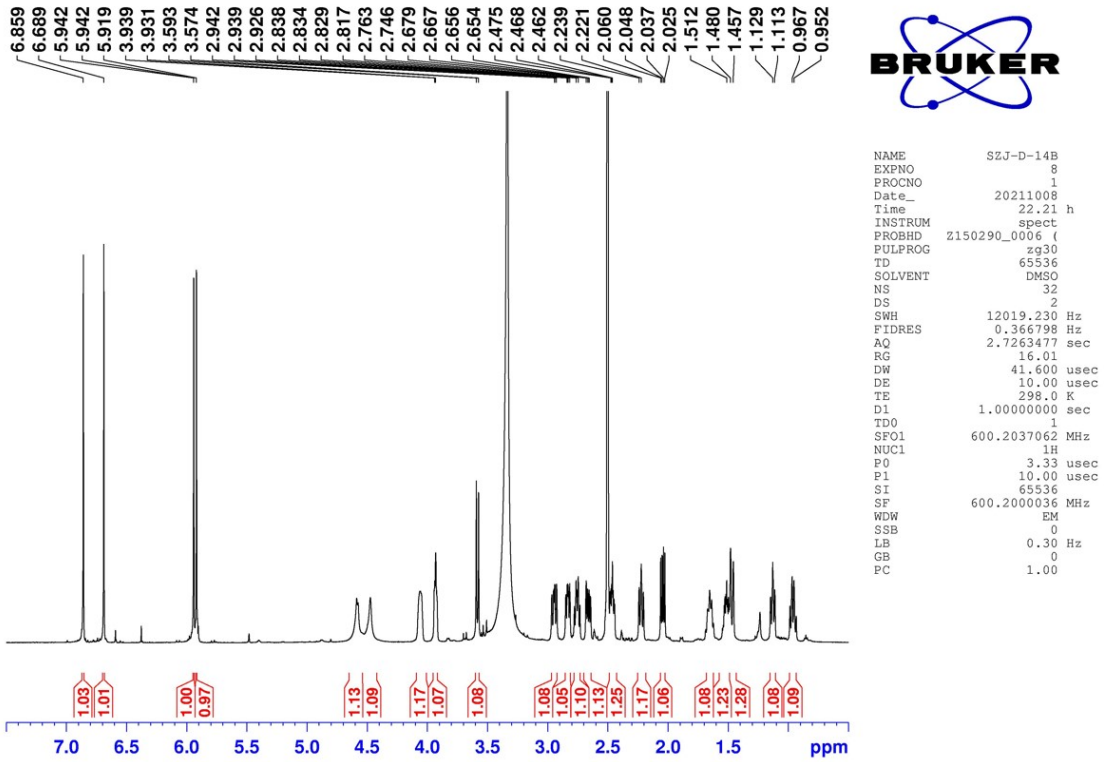

Figure S76. ^{1}H NMR spectrum of compound **15** (600 MHz, DMSO-d_6)

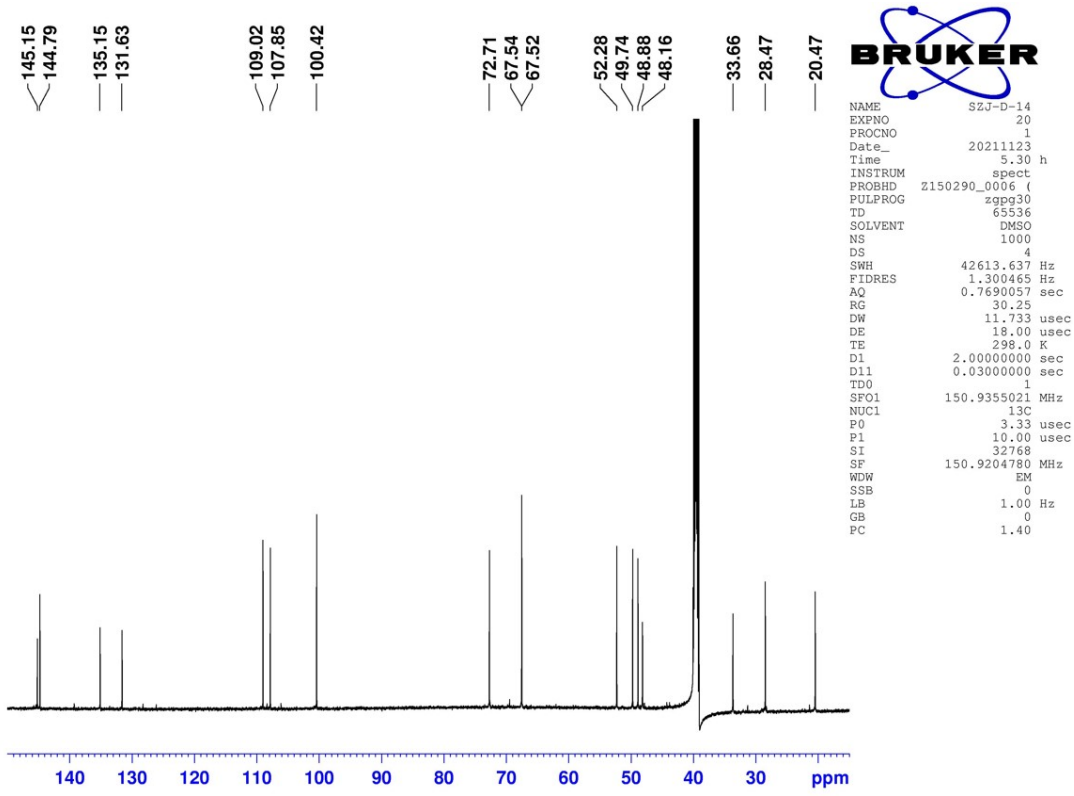

Figure S77. ^{13}C NMR spectrum of compound **15** (150 MHz, DMSO-d_6)

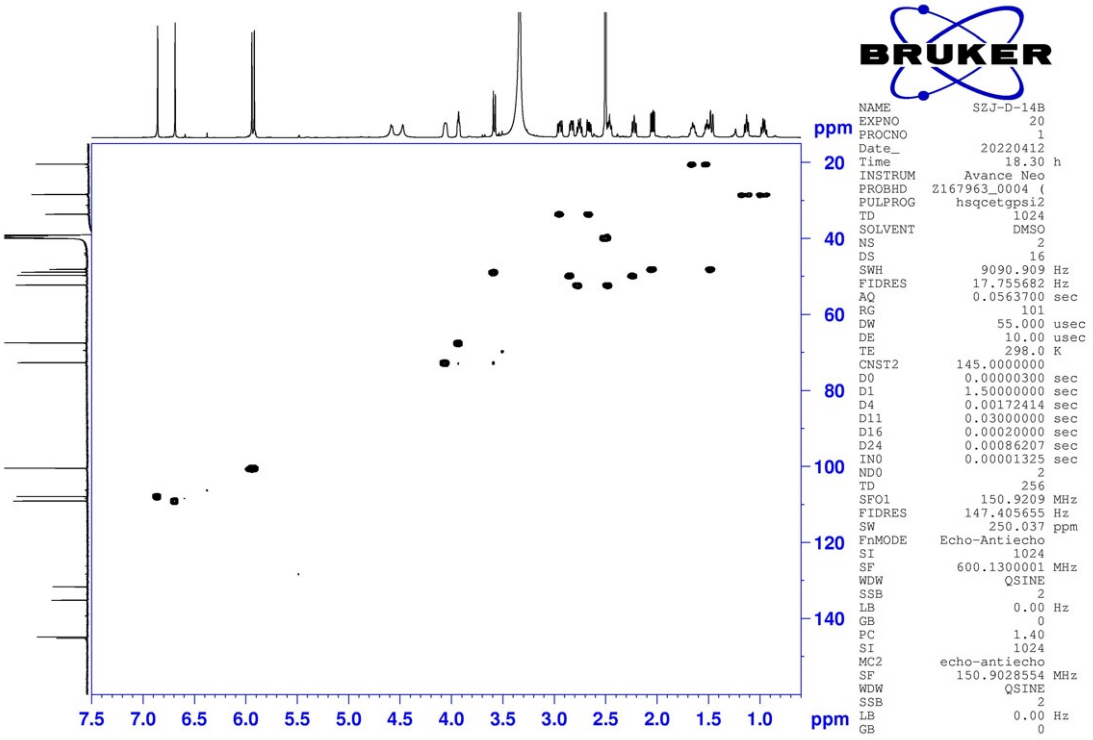

Figure S78. HSQC spectrum of compound **15** (600 MHz, DMSO-d_6)

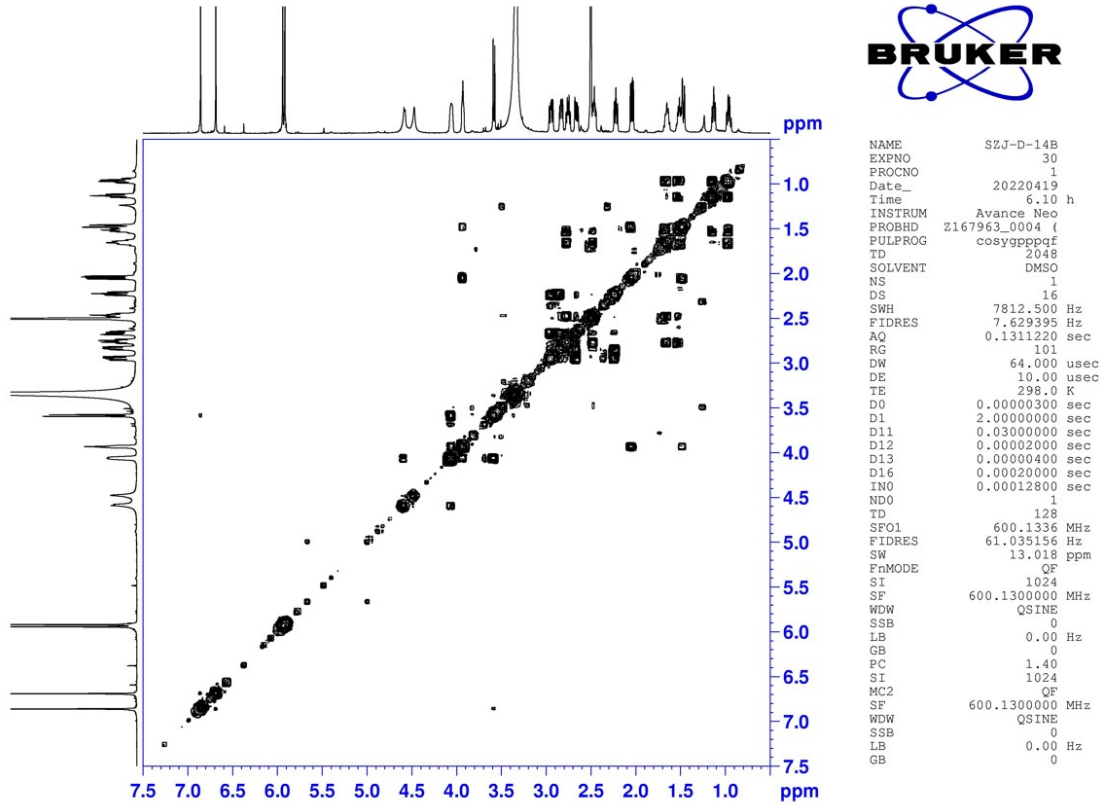

Figure S79. ^{1}H-^{1}H COSY spectrum of compound **15** (600 MHz, DMSO-d_6)

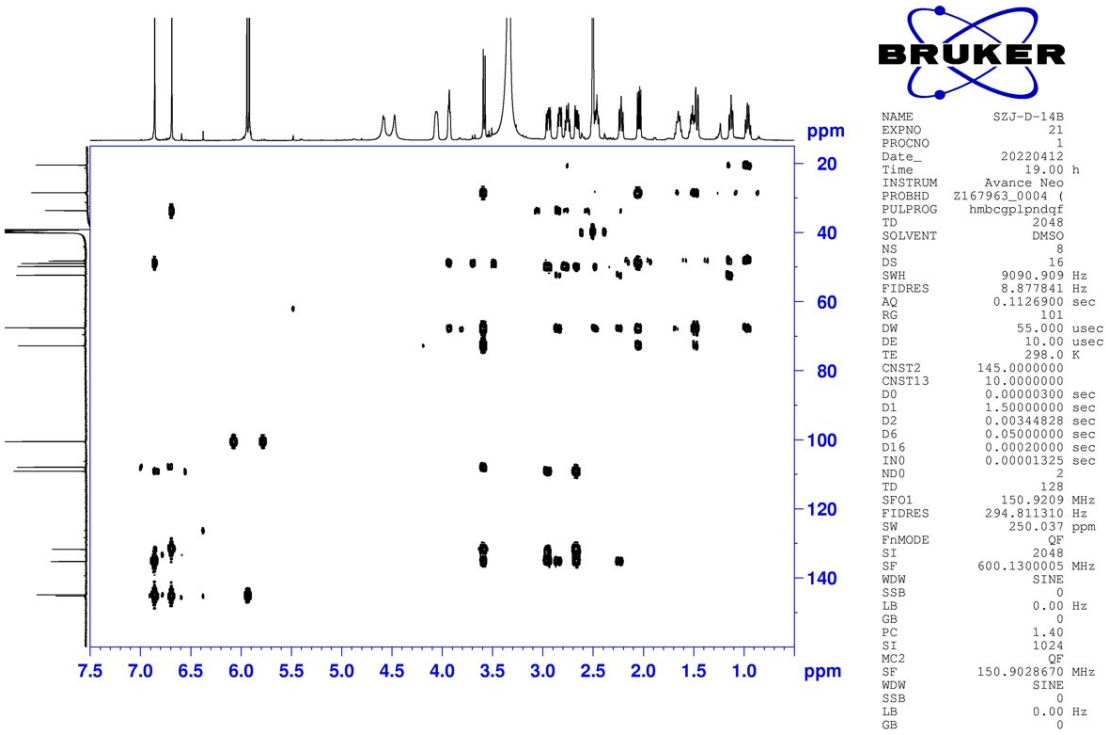

Figure S80. HMBC spectrum of compound **15** (600 MHz, DMSO-d_6)

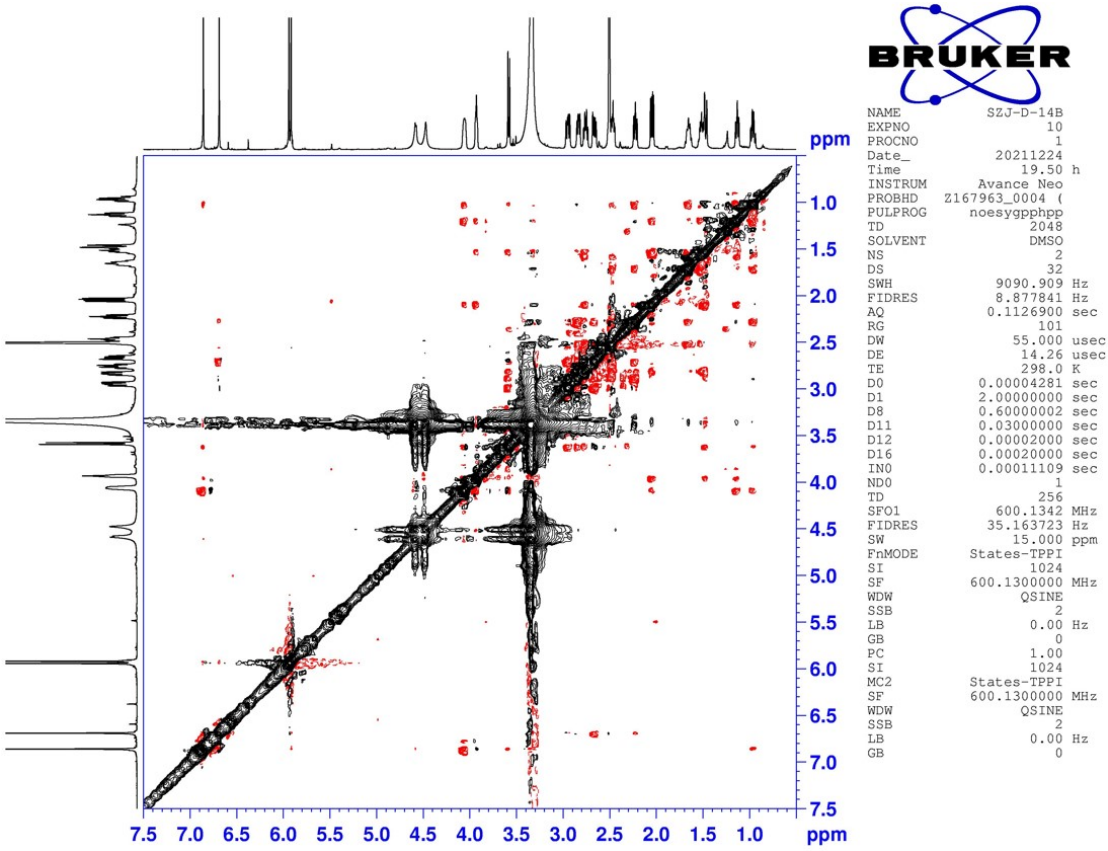

Figure S81. NOESY spectrum of compound **15** (600 MHz, DMSO-d_6)

Elemental Composition Report **Page 1**

Single Mass Analysis
Tolerance = 5.0 mDa / DBE: min = -1.5, max = 50.0
Element prediction: Off
Number of isotope peaks used for i-FIT = 3

Monoisotopic Mass, Even Electron Ions
217 formula(e) evaluated with 1 results within limits (up to 50 best isotopic matches for each mass)
Elements Used:
C: 23-23 H: 0-60 N: 0-7 O: 0-200
SZJ-D-5A 62 (0.366)
1: TOF MS ES+

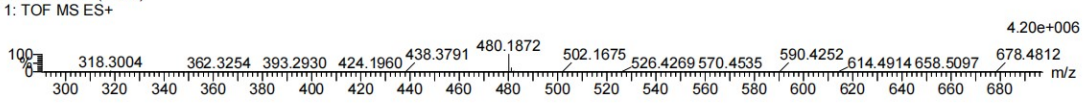

Minimum:				-1.5				
Maximum:		5.0	10.0	50.0				
Mass	Calc. Mass	mDa	PPM	DBE	i-FIT	Norm	Conf(%)	Formula
480.1872	480.1870	0.2	0.4	9.5	808.0	n/a	n/a	C23 H30 N O10

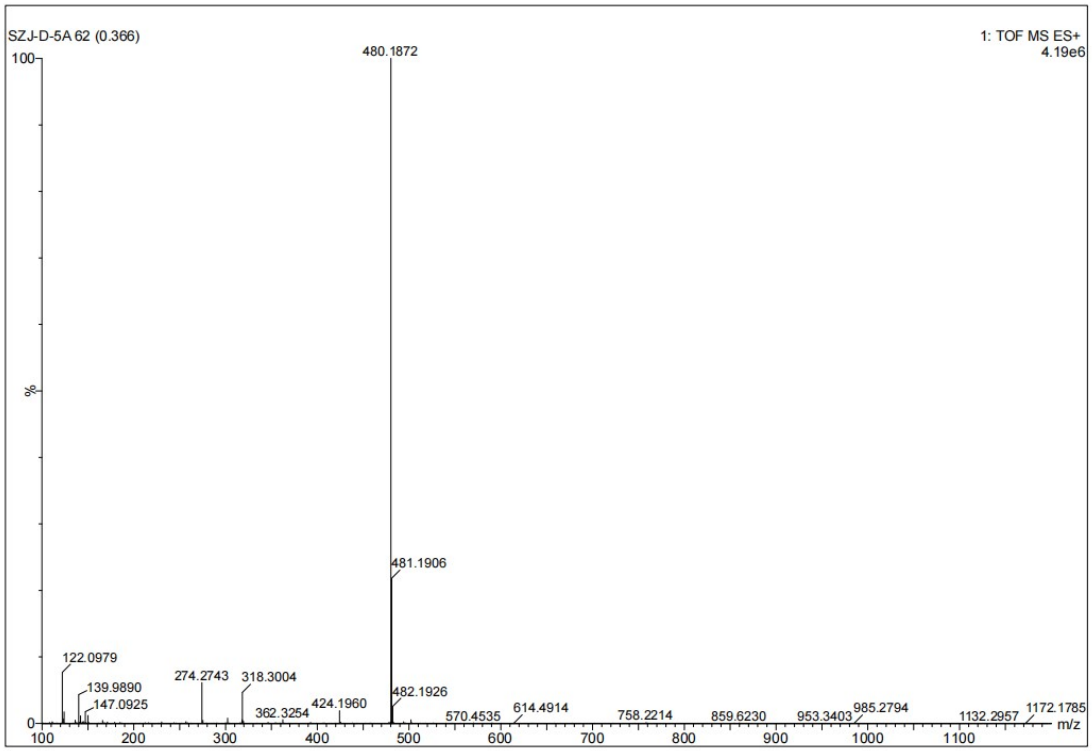

Figure S82. HRESIMS spectrum of **17**

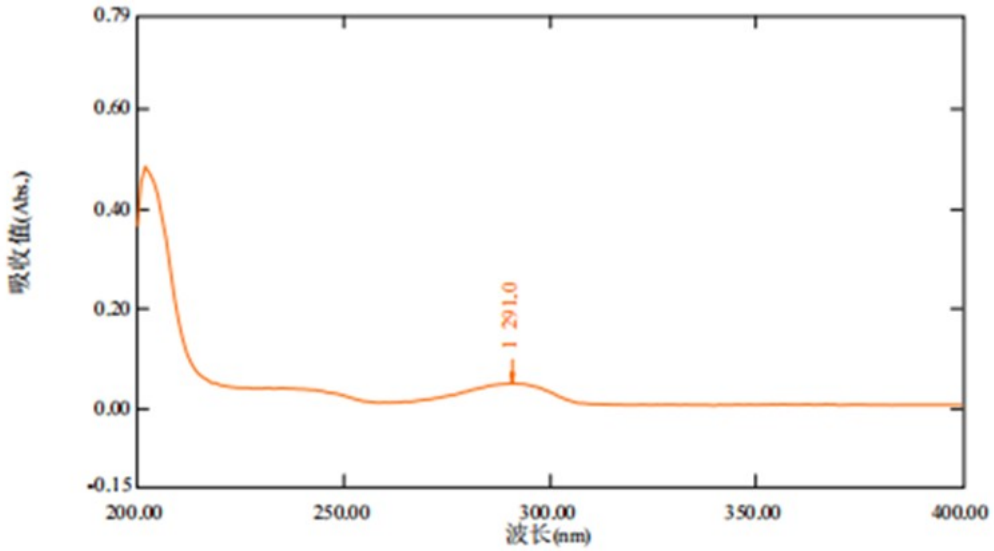

Figure S83. UV spectrum of compound **17**

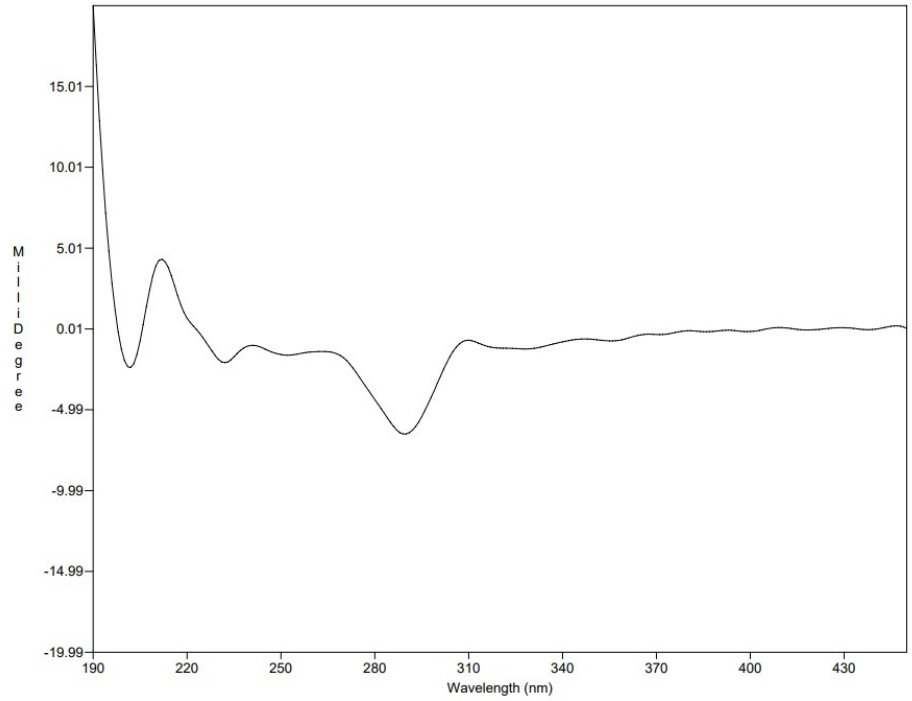

Figure S84. Experimental ECD spectrum of **17**

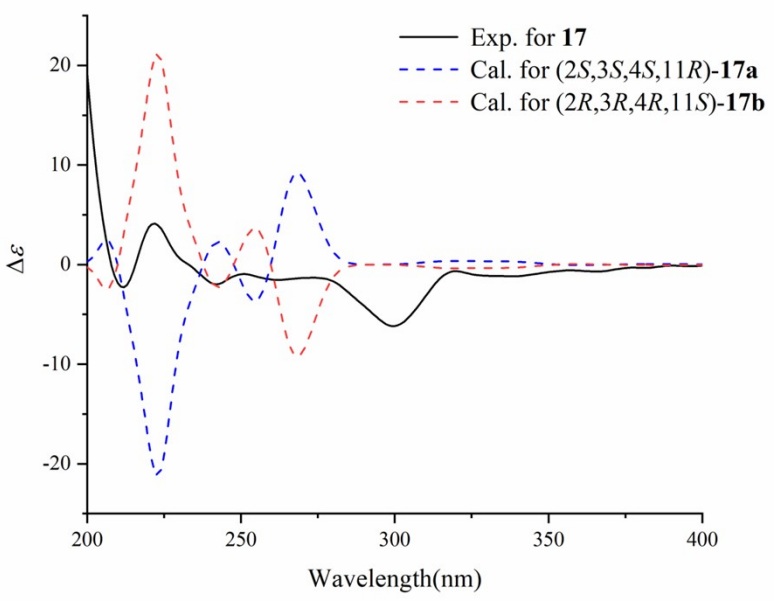

Figure S85. Experimental ECD spectrum of **17**, and B3LYP/6-31G(d,p)-calculated ECD spectra of the aglycone **17a** and **17b**

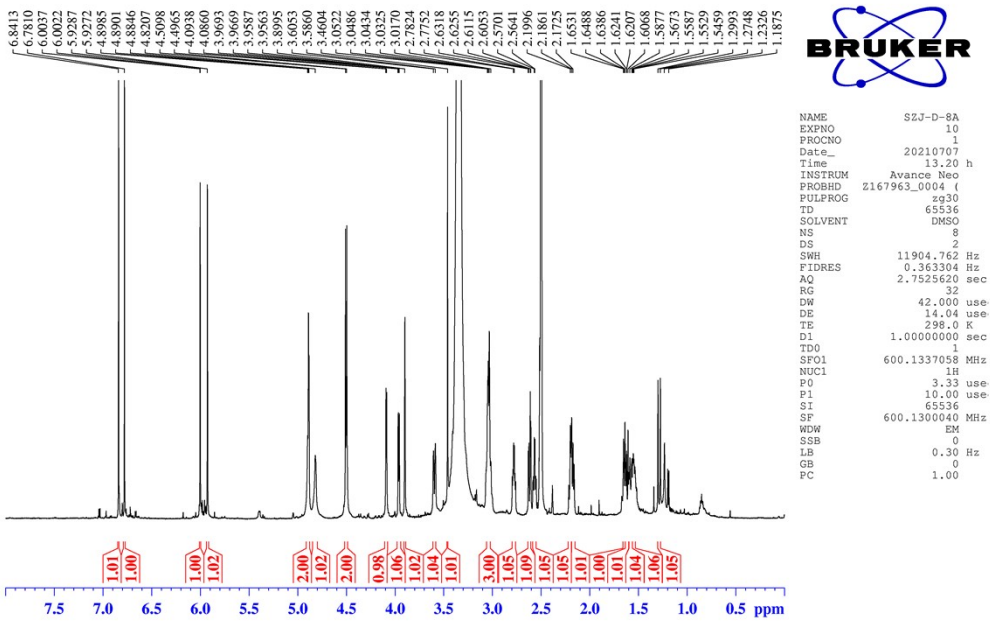

Figure S86. ^{1}H NMR spectrum of compound **17** (600 MHz, DMSO-d_6)

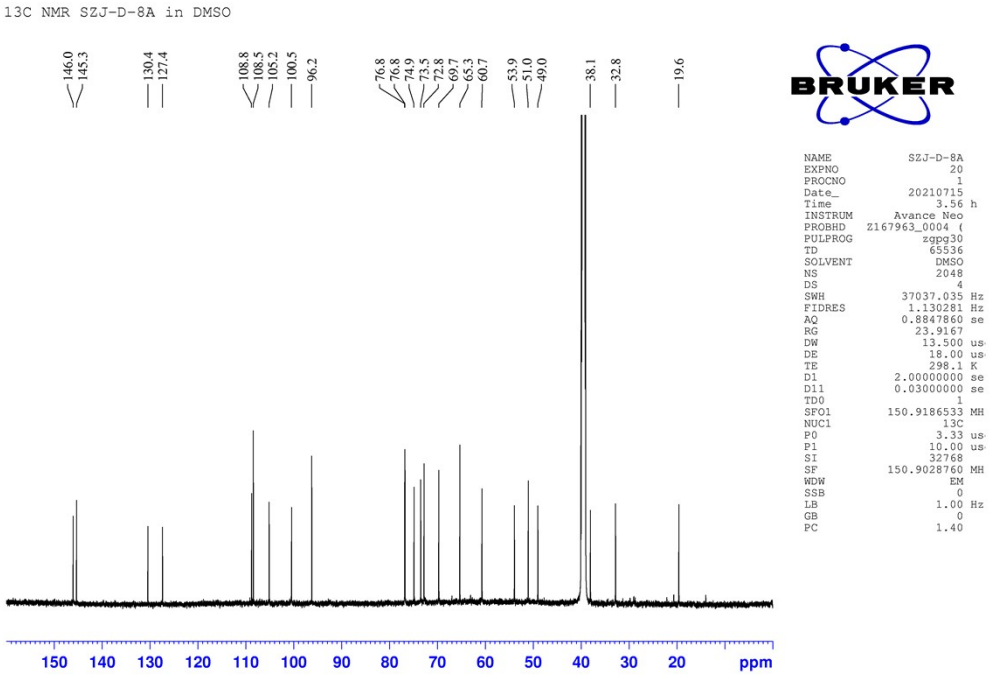

Figure S87. ^{13}C NMR spectrum of compound **17** (150 MHz, DMSO-d_6)

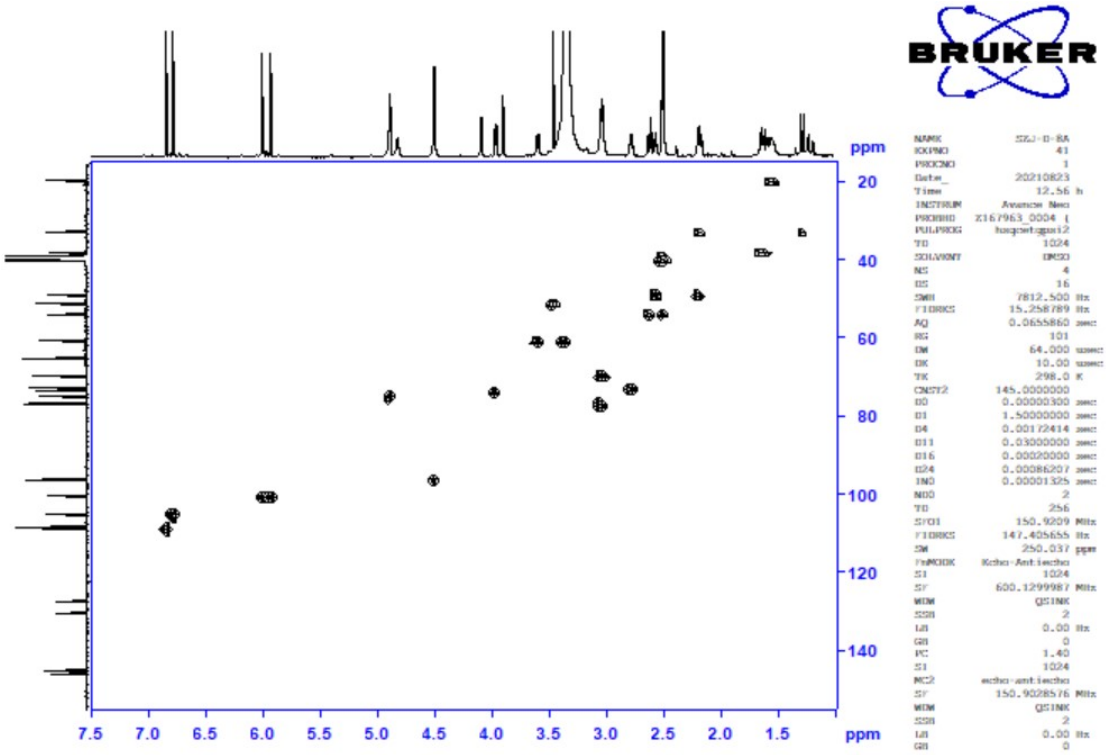

Figure S88. HSQC spectrum of compound **17** (600 MHz, DMSO-d_6)

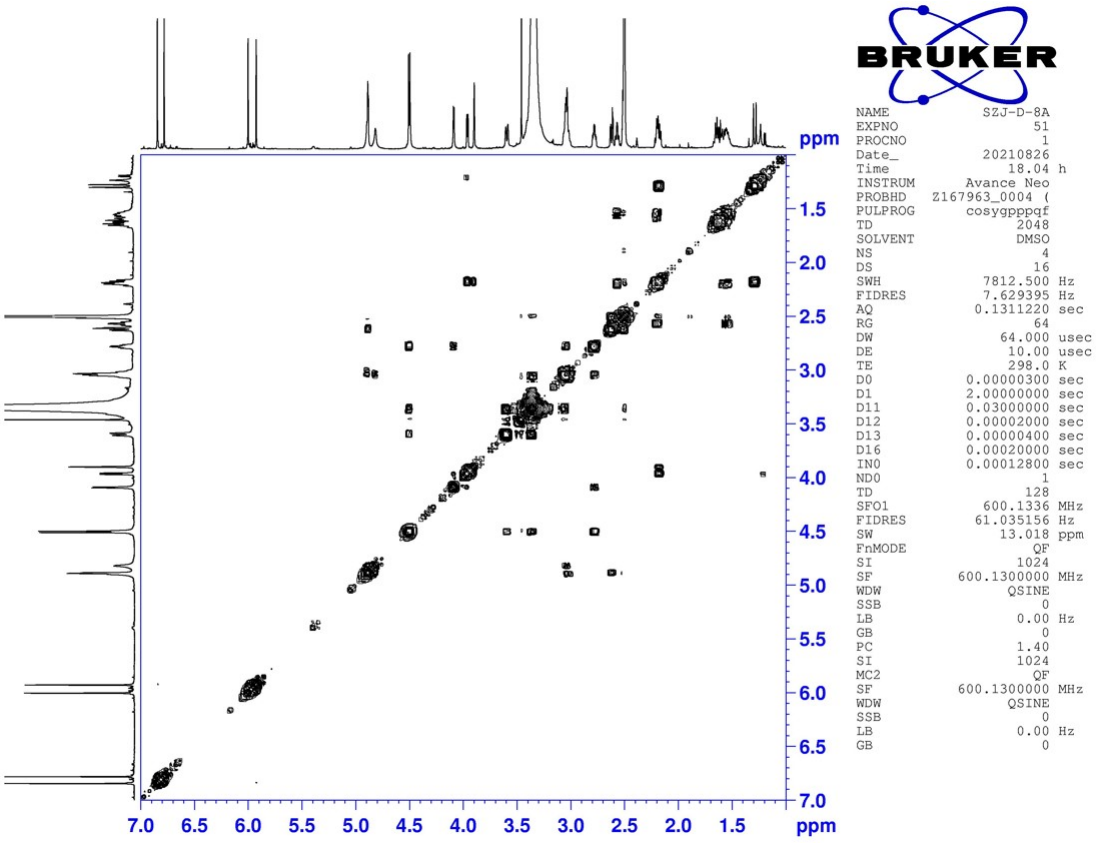

Figure S89. ^{1}H-^{1}H COSY spectrum of compound **17** (600 MHz, DMSO-d_6)

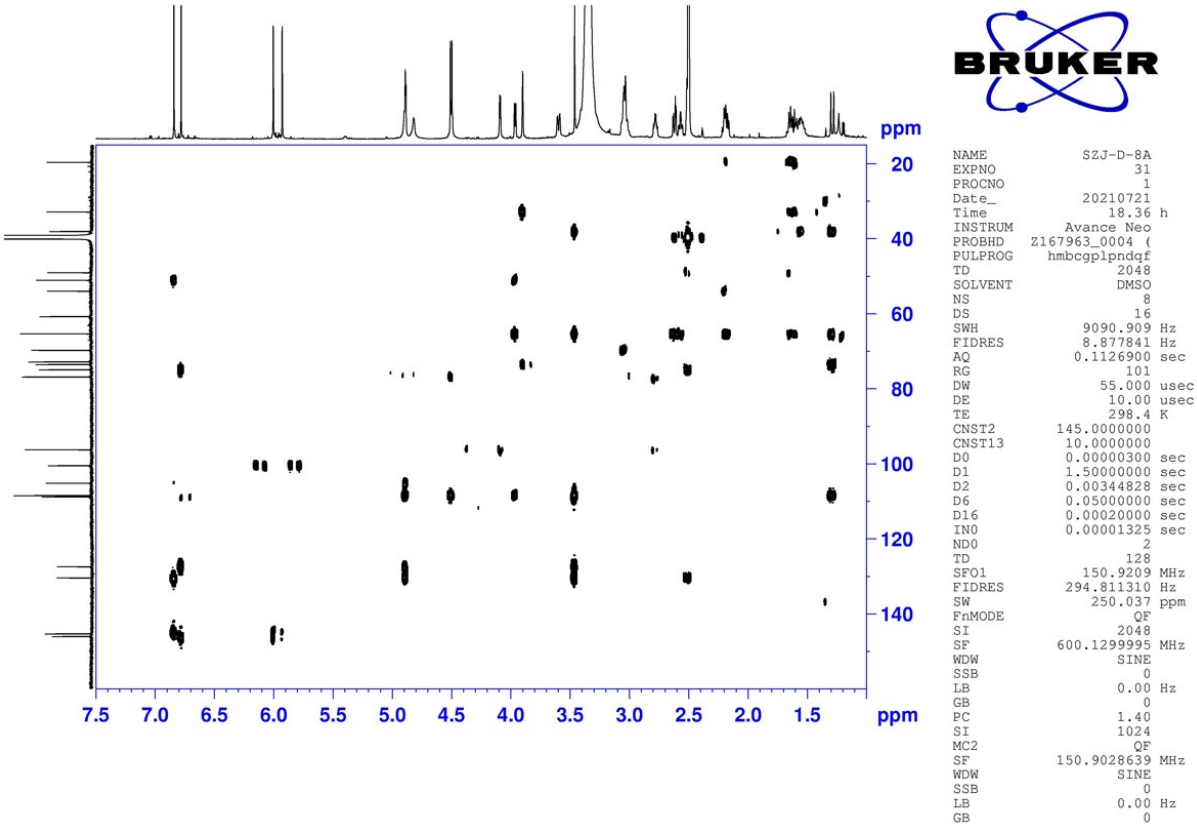

Figure S90. HMBC spectrum of compound **17** (600 MHz, DMSO-d_6)

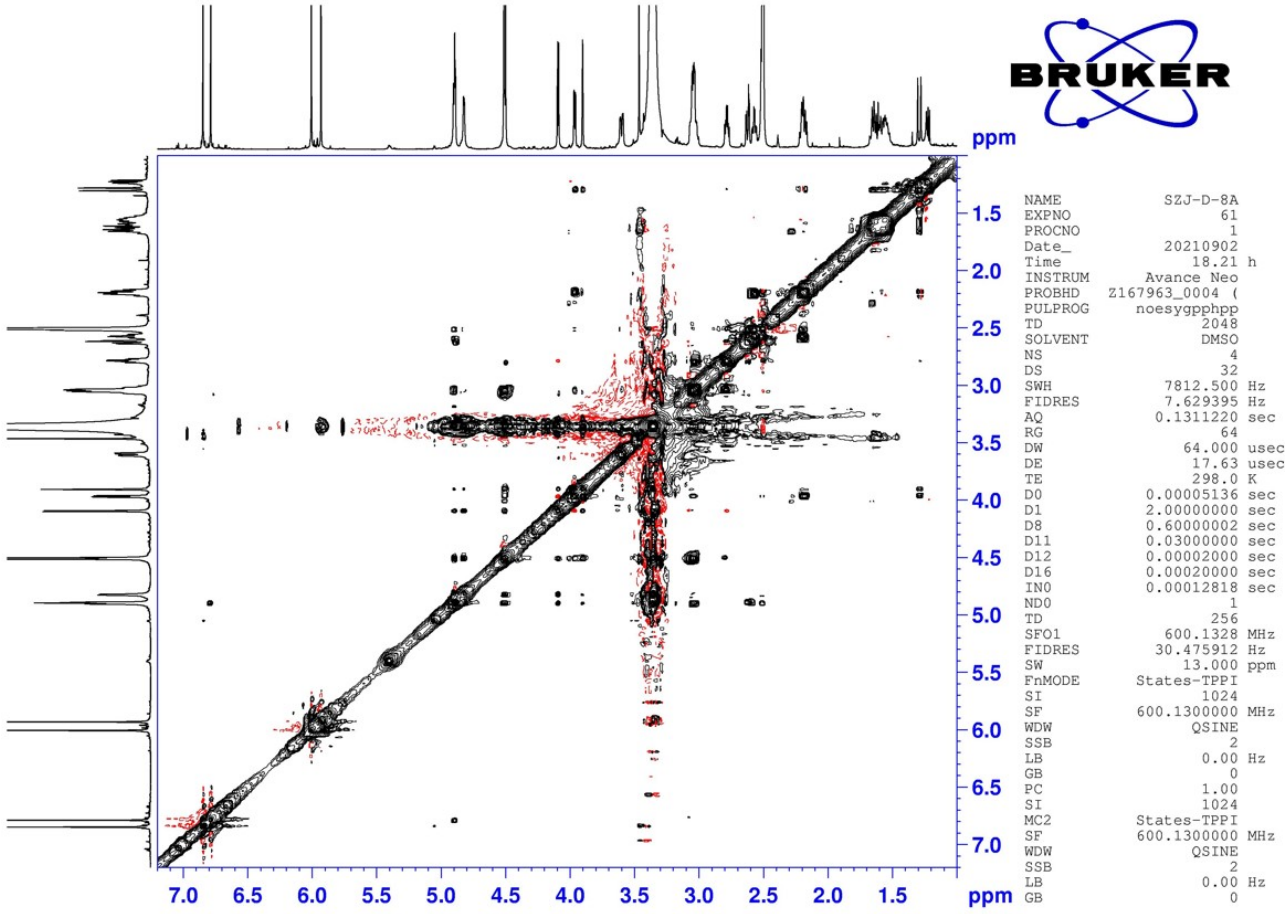

Figure S91. NOESY spectrum of compound **17** (600 MHz, DMSO-d_6)

Table S1. X-ray crystallographic data for **1**

Chemical formula	$C_{20}H_{27}NO_6$
Formula weight	377.42
Temperature	153(2) K
Crystal system	orthorhombic
Space group	P 21 21 21
Unit cell dimensions	a = 7.0303(2) Å $\alpha = 90°$
	b = 9.8072(3) Å $\beta = 90°$
	c = 27.1272(8) Å $\gamma = 90°$
Volume	1870.35(10) $Å^3$
Z	4
Density (calculated)	1.340 g/cm^3
Absorption coefficient	0.815 mm^{-1}
F (000)	808
Crystal size	0.200 x 0.200 x 0.300 mm
Wavelength	1.54178 Å
Radiation	Cu Kα, λ = 1.54178 Å
Theta range for data collection	4.79 to 72.58°
Index ranges	-8<=h<=8, -12<=k<=11, -31<=l<=33
Reflections collected	13371
Independent reflections	3655 [R(int) = 0.0162]
Data / restraints / parameters	3655 / 0 / 249
Goodness-of-fit on F2	1.033
Final R indices	3621 data; I>2σ(I) $R_1 = 0.0257$, $wR_2 = 0.0679$
	all data $R_1 = 0.0261$, $wR_2 = 0.0681$
Weighting scheme	w=1/[σ2(Fo2) + (0.0379P)2+0.4058P]
	where P=(Fo2+2Fc
	2)/3
Largest diff. peak and hole	0.261 and -0.176 eÅ-3
R.M.S. deviation from mean	0.031 eÅ-3
Flack parameter	0.07(2)

Table S2. X-ray crystallographic data for **6**

Chemical formula	$C_{20}H_{31}NO_7$
Formula weight	397.46
Temperature	153(2) K
Crystal system	monoclinic
Space group	P 1 21 1
Unit cell dimensions	a = 9.2538(3) Å α = 90°
	b = 9.4315(3) Å β = 95.7140(10)°
	c = 11.3689(3) Å γ = 90°
Volume	987.32(5) Å3
Z	2
Density (calculated)	1.337 g/cm^3
Absorption coefficient	0.834 mm^{-1}
F (000)	428
Crystal size	0.080 x 0.100 x 0.100 mm
Wavelength	1.54178 Å
Radiation	Cu Kα, λ = 1.54178 Å
Theta range for data collection	3.91 to 72.54°
Index ranges	-11<=h<=11, -11<=k<=11, -14<=l<=13
Reflections collected	16388
Independent reflections	3850 [R(int) = 0.0207]
Data / restraints / parameters	3850 / 1 / 274
Goodness-of-fit on F2	1.047
Final R indices	3797 data; I>2σ(I) R_1 = 0.0246, wR_2 = 0.0640
	all data R_1 = 0.0250, wR_2 = 0.0645
Weighting scheme	w=1/[σ2(Fo2) + (0.0393P)2+0.1317P]
	where P=(Fo2+2Fc2)/3
Largest diff. peak and hole	0.163 and -0.155 eÅ-3
R.M.S. deviation from mean	0.038 eÅ-3
Flack parameter	0.05(3)

Table S3. X-ray crystallographic data for **13**

Chemical formula	$C_{37}H_{42}Cl_4N_2O_{10}$
Formula weight	816.52
Temperature	153(2) K
Crystal system	monoclinic
Space group	P 1 21 1
Unit cell dimensions	a = 7.8741(4) Å $\alpha = 90°$
	b = 27.6610(14) Å $\beta = 100.292(3)°$
	c = 7.9804(4) Å $\gamma = 90°$
Volume	1710.21(15) Å3
Z	2
Density (calculated)	1.586 g/cm^3
Absorption coefficient	3.707 mm^{-1}
F (000)	852
Crystal size	0.100 x 0.100 x 0.100 mm
Wavelength	1.54178 Å
Radiation	Cu Kα (λ = 1.54178 Å)
Theta range for data collection	3.19 to 81.22°
Index ranges	-10<=h<=9, -33<=k<=34, -10<=l<=10
Reflections collected	18258
Independent reflections	6536 [R(int) = 0.1756]
Data / restraints / parameters	6536 / 1 / 484
Goodness-of-fit on F2	1.492
Final R indices	4246 data; I>2σ(I) $R_1 = 0.1098$, $wR_2 = 0.2612$
	all data $R_1 = 0.1684$, $wR_2 = 0.3052$
Weighting scheme	w=1/[σ2(Fo2) + (0.1000P)2]
	where P=(Fo2+2Fc2)/3
Largest diff. peak and hole	1.010 and -0.966 eÅ-3
R.M.S. deviation from mean	0.175 eÅ-3
Flack parameter	0.21(2)

Table S4. ^{1}H NMR and ^{13}C NMR data of compounds **14a** and **14** (600 MHz, DMSO-d_6)

	14a		**14**	
Position	δ_H, (J in Hz)	δ_C, type	δ_H, (J in Hz)	δ_C, type
1	2.90, d (7.0)	54.9, CH	2.47, m	56.6, CH
2	4.25, m	66.7, CH	4.16, t (7.3)	68.0, CH
3	4.08, m	72.7, CH	3.98, m	72.7, CH
4	2.99, d (4.1)	53.9, CH	2.48, m	57.5, CH
5		79.6, C		75.9, C
6	1.80, m	33.1, CH_2	1.63, m	34.9, CH_2
	2.12, m		1.74, m	
7	2.03, m	23.8, CH_2	1.74, m	26.1, CH_2
	2.19, m		1.87, m	
8	3.13, m	54.1, CH_2	2.40, m	54.4, CH_2
	3.27, m		2.81, m	
10	3.30 (2H, m)	67.7, CH_2	2.69, d (7.3)	71.0, CH_2
			2.75, d (7.3)	
11		81.0, C		82.3, C
12		135.2, C		138.7, C
13		125.7, C		128.9, C
14	6.54, s	110.1, CH	6.42, s	109.4, CH
15		145.6, C		144.5, C
16		146.6, C		145.2, C
17	6.88, s	103.2, CH	6.85, s	102.9, CH
18	5.97, s	100.7, CH_2	5.90, s	100.1, CH_2
	5.96, s		5.87, s	
2-OH	4.67, d (4.4)		4.05, br s	
3-OH	3.96, d (7.4)		3.54, d (6.5)	
11-OH	5.66, br s		4.58, br s	

Table S5. ^{1}H NMR and ^{13}C NMR data of compounds **14a** and **14** (310 K $CDCl_3/CD_3OD$ 4:1)

	14a		**14**	
Position	δ_H, (*J* in Hz)	δ_C, type	δ_H, (*J* in Hz)	δ_C, type
1	2.82, d (7.0)	55.8, CH	2.65, d (7.0)	56.6, CH
2	4.24, t (7.5)	67.8, CH	4.29, t (7.5)	68.7 CH
3	4.06, dd (7.5, 5.1)	73.4, CH	4.20, dd (7.5, 5.2)	73.5, CH
4	3.04, d (4.2)	54.5, CH	2.70, d, (5.2)	57.2, CH
5		80.7, C		76.3, C
6	1.85, m	33.9, CH_2	1.72, m	35.2, CH_2
	2.10, m		1.88, m	
7	1.93, m	24.7, CH_2	1.80, m	26.1, CH_2
	2.10, m		1.98, m	
8	2.93, m	54.9, CH_2	2.54, m	55.1, CH_2
	3.38, m		3.00, m	
10	3.38, d (10.0)	68.3, CH_2	2.85, d (8.0)	70.1, CH_2
	3.08, d (10.0)		3.07, d (8.0)	
11		81.4, C		82.7, C
12		134.3, C		137.5, C
13		124.8, C		127.1, C
14	6.48, s	110.4, CH	6.53, s	109.8, CH
15		147.2, C		146.1, C
16		148.3, C		146.8, C
17	6.87, s	103.5, CH	7.01, s	103.3, CH
18	5.81, s	100.7, CH_2	5.90, s	100.7, CH_2
	5.80, s		5.87, s	

Table S6. Original data on antiproliferative effects on THP-1 and K562 cells of **1-32**

	K562			MEAN	SD	THP-1			MEAN	SD
1	22.50	21.07	23.31	22.29	1.13	19.80	17.56	22.20	21.34	4.74
2	21.20	21.91	25.27	22.79	2.17	21.4	16.95	26.58	24.71	2.87
3	18.20	25.21	21.72	21.71	4.96	18.43	14.68	20.5	17.86	2.95
4	20.42	19.78	20.62	20.22	2.51	22.21	23.64	21.18	22.52	1.78
5	26.13	29.32	24.35	26.59	2.52	16.61	17.03	26.92	17.83	1.78
6	21.50	20.16	27.57	23.08	3.95	20.83	15.79	16.98	17.86	2.62
7	>40	>40	>40			>40	>40	>40		
8	22.8	27.69	21.31	23.93	3.34	18.02	14.86	13.58	15.48	2.27
9	16.3	18.42	19.92	18.21	1.82	19.13	16.85	21.65	19.20	2.40
10	27.0	24.9	25.67	25.86	1.06	16.65	16.31	16.38	16.43	0.15
11	26.02	28.06	26.74	26.94	1.03	14.8	18.7	16.23	16.24	2.18
12	26.61	29.69	22.77	26.36	3.47	16.58	17.26	15.88	16.23	1.49
13	24.0	19.19	24.16	22.45	2.82	17.05	14.07	22.70	17.92	4.39
14	17.8	23.79	25.91	20.83	3.00	11.63	14.71	17.81	14.71	3.11
15	>40	>40	>40			16.50	17.52	16.42	16.88	2.50
16	27.56	28.28	28.87	28.24	0.66	16.02	15.59	15,82	15.51	2.01
17	20.3	26.48	30.02	25.60	4.92	18.02	18.42	17.42	17.48	1.26
18	20.35	25.18	22.65	22.73	2.42	12.88	13.02	13.32	12.97	2.67
19	31.05	28.28	23.77	27.70	3.67	17.56	18.02	16.59	17.25	1.33
20	26.2	21.62	20.64	22.82	2.97	21.75	19.7	21.66	21.02	1.14
21	30.2	26.57	31.87	29.55	2.71	22.93	13.93	20.85	19.23	4.70
22	21.8	24.32	20.41	22.18	1.98	21.23	16.85	26.41	24.49	2.86
23	>40	>40	>40			>40	>40	>40		
24	19.6	19.45	21.19	20.08	0.96	14.95	12.01	27.57	16.22	5.01
25	29.11	26.9	20.38	25.46	4.54	15.59	16.02	14.88	15.27	1.47
26	9.02	8.82	7.92	8.23	2.78	10.02	9.45	9.62	9.93	2.44
27	23.16	33.43	28.81	28.47	5.14	14.85	22.7	16.23	17.09	3.66
28	22.03	23.77	26.98	24.26	2.51	18.52	17.59	16.80	17.22	1.49
29	20.54	29.24	26.54	25.44	4.45	16.89	19.02	16,04	16.66	2.18
30	5.11	3.46	4.37	4.31	0.83	2.38	3.36	3.33	3.02	0.56
31	0.36	0.23	0.27	0.29	0.07	0.21	0.18	0.32	0.24	0.07
32	21.0	20.42	16.9	19.44	2.22	12.97	12.47	10.85	11.91	2.05

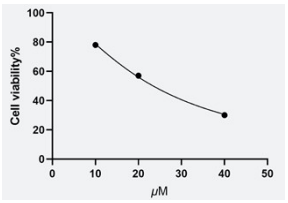

1

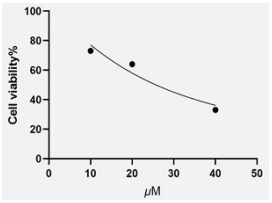

2

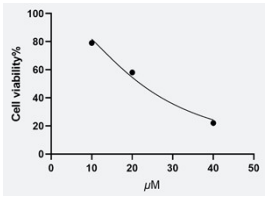

3

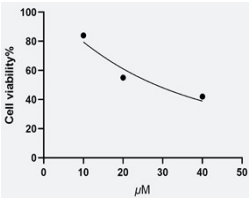

4

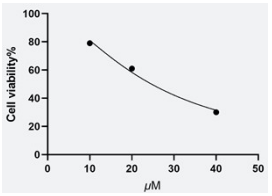

5

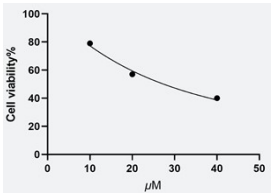

6

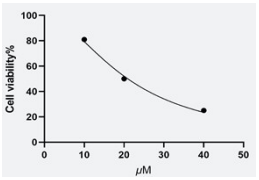

8

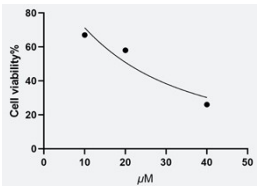

9

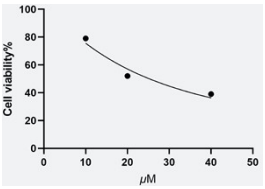

10

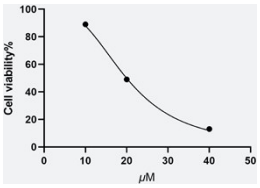

11

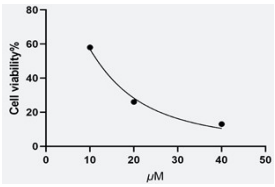

12

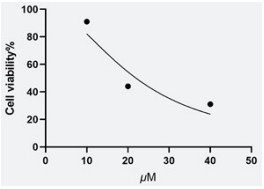

13

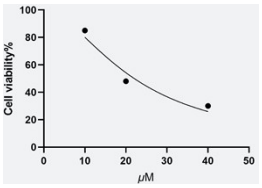

14

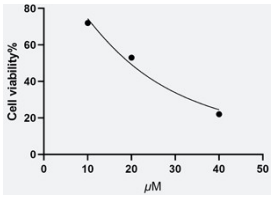

16

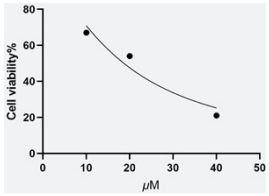

17

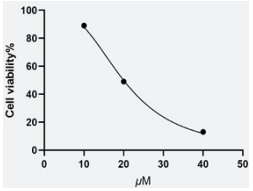

18

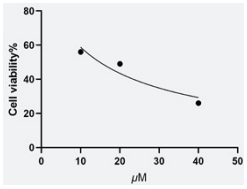

19

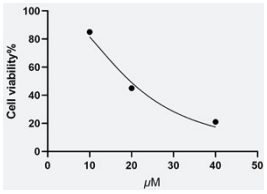

20

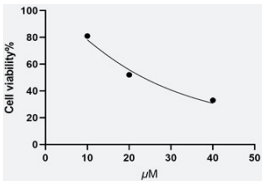

21

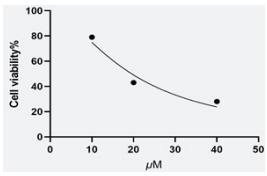

22

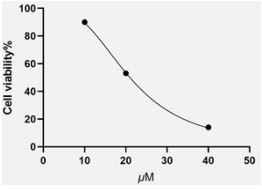

24

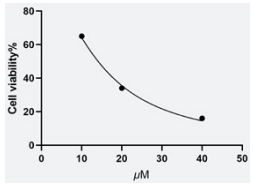

25

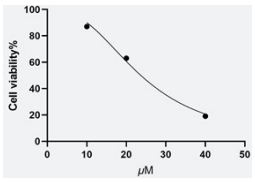

26

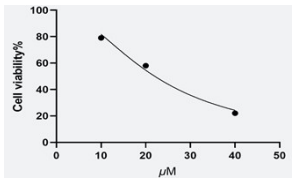

27

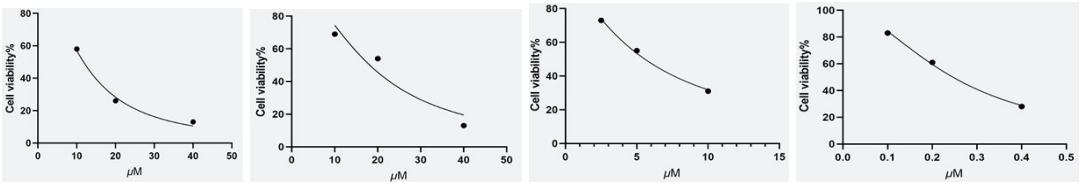

28 **29** **30** **31**

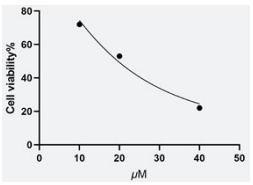

32

Figure S92. Inhibitory curve on K562 cells and THP-1 cells of **1-32**